Geochemistry Geophysics Geosystems G3
AN ELECTRONIC JOURNAL OF THE EARTH SCIENCES
Published by AGU and the Geochemical Society

Review
Volume 4, Number 10
28 October 2003
1089, doi:10.1029/2003GC000533
ISSN: 1525-2027

Short-lived and discontinuous intraplate volcanism in the South Pacific: Hot spots or extensional volcanism?

Anthony A. P. Koppers and Hubert Staudigel
Institute of Geophysics and Planetary Physics, Scripps Institution of Oceanography, University of California, San Diego, La Jolla, CA 92093-0225, USA (akoppers@ucsd.edu; hstaudigel@ucsd.edu)

Malcolm S. Pringle
Argon Isotope Facility, Scottish Universities Environmental Research Center, Rankine Avenue, East Kilbride G75 0QF, UK (m.pringle@surrc.gla.ac.uk)

Jan R. Wijbrans
Laboratory of Isotope Geology, Vrije Universiteit Amsterdam, De Boelelaan 1085 1081 HV Amsterdam, Netherlands (wijj@geo.vu.nl)

[1] South Pacific intraplate volcanoes have been active since the Early Cretaceous. Their HIMU-EMI-EMII mantle sources can be traced back into the West Pacific Seamount Province (WPSP) using plate tectonic reconstructions, implying that these distinctive components are enduring features within the Earth's mantle for, at least, the last 120 Myr. These correlations are eminent on the scale of the WPSP and the South Pacific Thermal and Isotopic Anomaly (SOPITA), but the evolution of single hot spots emerges notably more complicated. Hot spots in the WPSP and SOPITA mantle regions typically display intermittent volcanic activity, longevities shorter than 40 Myr, superposition of hot spot volcanism, and motion relative to other hot spots. In this review, we use $^{40}Ar/^{39}Ar$ seamount ages and Sr-Nd-Pb isotopic signatures to map out Cretaceous volcanism in the WPSP and to characterize its evolution with respect to the currently active hot spots in the SOPITA region. Our plate tectonic reconstructions indicate cessation of volcanism during the Cretaceous for the Typhoon and Japanese hot spots; whereas the currently active Samoan, Society, Pitcairn and Marquesas hot spots lack long-lived counterparts in the WPSP. These hot spots may have become active during the last 20 Myr only. The other WPSP seamount trails can be only "indirectly" reconciled with hot spots in the SOPITA region. Complex age distributions in the Magellan, Anewetak, Ralik and Ratak seamount trails would necessitate the superposition of multiple volcanic trails generated by the Macdonald, Rurutu and Rarotonga hot spots during the Cretaceous; whereas HIMU-type seamounts in the Southern Wake seamount trail would require 350–500 km of hot spot motion over the last 100 Myr following its origination along the Mangaia-Rurutu "hotline" in the Cook-Austral Islands. These observations, however, violate all assumptions of the classical Wilson-Morgan hot spot hypothesis, indicating that long-lived, deep and fixed mantle plumes cannot explain the intraplate volcanism of the South Pacific region. We argue that the observed short-lived and discontinuous intraplate volcanism has been produced by another type of hot spot-related volcanism, as opposed to the strong and continuous Hawaiian-type hot spots. Our results also indicate that other geological processes (plate tension, hotlines, faulting, wetspots, self-propagating volcanoes) may act in conjunction with hot spot volcanism in the South Pacific. In all these scenarios, intraplate volcanism has to be controlled by "broad-scale" events giving rise to multiple closely-spaced mantle plumelets, each with a distinct isotopic signature, but only briefly active and stable over geological time. It seems most likely that these plumelets originate and dissipate at very shallow mantle depths, where they may shoot off as thin plumes from the top of a "superplume" that is present in the South Pacific mantle. The absence of clear age progressions in most

seamount trails and periodic flare-ups of massive intraplate volcanism in the South Pacific (such as the one in the Cretaceous and one starting 30 Myr ago) show that regional extension (caused by changes in the global plate circuit and/or the rise-and-fall of an oscillating superplume) may be driving the waxing and waning of intraplate volcanism in the South Pacific.

Components: 28,607 words, 14 figures, 3 tables, 1 dataset.

Keywords: Intraplate volcanism; hot spots; $^{40}Ar/^{39}Ar$ geochronology; Sr-Nd-Pb Geochemistry; seamounts; Pacific plate; extension; mantle plumes and plumelets.

Index Terms: 3040 Marine Geology and Geophysics: Plate tectonics (8150, 8155, 8157, 8158); 8155 Tectonophysics: Plate motions—general; 8120 Tectonophysics: Dynamics of lithosphere and mantle—general.

Received 27 February 2003; **Revised** 23 June 2003; **Accepted** 26 June 2003; **Published** 28 October 2003.

Koppers, A. A. P., H. Staudigel, M. S. Pringle, and J. R. Wijbrans, Short-lived and discontinuous intraplate volcanism in the South Pacific: Hot spots or extensional volcanism?, *Geochem. Geophys. Geosyst.*, *4*(10), 1089, doi:10.1029/2003GC000533, 2003.

1. Introduction

[2] Age progressive trails of intraplate volcanoes are attractive research targets in the Earth sciences. Some of the most fundamental concepts about deep mantle plumes and hot spots, absolute plate motion, and many aspects of chemical and physical geodynamics are based on our research of such volcanic lineaments. Despite their importance, these concepts are still vigorously debated, in particular, the fixed framework of long-lived hot spots. There are many robust observations that support the concept of hot spots. It was first noted by *Darwin* [1837, 1842] that ocean islands often exist in chains that go through a sequence of subsidence from volcanic islands to atolls. A few years later *Dana* [1849] observed that in these chains only one end is volcanically active, whereas to the other end the volcanoes progressively erode, subside and become older. He even predicted the existence of drowned islands (i.e., guyots) to the west of the Hawaiian Islands, which were only to be discovered by *Hess* [1946]. This very early recognition of age progressive island chains was put on a quantitative basis with K-Ar age determinations [*McDougall*, 1964, 1971] and the resulting "linear" age-distance relationship in the Hawaiian-Emperor seamount trail inspired the "fixed" hot spot concept [*Wilson*, 1963; *Morgan*, 1971, 1972a, 1972b]. Subsequently, the 80 Myr long history of the Hawaiian-Emperor trail has become the cornerstone in our modeling of absolute Pacific plate motion [*Epp*, 1984; *Duncan and Clague*, 1985; *Henderson*, 1985; *Engebretson et al.*, 1985; *Lonsdale*, 1988; *Wessel and Kroenke*, 1997; *Steinberger*, 2000; *Harada and Hamano*, 2000; *Koppers et al.*, 2001] together with the Louisville seamount trail in the South Pacific (Figure 1) [*Hawkins et al.*, 1987; *Lonsdale*, 1988; *Watts et al.*, 1988]. The concept of stationary hot spots has been so successful that it has been a largely unquestioned paradigm throughout all major Earth science textbooks and through much of the scientific literature for several decades.

[3] However, over the last few years it has become clear that the concept of a stationary hot spot cannot be applied to all linear intraplate volcanoes, and it does not even strictly apply to its type-example, the Hawaiian-Emperor chain. For example, *Cande et al.* [1995] pointed out that the bend in the Hawaiian-Emperor chain does not coincide with any major plate reorganization in the global plate circuit, leading to proposals that the Hawaiian hot spot actually moved over geological time due to the massive return-flow of subducted oceanic lithosphere toward the spreading ridges within the deep convecting Pacific mantle [*Steinberger and O'Connell*, 1998; *Steinberger*, 2000; *Wang and Wang*, 2001].

[4] The classic concept of a stationary hot spot may have to be further modified when it is applied to most other volcanic island and seamount trails.

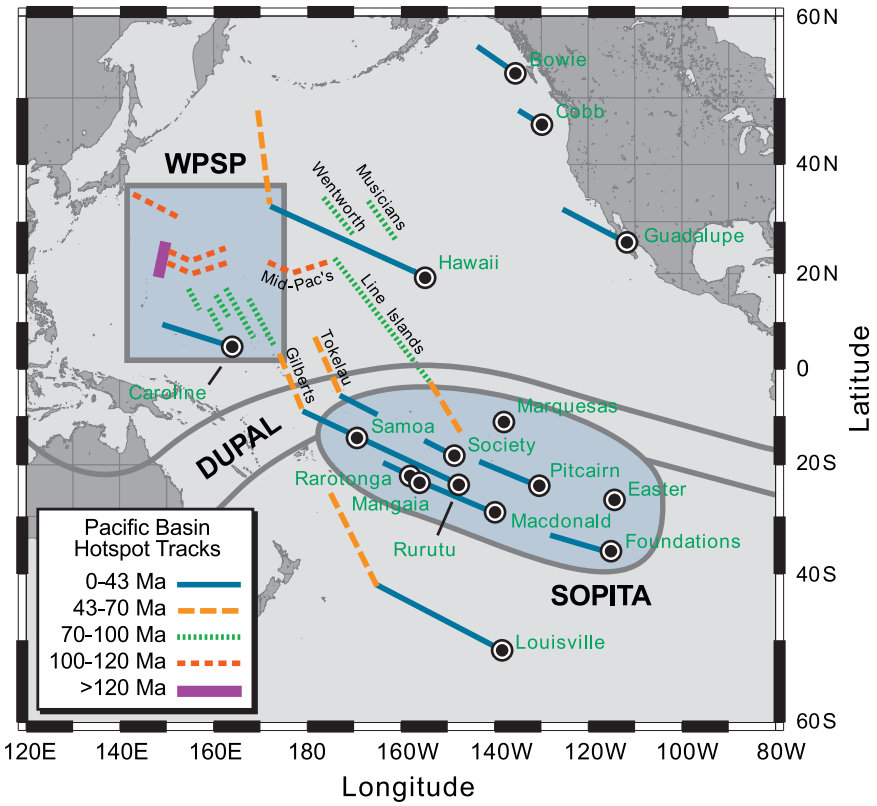

Figure 1. Location of the West Pacific Seamount Province (WPSP) with reference to the South Pacific isotopic and thermal mantle anomaly (SOPITA [*Staudigel et al.*, 1991]) and the DUPAL isotopic mantle anomaly [*Hart*, 1984]. Only those hot spot trails of which radiometric age information is available (see legend for age ranges) and those hot spots assumed to be currently active in the Pacific Basin (filled circles) are plotted.

In the South Pacific, seamount trails are typically shorter, less voluminous than Hawaii, and discontinuous (Figure 2) [cf. *Vogt*, 1972; *Pringle et al.*, 1994; *McNutt et al.*, 1997; *Koppers et al.*, 1998; *Clouard and Bonneville*, 2001; *Nikishin et al.*, 2002; this study]. They also are often non-age-progressive [cf. *Jackson*, 1976; *Bonatti and Harrison*, 1976; *Turner and Jarrard*, 1982; *McNutt et al.*, 1997; *Dickinson*, 1998; *Davis et al.*, 2002; this study]. These observations require major modifications to the general concept of hot spots, or maybe even the definition of new types of hot spot volcanism. In either case, many or all premises of the Wilson-Morgan hot spot hypothesis appear to be open to questions—diminishing the simplicity and age-predictive power of the classical mantle plume hypothesis [*Smith and Lewis*, 1999; *Foulger and Natland*, 2003].

[5] A similar conclusion was reached by *Courtillot et al.* [2002] who suggested that three distinct types of hot spots can be recognized in the Earth's mantle. They recognized only seven "primary" Wilson-Morgan hot spots (including the Hawaiian, Louisville and Eastern hot spots for the Pacific mantle region) based on the presence of clear linear age progressions, large buoyancy fluxes and high $^{3}He/^{4}He$ ratios reflecting a deep mantle source. All other hot spots are considered "secondary" or "tertiary" either caused by shallow mantle plume-lets rising from the top of "superplumes" [cf. *Davaille*, 1999; *Davaille et al.*, 2002, 2003] or extensional features in the oceanic lithospheres [cf. *Anderson*, 2001, 2002].

[6] By far the largest number of secondary hot spots can be found in the "South Pacific Thermal and Isotopic Anomaly" or the "Superswell" (SOPITA; Figure 1) offering a unique opportunity to study these hot spots over a long geological time period. In fact, the SOPITA represents the only locus of intraplate volcanism in the Pacific that

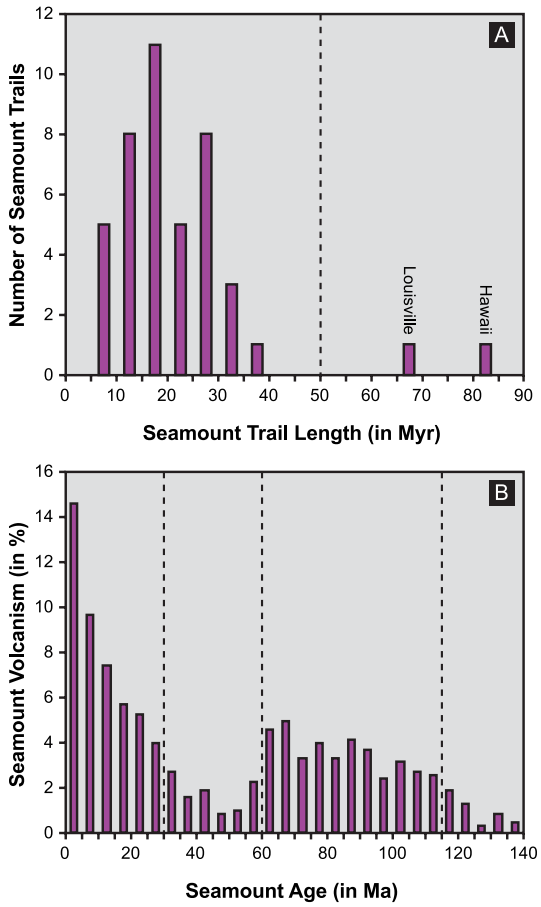

Figure 2. Histograms displaying timescales and periodicity of Pacific hot spot volcanism. (a) Typical overall duration of volcanism per hot spot trail in Myr (n = 43). Segments of seamount trails where measured from the predicted bathymetry database of *Smith and Sandwell* [1996, 1997] and their lengths (in angular distance) were converted to timescales based on the Pacific stage pole model of *Koppers et al.* [2001]. (b) Cumulative periodicity of seamount volcanism in the Pacific basin using 5 Myr bins. In both histograms we use the same data set, which excludes intraplate volcanism producing oceanic plateaus.

continuously has been producing seamounts over the last 140 Myr. Its Cretaceous counterpart is preserved in a large range of seamounts and guyots found in the West Pacific Seamount Province (WPSP; Figures 1 and 3). In addition, the SOPITA hot spots display very distinct and long-lived isotopic signatures [*Staudigel et al.*, 1991] that offer the possibility to combine source region chemistry and seamount geochronology to map out these mantle melting anomalies over geological time. The results of these hot spot mappings may resolve many important issues regarding the stationary character, continuity and longevity of the SOPITA melting anomaly in the South Pacific mantle—and its secondary hot spots.

[7] In this review, we use $^{40}Ar/^{39}Ar$ seamount ages and Sr-Nd-Pb isotopic signatures to map out Cretaceous volcanism in the WPSP and to characterize its evolution with respect to the currently active hot spots in the SOPITA region. We will exploit the resulting relationships to evaluate the validity of the classic concepts of mantle plumes and stationary hot spots [*Wilson*, 1963; *Morgan*, 1971, 1972a, 1972b] and to shed light on alternative models for intraplate volcanism in the South Pacific as being controlled by lithospheric architecture and stress [cf. *Jackson and Shaw*, 1975; *Winterer and Sandwell*, 1987; *Sandwell et al.*, 1995; *Wessel et al.*, 1996; *Smith and Lewis*, 1999; *Favela and Anderson*, 2000; *Hieronymus and Bercovici*, 2000; *Anderson*, 2001, 2002; *Foulger and Natland*, 2003] or "superplume" mantle convection [cf. *McNutt*, 1998; *Janney et al.*, 1999; *Courtillot et al.*, 2002; *Davaille et al.*, 2002, 2003]. We will start out by briefly reviewing the geological framework and the analytical techniques for a large suite of new data based on

Figure 3. (opposite) Sample locations and $^{40}Ar/^{39}Ar$ data of the West Pacific Seamount Province. (a) Simplified map delineating the proposed seamount trails (see legend for age ranges) as distinguished on basis of their azimuth and $^{40}Ar/^{39}Ar$ age data. (b) Japanese seamount trail. (c) Northern Wake, Southern Wake and Typhoon seamount trails. (d) Magellan, Ujlan and Anewetak seamount trails. (e) Ralik and Ratak seamount trails. All recombined $^{40}Ar/^{39}Ar$ ages are shown in conjunction with the Jurassic geomagnetic reversals (red lines) and fracture zones (blue lines) for the oceanic basement [*Nakanishi et al.*, 1992; *Abrams et al.*, 1993; *Nakanishi*, 1993]. Fracture zones are based on the geomagnetic reversal patterns, except for Osagawara FZ#1 and FZ#2 that are based on seismic profiling [*Abrams et al.*, 1993]. All bathymetric maps have been produced using Generic Mapping Tools (GMT) version 3.0 [*Wessel and Smith*, 1995] from the predicted bathymetry database of *Smith and Sandwell* [1996, 1997] on basis of altimetric gravity data. Contours represent 200 m depth intervals. Polarity timescale after *Cande and Kent* [1992]. Conventional K-Ar ages have been omitted from this compilation since these ages may be inaccurate due to pervasive seawater alteration [cf. *Koppers et al.*, 2000].

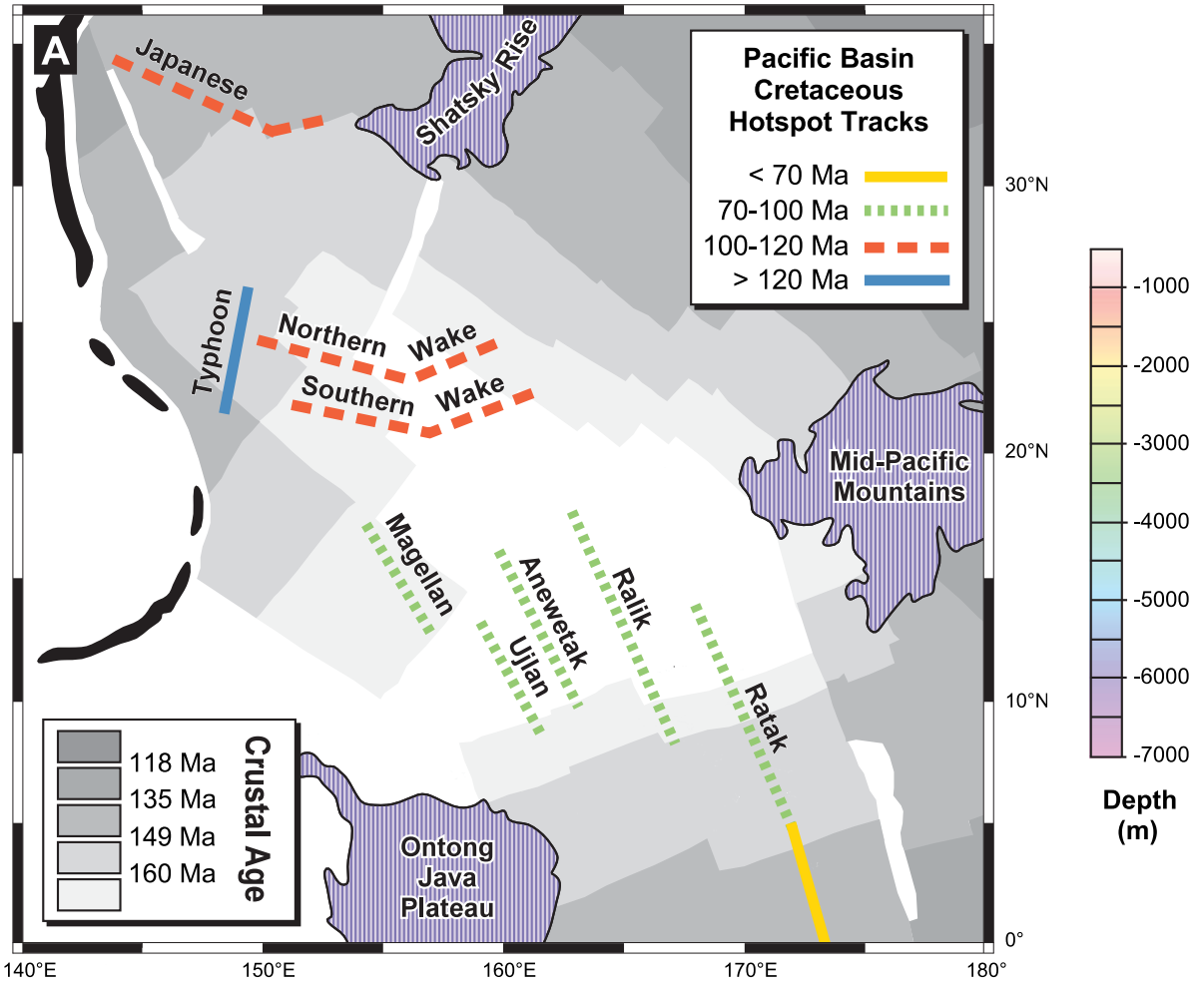
A
Japanese
Shatsky Rise
Pacific Basin
Cretaceous
Hotspot Tracks
< 70 Ma
70-100 Ma
100-120 Ma
> 120 Ma
Typhoon
Northern Wake
Southern Wake
Mid-Pacific
Mountains
Magellan
Anewetak
Ujlan
Ralik
Ratak
Ontong
Java
Plateau
Crustal Age
118 Ma
135 Ma
149 Ma
160 Ma
30°N
20°N
10°N
0°
140°E
150°E
160°E
170°E
180°
-1000
-2000
-3000
-4000
-5000
-6000
-7000
Depth
(m)

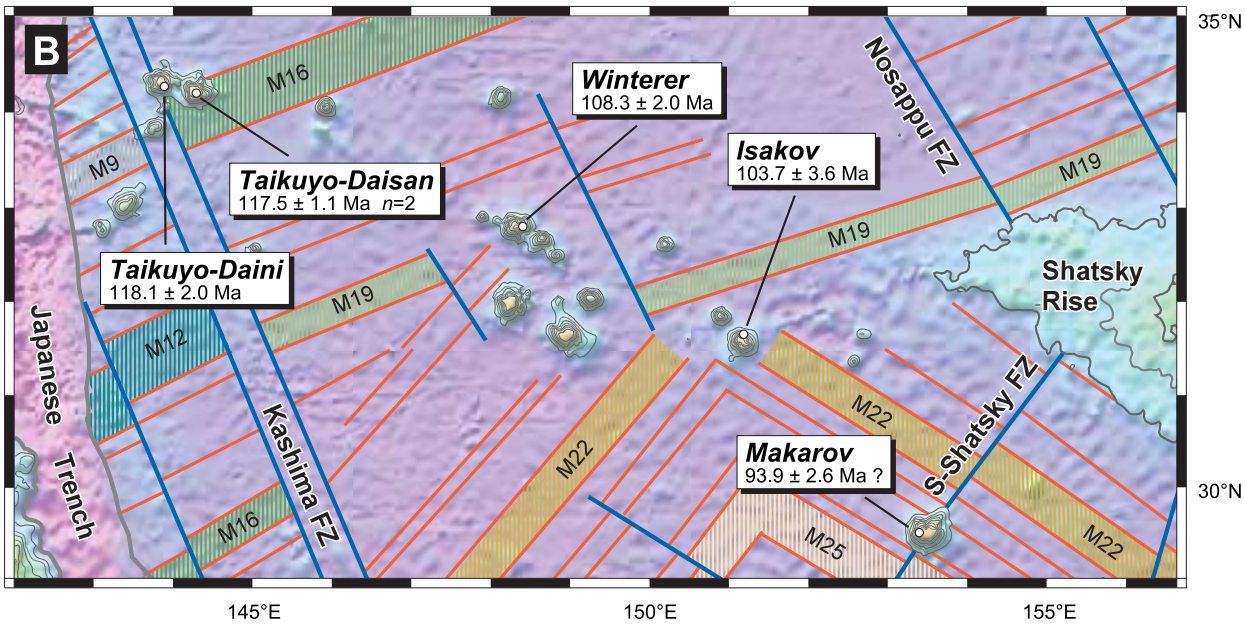
B
M16
M9
Winterer
108.3 ± 2.0 Ma
Nosappu FZ
Isakov
103.7 ± 3.6 Ma
Taikuyo-Daisan
117.5 ± 1.1 Ma n=2
M19
M19
Taikuyo-Daini
118.1 ± 2.0 Ma
Shatsky
Rise
M12
M19
Japanese
Trench
Kashima FZ
M22
M22
S-Shatsky FZ
Makarov
93.9 ± 2.6 Ma ?
M16
M25
M22
35°N
30°N
145°E
150°E
155°E

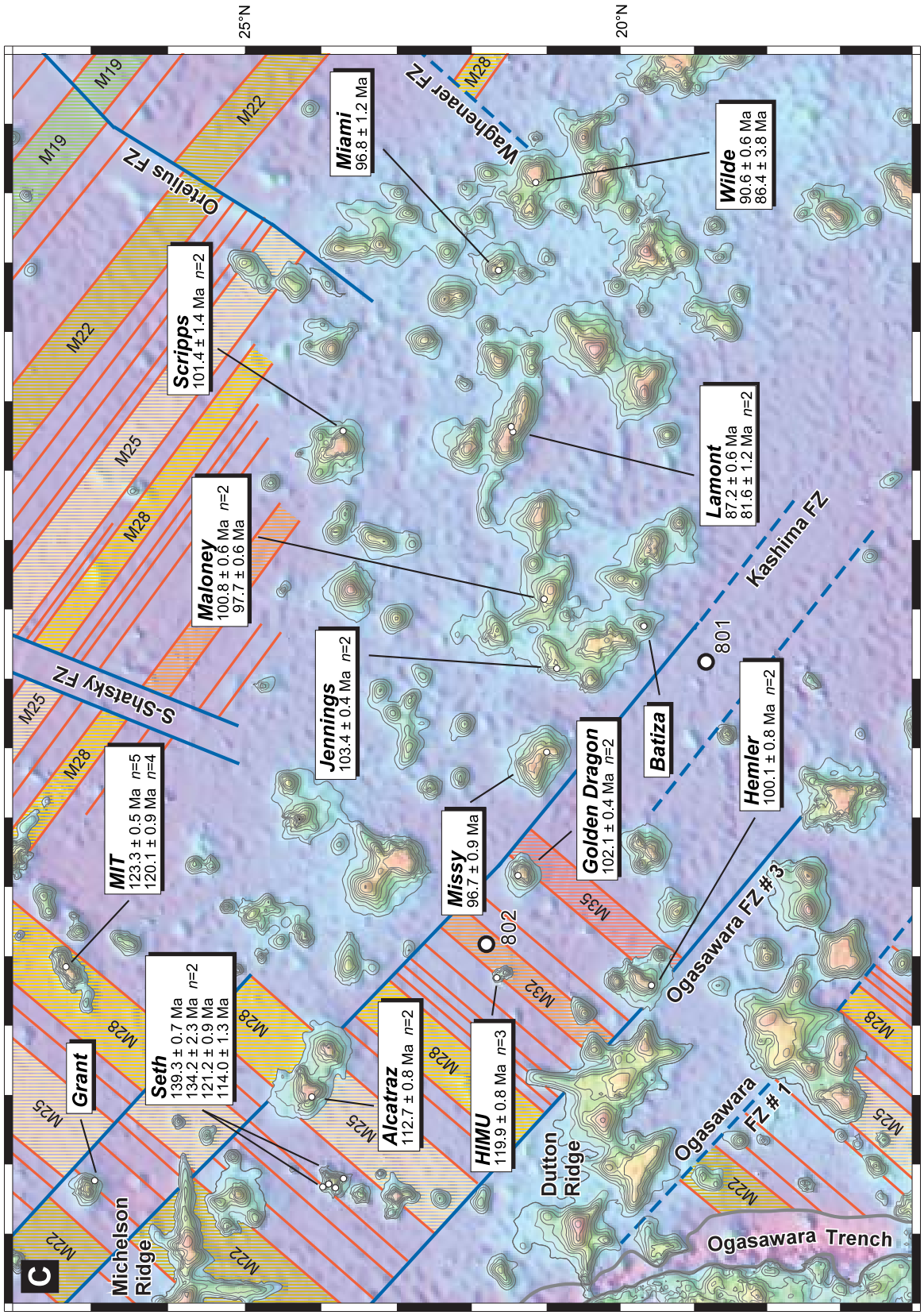

Figure 3. (continued)

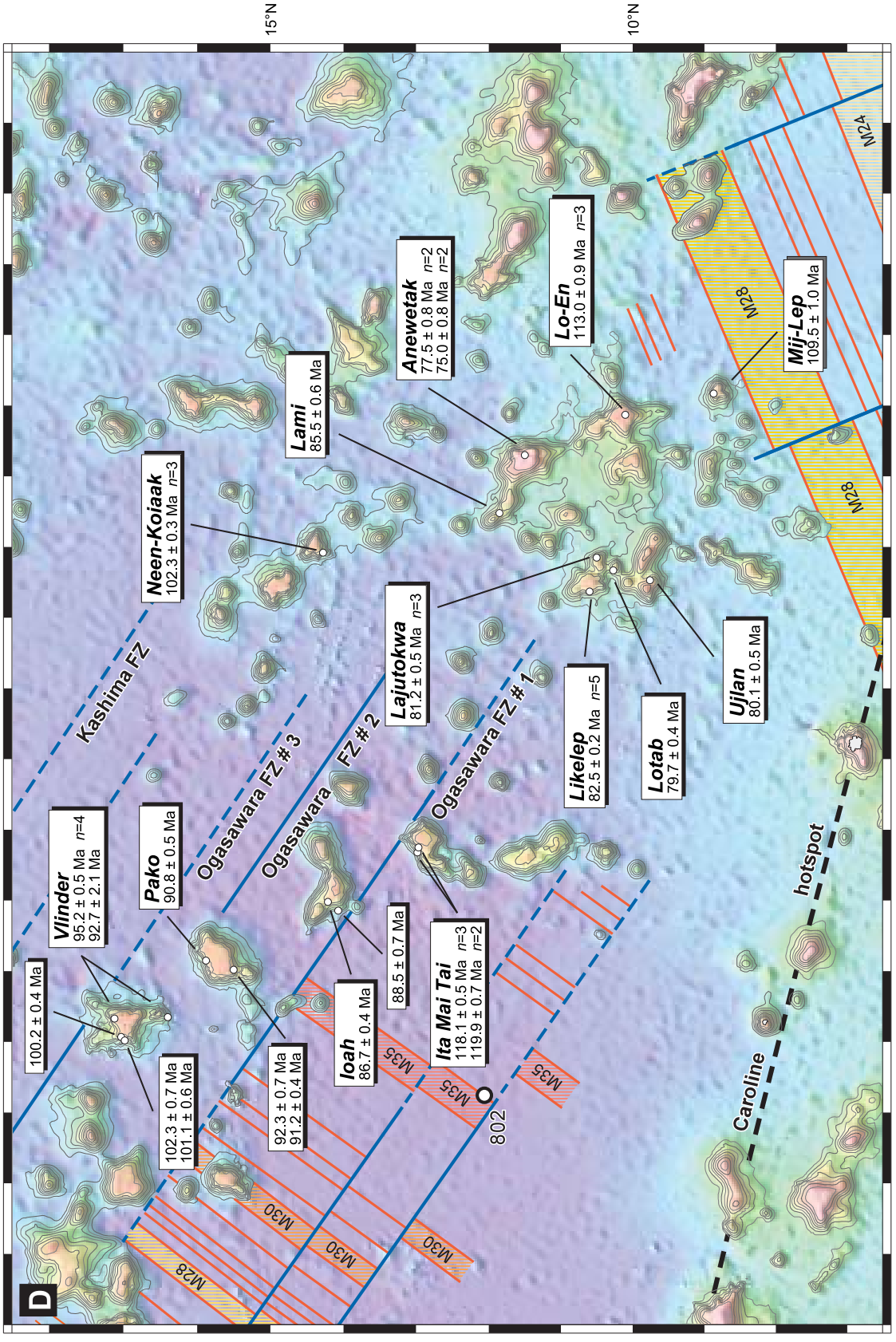

Figure 3. (continued)

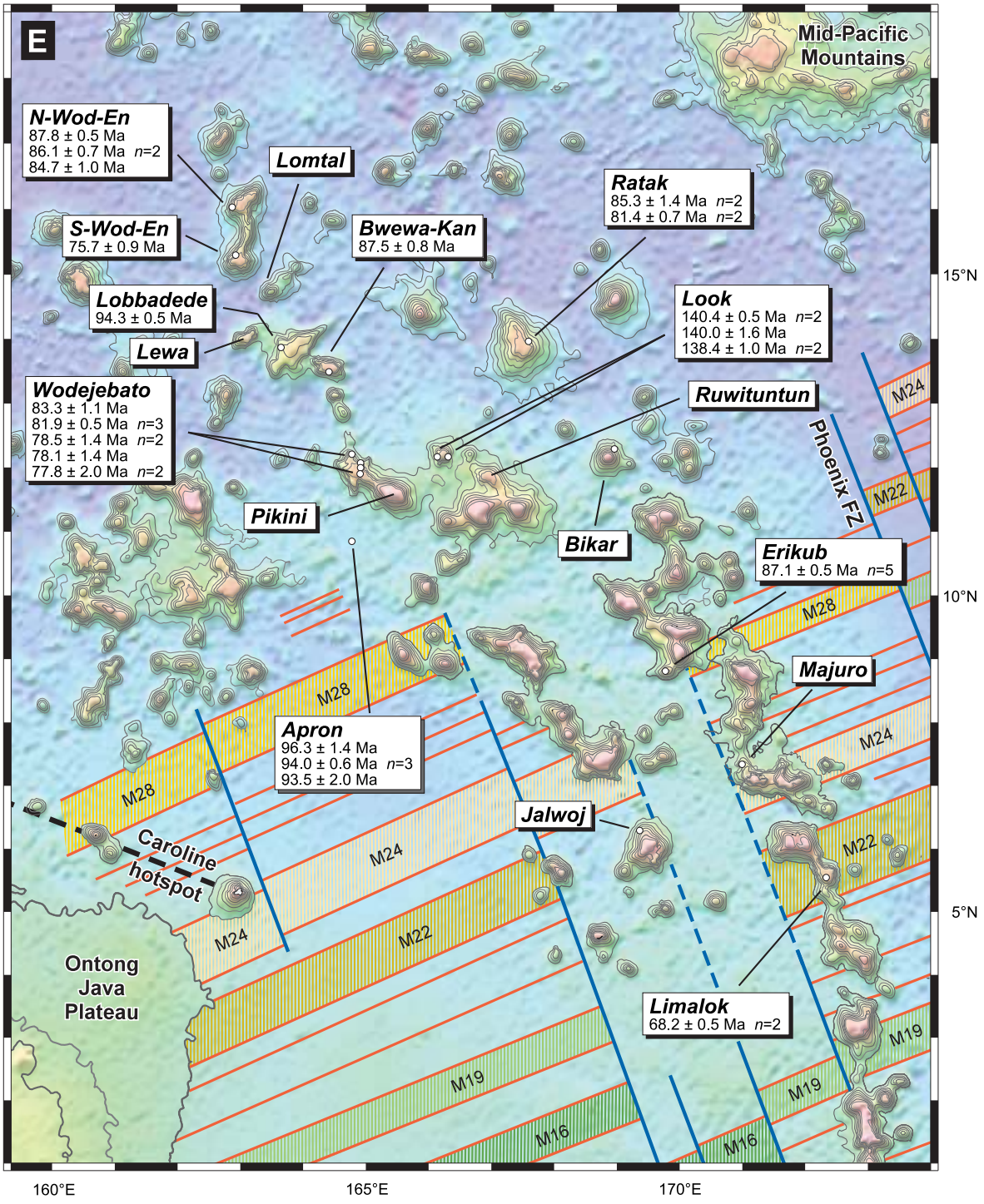

Figure 3. (continued)

the Ph.D. thesis of *Koppers* [1998]. In Sections 4 and 5, we will discuss the $^{40}Ar/^{39}Ar$ geochronology and the apparent (lack of) age progressions in the WPSP seamount trails and their distinct Sr-Nd-Pb isotopic characteristics. In the discussion, we will use "backtracking" and "hot spotting" techniques to actually map out the evolution of the South Pacific hot spots over the last 140 Myr. Note that

throughout this review, we will use the term "hot spot" as a generic term describing intraplate volcanism due to any type of mantle melting, either caused by a plume-like upwelling, wetspots or decompression melting due to plate extension.

2. Geological Framework

[8] This paper focuses on the West Pacific Seamount Province (WPSP) that stretches all the way from the Mid-Pacific Mountains to the Mariana trench in the Western Pacific basin (Figure 3a). The WPSP was originally formed in the South Pacific—a region that today exhibits active intraplate volcanism and that has been referred to as the "Superswell" for its unusually shallow ocean floor [*Menard*, 1964; *McNutt et al.*, 1996; *McNutt*, 1998] or the "South Pacific Isotopic and Thermal Anomaly" (SOPITA) for the coincidence of an isotopically and thermally anomalous mantle region [*Staudigel et al.*, 1991].

2.1. The South Pacific Isotopic and Thermal Anomaly

[9] The mantle underneath the French Polynesian region in the South Pacific ocean is both thermally and isotopically unusual [*Hart*, 1984; *Staudigel et al.*, 1991; *McNutt et al.*, 1996]. One of the largest concentrations of hot spots in any ocean (eleven hot spots) has produced an anomalously large number of seamounts and volcanic islands over the last 20 Myr [*Stefanick and Jurdy*, 1984; *Duncan and Richards*, 1991; *Bemis and Smith*, 1993]. These intraplate volcanoes are located on relatively thin and hot oceanic lithosphere of the South Pacific Superswell [*McNutt and Fischer*, 1987; *McNutt and Judge*, 1990; *Larson*, 1991; *Cazenave and Thoraval*, 1994; *McNutt et al.*, 1996, 1997; *McNutt*, 1998]. This Superswell coincides with a negative geoid anomaly that necessitates dynamic support from broad-scale convection in the upper mantle [*Castillo*, 1988; *McNutt*, 1998]. Most tomography studies picture this "superplume" with enough resolution, in some cases all the way from the core-mantle boundary to the bottom of the lithosphere [cf. *Gu et al.*, 2001; *Romanowicz and Gung*, 2002]. The SOPITA volcanoes also have unusual isotope compositions for their underlying mantle [*Vidal et al.*, 1984; *Zindler and Hart*, 1986; *Staudigel et al.*, 1991; *Chauvel et al.*, 1992; *Woodhead and Devey*, 1993]. It was *Hart* [1984] who first drew attention to this isotopic anomaly by relating them to a globe-encircling zone of intraplate volcanoes with common (isotopic) source region characteristics. This DUPAL anomaly (Figure 1) includes both high $^{87}Sr/^{86}Sr$ ratios and high Pb isotope ratios deviating from an average northern hemisphere trend. However, *Staudigel et al.* [1991] observed that the SOPITA anomaly (Figure 1) is distinct from the DUPAL anomaly by covering the entire spectrum between isotope end-members for ocean island basalts (HIMU-EM1-EM2) [*Zindler and Hart*, 1986]. Most of these mantle components can be linked to the subduction of crustal components into the mantle, suggesting that the South Pacific mantle is unusually enriched in subducted components [*Hofmann and White*, 1982; *White and Hofmann*, 1982; *Zindler and Hart*, 1986; *Staudigel et al.*, 1991], where HIMU represents old and recycled (altered) oceanic crust that is characterized by high $^{206}Pb/^{204}Pb$ ratios and EM1-EM2 represents subducted oceanic crust with a few percent pelagic or continental sediment intermixed [cf. *Zindler and Hart*, 1986; *Chauvel et al.*, 1992]. Alternatively, the mantle itself may not be enriched in these components, but these subducted components may be delivered more efficiently to the intraplate volcanoes in this region because they are particularly enriched in recycled volatiles that may enhance heat transfer and, therefore, promote ductile flow and partial melting [*Staudigel et al.*, 1991]. In either case, the unusual abundance of these subducted components seems responsible for the coincidence of isotopic and thermal anomalies in the South Pacific.

2.2. West Pacific Seamount Province

[10] The West Pacific Seamount Province (WPSP) is located on the oldest part of the Pacific plate and offers an ancient record of SOPITA intraplate volcanism. The WPSP includes all "seamounts" with an age older than 70 Ma that are located in the West Pacific. It marks the convergence of numer-

ous seamount trails and oceanic plateaus that may be arranged geometrically in nine different seamount trails (Figure 3a). The WPSP sits on unusually shallow seafloor with a thin elastic plate thickness [*McNutt and Fischer*, 1987; *Smith et al.*, 1989; *Wolfe and McNutt*, 1991; *Winterer et al.*, 1993; *McNutt*, 1998] and a slower than normal subsidence when compared to conductive heat loss models [*Parsons and Sclater*, 1977]. These observations are best explained by a thermal rejuvenation of the WPSP lithosphere occurring ~70 Myr subsequent to formation at its Jurassic spreading centers [*Schlanger et al.*, 1981; *Epp*, 1984; *Schlanger et al.*, 1987; *Smith et al.*, 1989; *Lincoln et al.*, 1993; *Larson et al.*, 1995; *Haggerty and Premoli Silva*, 1995; *Nagihara et al.*, 1996]. Concentrated intraplate volcanism in the Wake seamounts, Marshall Islands, Mid-Pacific Mountains and Line Islands were causally related to this thermal rejuvenation forming the Darwin Rise [*Menard*, 1964, 1984a, 1984b; *Crough*, 1978; *Detrick and Crough*, 1978; *Wolfe and McNutt*, 1991]. This ancient "Superswell" resulted in a lithospheric uplift of 200–700 m causing the exposure and erosion of many carbonate reefs during the Cretaceous [*Winterer et al.*, 1993].

2.3. Models for Intraplate Volcanism

[11] Different expressions of intraplate volcanism can be reconciled under one generalized "hot spot" model, but only if several types of hot spots are distinguished. In previous studies a distinction was made between strong Hawaiian-type and weak Marquesian-type hot spots based on their (geophysical and) geochemical evolution [*Duncan et al.*, 1986; *Haase*, 1996]. These distinctions were recently restated by *Courtillot et al.* [2002] by labeling these "primary" and "secondary" hot spots. In the first model, focused mantle plumes penetrate the lithosphere producing Hawaiian-type hot spots that are continuously active over extended geological periods (i.e., more than 80 Myr) while producing voluminous volcanic edifices aligned in age progressive seamount trails. As a consequence, their isotopically-enriched tholeiitic shield-building lavas are predominantly derived from plume melts, while post-shield lavas have more depleted isotopic signatures and are increasingly derived from lithospheric melts [*Chen and Frey*, 1983; *Clague et al.*, 1989]. These primary hot spots are speculated to have a deep origin, possibly at the core-mantle boundary [*Courtillot et al.*, 2002]. In the second model, broad and diffuse mantle plumes spread out underneath the overlying lithosphere producing multiple weak Marquesian-type hot spots [*Sleep*, 1984; *Duncan et al.*, 1986; *Woodhead*, 1992; *McNutt et al.*, 1997]. At these Marquesian-type hot spots, shield-building and post-shield lavas are mainly derived from lithospheric melts, whereas enriched isotopic plume signatures are restricted to the post-shield stage of intraplate volcanism when sufficient time has elapsed to entrain plume material in the lithospheric melts [*Hauri et al.*, 1994; *Janney et al.*, 1999]. These secondary hot spots are speculated to have been formed at shallow depths in the upper mantle, where they may have originated as parasitic plumelets on top of superplumes [*McNutt*, 1998; *Davaille*, 1999; *Courtillot et al.*, 2002]. In this context, most active and ancient hot spots in the SOPITA and WPSP regions may be considered weak Marquesian-type or secondary hot spots, because their seamount trails are short of length (10–40 Myr; Figure 2a) and because they (almost) completely lack the typical tholeiitic basalts that are illustrative of strong Hawaiian-type hot spots [cf. *Hart et al.*, 2000].

[12] These modifications of the classic hot spot concept make it more complicated, and less appealing as a unique and predictive model. For this reason, it is important to explore alternative concepts to explain intraplate volcanism. Numerous studies (including this study) show that seamount trails quite often have complex and non-linear age distributions. This is particularly true for the Line Islands in the Central Pacific, where coincidences of multiple hot spot trails may play an important role and/or alternative mechanisms that produce intraplate volcanism [cf. *Henderson and Gordon*, 1982; *Schlanger et al.*, 1984; *Epp*, 1984; *Davis et al.*, 2002]. *Epp* [1984] suggested many alternative models to explain the complex age distribution in the Line Islands, including flow toward mid-oceanic ridge segments, thermal feedback, re-melting of

the lithosphere and interaction with transform faults. In addition, *Davis et al.* [2002] proposed that two major episodes of volcanism (around 70 and 83 Ma) occurred synchronously over distances up to 1,500 km. Each of these episodes lasted for ~5 Myr and, according to these authors, are related to the periodic upwelling of the eastern "Superswell" during the Cretaceous that caused intraplate tensional stresses and volcanism. *Bonatti and Harrison* [1976] suggested that simultaneous volcanism along lineaments in the South Pacific may be due to a hotline in the mantle, rather than a hot spot. Complex age distributions are also typical for the "closely-spaced" seamount trails and en echelon ridges [*Winterer and Sandwell*, 1987; *Sandwell et al.*, 1995; *McNutt et al.*, 1997; *Dickinson*, 1998] in the SOPITA region, which indicate non-age-progressive volcanism running slightly oblique to the general plate motion trend [*McNutt et al.*, 1997; *Winterer*, 2002]. Cracking of the lithosphere through tensional stresses [*Sandwell et al.*, 1995] or bending through uneven thermal contractions in young lithosphere [*Gans et al.*, 2003] may explain these ridges that often occur in gravity lows, such as the Pukapuka ridge. These cracking and bending mechanisms require no elevated "hot spot" temperatures or (deep) mantle plumes [*Smith and Lewis*, 1999; *Favela and Anderson*, 2000; *Winterer*, 2002; *Foulger and Natland*, 2003]; they also may explain seamount trails that show volcanic phases up to 10 Myr older than expected [*Koppers et al.*, 1998] or that have completely erratic age distributions as shown in this study. *Courtillot et al.* [2002] labeled these features "tertiary" hot spots.

[13] Plate deformation and cracking of the lithosphere to generate leaking transform faults is not that surprising in the context of plate tectonics. Lithospheric plates are not believed to be "completely" rigid anymore [*Anderson*, 2001, 2002; *Gans et al.*, 2003] and, as a consequence, they can experience thinning and form weak zones under tensional and geothermal stresses. Intraplate volcanism can form over (and enhance) these weak zones where decompression-generated melts penetrate the lithosphere and form seamount trails that typically are non-age-progressive. In these models, shallow mantle melting is facilitated by increased thermal stresses surrounding fractures and by the presence of H_2O-rich metasomatized mantle domains or "wetspots" that sufficiently lower the solidus of the mantle underneath the fractures to induce partial melting [*Bonatti*, 1990; *Smith and Lewis*, 1999; *Favela and Anderson*, 2000].

[14] Although many models have been proposed to explain intraplate volcanism, the "plume theory" has dominated geodynamics over the last decades with only a few challenges. This is largely due to its perceived success and predictive power in explaining intraplate volcanism, geodynamics and absolute plate motion. In contrast, the alternative "extensional" models are relatively vague about the exact location of an intraplate volcano; they have no predictive power to explain age progressions and, therefore, leave us without a simple concept for absolute plate motion. Throughout this review paper we will focus on what we do observe at seamount trails, in terms of their geospatial distributions over the last 140 Myr and their geochemistry, laying out the available geological data that may support hot spot or extensional models, or both.

3. Analytical Methods

[15] All data reviewed in this paper were previously published, either in the peer-reviewed literature or in the Ph.D. thesis of *Koppers* [1998]. In total we will review $^{40}Ar/^{39}Ar$ geochronological and Sr-Nd-Pb isotope data from 41 seamounts and guyots in the WPSP (Figure 3; Table 1, 2). New $^{40}Ar/^{39}Ar$ incremental heating experiments are listed in Table 1 and displayed in the age plateau diagrams of Figure 4; new Sr-Nd-Pb radiogenic isotope data are listed in Table 2 and displayed in Figures 6 and 7. Analytical data and sample details can be found in the Appendices A through D. References to all previously published data have been listed in Table 1 and 2. Data tables and Appendices can be downloaded from the EarthRef Digital Archive by using the http://earthref.org/cgi-bin/err.cgi?n=1445 link and by following the Quick Links. You can also

Table 1 (Representative Sample). Overview $^{40}Ar/^{39}Ar$ Data of the West Pacific Seamount Province[a] [The full Table 1 is available in the HTML version of this article at http://www.g-cubed.org.]

Sample								Analyses			Age Spectrum				
				Location											
Seamount	Field Number	Lab Code	Rock Type	Lat	Lon	Depth, m	Dredge Site	Analyses Number	Sample Type	Ref.	Age ± 2σ (Ma)	K/Ca	^{39}Ar, %	MSWD	n
Magellan Seamount Trail															
Vlinder	TUNES 6 29-1	VLI-1	hawaiite	17.12	154.33	2200	rim	97M0266	grndm	(2)	95.0 ± 0.7	0.47	52	16.5	6
	TUNES 6 29-29	VLI-4	hawaiite	17.12	154.33	2200	rim	93M0054	plag	(1)	95.4 ± 1.5	0.01	49	5.2	4
								95M0259	grndm	(1)	96.6 ± 0.7	0.34	41	6.6	5
	TUNES 6 29-10	VLI-8	alk basalt	17.12	154.33	2200	rim	97M0272	plag	(2)	92.3 ± 1.7	0.01	96	1.1	7
	TUNES 6 32-14	OMA-1	hawaiite	16.40	154.35	3400	satellite	93M0056	plag	(2)	95.6 ± 0.7	0.01	49	0.9	4
								97M0242	*repeat*	(2)	93.3 ± 2.2	0.01	80	0.3	4
	TUNES 6 27-10a	VLI-6	hbl basanite	16.98	154.02	3100	pedestal	97M0261	grndm kfs	(2)	102.4 ± 0.5	6	100	4.1	8
	TUNES 6 27-9a	VLI-9	hbl basanite	16.98	154.02	3100	pedestal	97M0260	grndm kfs	(2)	101.6 ± 0.6	5.73	100	7.4	11
	TUNES 6 28-1	VLI-5	hbl basanite	17.03	154.07	2400	pedestal	95M0193	hbl	(2)	100.2 ± 0.4	0.11	93	1.5	11
Pako	MW8805 RD-66-1	PAK-1	hawaiite	15.88	155.15	2025	rim	95M0220	plag	(2)	90.9 ± 0.5	0.04	65	1.3	9
	MW8805 RD-67-3	PAK-2	hawaiite	15.50	155.02	1600	rim	97M0265	aph bas	(2)	92.3 ± 0.7	0.31	19	2.9	3
	MW8805 RD-67-2	PAK-3	hawaiite	15.50	155.02	1600	rim	97M0267	aph bas	(2)	91.2 ± 0.4	0.8	25	2.1	3
Ioah	PUSH I-065-5	IOA-3	hawaiite	14.13	155.88	4000	flank	97M0264	grndm	(2)	88.5 ± 0.7	0.65	53	2.8	9

[a] K/Ca values are calculated as weighted means for the age spectra or using recombined totals of $^{39}Ar_K$ and $^{37}Ar_{Ca}$ for the total fusions. MSWD values for the age plateaus and inverse isochrons are calculated using N-1 and N-2 degrees of freedom, respectively. All Vrije Universiteit samples where monitored against Taylor Creek Rhyolite sanidine (27.92 Ma). Reported errors on the $^{40}Ar/^{39}Ar$ ages are on the 95% confidence level including 0.2–0.3% standard deviation in the J-value. The analyses normally represent incremental heating experiments on acid-leached materials, unless they are denoted by: C, incremental heating experiments performed on whole rock cores; F = total fusion experiments; N, non-leached materials. This compilation table contains 38 new incremental heating experiments from *Koppers* [1998]; all other data are from (1) *Koppers et al.* [2000]; (2) *Koppers et al.* [1998]; (3) *Davis et al.* [1989]; (4) *Smith et al.* [1989]; (5) *Lincoln et al.* [1993]; (6) *Winterer et al.* [1993]; (7) *Pringle and Duncan* [1995a]; (8) *Pringle and Duncan* [1995b]; (9) *Ozima et al.* [1977]; (10) *Wijbrans et al.* [1995]. Some unleached whole rock (core) analyses are denoted by light gray background colors indicating that they are most likely affected by alteration based on comparison with comagmatic samples.

Table 2 (Representative Sample). Overview Sr-Nd-Pb Isotope Compositions of the West Pacific Seamount Province[a] [The full Table 1 is available in the HTML version of this article at http://www.g-cubed.org.]

Lab Code	Location		Sample Type	Ref.	Measured Values											
	Lat	Lon			Rb ppm	Sr ppm	$^{87}Rb/^{86}Sr$	$^{87}Sr/^{86}Sr$	Sm ppm	Nd ppm	$^{147}Sm/^{144}Nd$	$^{143}Nd/^{144}Nd$	U ppb	Th ppb	Pb ppm
Alcatraz Guyot															
ALC-2	24.10	149.95	plagioclase					0.702607							
Golden Dragon Seamount															
GLD-3	21.37	153.15	plagioclase					0.702950							
			unleached WR		208[b]	383[b]	1.571	0.705923	8.3[b]	74[b]	0.068	0.512840	2700[b]	42.6[b]	28.3[b]
			leached WR		214[c]	375[c]	1.649	0.705225	2.1[c]	15.2[c]	0.085	0.512836	3760[c]	27.4[c]	17.0[c]
			leached WR		245[b]	500[b]	1.419	0.705055		18[b]		0.512844	2100[b]	27.7[b]	
GLD-5	21.37	153.15	clinopyroxene			111.6		0.702813	6.39	21.05	0.183	0.512879	12.7		0.080
			hornblende			859.3		0.702868	8.19	34.73	0.143	0.512878	1.9		
			leached WR		28[b]	186[b]	0.438	0.703388	6.1[d]	41[b]	0.090	0.512866	1000[b]	4.6[b]	<dl
GLD-9	21.35	153.33	leached WR	(1)			0.028	0.702984			0.125	0.512961			
GLD-10	21.35	153.33	leached WR	(1)			0.525	0.703610			0.140	0.512850			
			leached WR	(1)			0.394	0.703275							
Hemler Guyot															
HEM-1	19.55	151.57	plagioclase					0.705058							
			clinopyroxene		2.32	132.8	0.051	0.704737	6.57	26.09	0.152	0.512740	75.6		0.308
			clinopyroxene		2.32	132.8	0.051	0.704712	6.57	26.09	0.152	0.512739	75.6		0.308
			leached WR	(1)			0.010	0.704761			0.140	0.512758			
			leached WR	(1)				0.704698							
HEM-2	19.55	151.57	nefeline					0.704801							
			clinopyroxene		0.48	117.5	0.012	0.704661	5.74	21.91	0.158	0.512733	53.7		0.352
			leached WR		4[c]	260[c]	0.042	0.704710	7.2[c]	32.9[c]	0.132	0.512736	170[c]	2.4[c]	5.0[c]
HEM-3	19.55	151.57	leached WR	(1)			0.855	0.705257				0.512745			
			leached WR	(1)				0.705110							
HEM-4	19.88	151.90	leached WR	(1)			0.098	0.705065			0.094	0.512722			
HEM-5	19.37	151.97	leached WR	(1)			0.116	0.704686			0.089	0.512685			

[a] Abundances are determined by isotope dilution mass spectrometry. Exponential Sr and Nd isotopic mass fractionation corrections are based on $^{86}Sr/^{88}Sr = 0.1194$ and $^{146}Nd/^{144}Nd = 0.7219$. Mass fractionation (1σ SD) is -0.00400 ± 0.00089 amu^{-1} for Rb, 0.00300 ± 0.00037 amu^{-1} for U (U500 standard) and 0.00124 ± 0.00028 amu^{-1} for Pb (NBS981 standard). Measured isotope ratios for Sr and Nd are normalized to Vrije Universiteit standard values (2σ SD) for NBS987 Sr, $^{87}Sr/^{86}Sr = 0.710243 \pm 14$, for the internal standard VITRON Nd, $^{143}Nd/^{144}Nd = 0.511336 \pm 16$ and for La-Jolla Nd, $^{143}Nd/^{144}Nd = 0.511851 \pm 15$. Within-run errors (not listed) are always smaller than the reproducibility of the standards. Total blank-sample ratios are lower than 0.1%. Calculated initial ratios that are higher than expected based on comparison with comagmatic phases probably are affected by alteration and, therefore, denoted by light gray background colors. 1. Initial isotope ratios denoted in red colors could not corrected for radiogenic ingrowth, because the parent-daughter ratios were not analyzed. All data are from *Koppers* [1998].

[b] Abundances are determined by XRF.

[c] Abundances are determined by ICP-MS.

[d] Abundances are determined by INA.

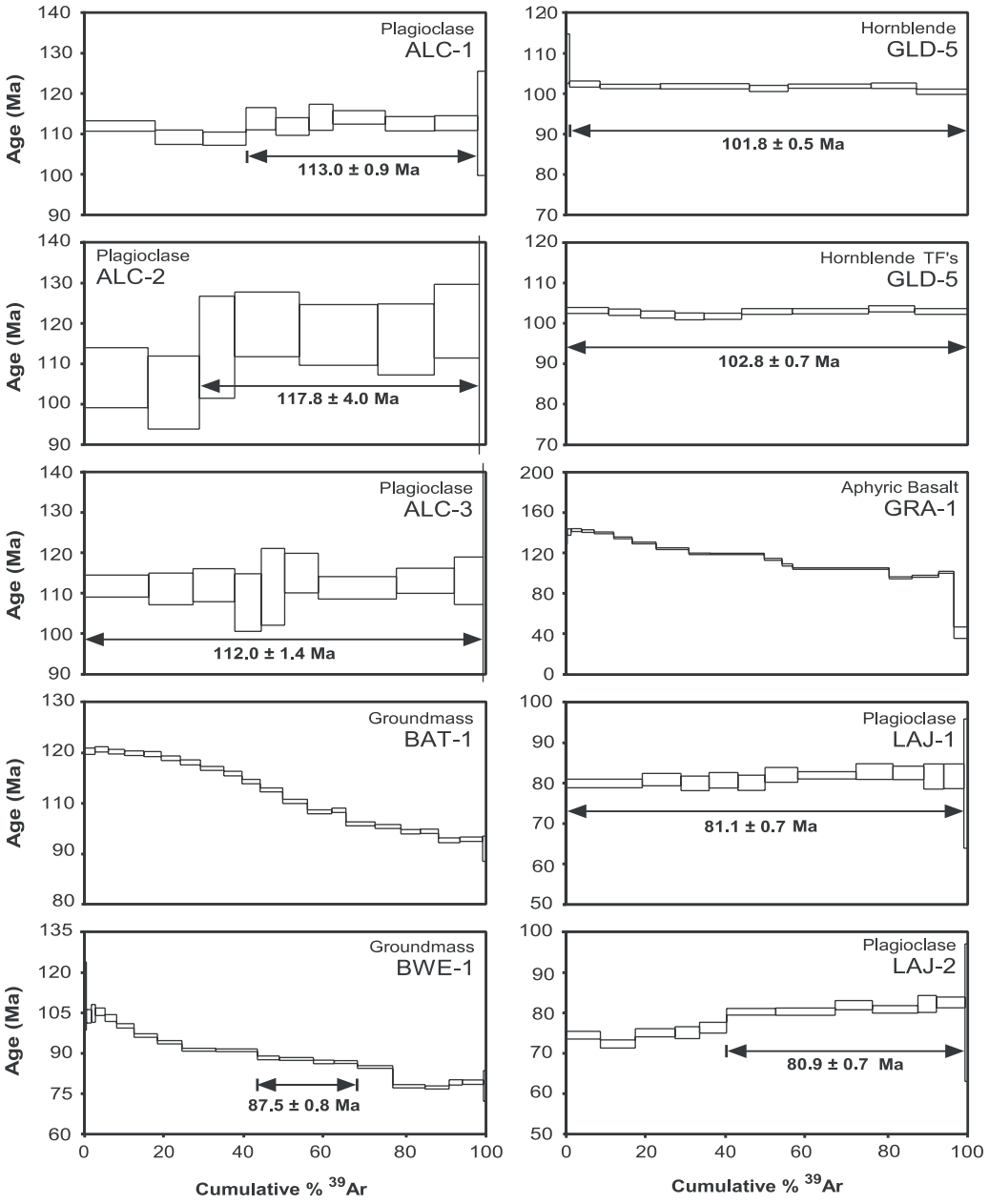

Figure 4. Incremental heating $^{40}Ar/^{39}Ar$ analyses for West Pacific Seamount Province basalts. Reported $^{40}Ar/^{39}Ar$ ages are weighted age estimates and errors on the 95% confidence level including 0.2–0.3% standard deviation in the J-value. All samples where monitored against Taylor Creek Rhyolite sanidine (27.92 Ma). Data are listed in Table 1.

search by Reference or Keywords from the http://earthref.org/databases/ERR/ web page.

3.1. $^{40}Ar/^{39}Ar$ Geochronology

[16] Incremental heating $^{40}Ar/^{39}Ar$ age determinations were performed on hornblende, plagioclase, groundmass K-feldspar and crystalline groundmass separates using an argon laserprobe combined with a MAP-215/50 mass spectrometer at the Vrije Universiteit Amsterdam [*Wijbrans et al.*, 1995]. Sample preparation, acid leaching and argon mass-spectrometry are described in *Koppers et al.* [2000]. All argon ages are normalized to the flux monitor standard Taylor Creek Rhyolite sanidine (age = 27.92 Ma). Incremental heating plateau ages and argon-isotope isochron ages were calculated as weighted means using $1/\sigma^2$ as weighting factor [*Taylor*, 1982] and as YORK2

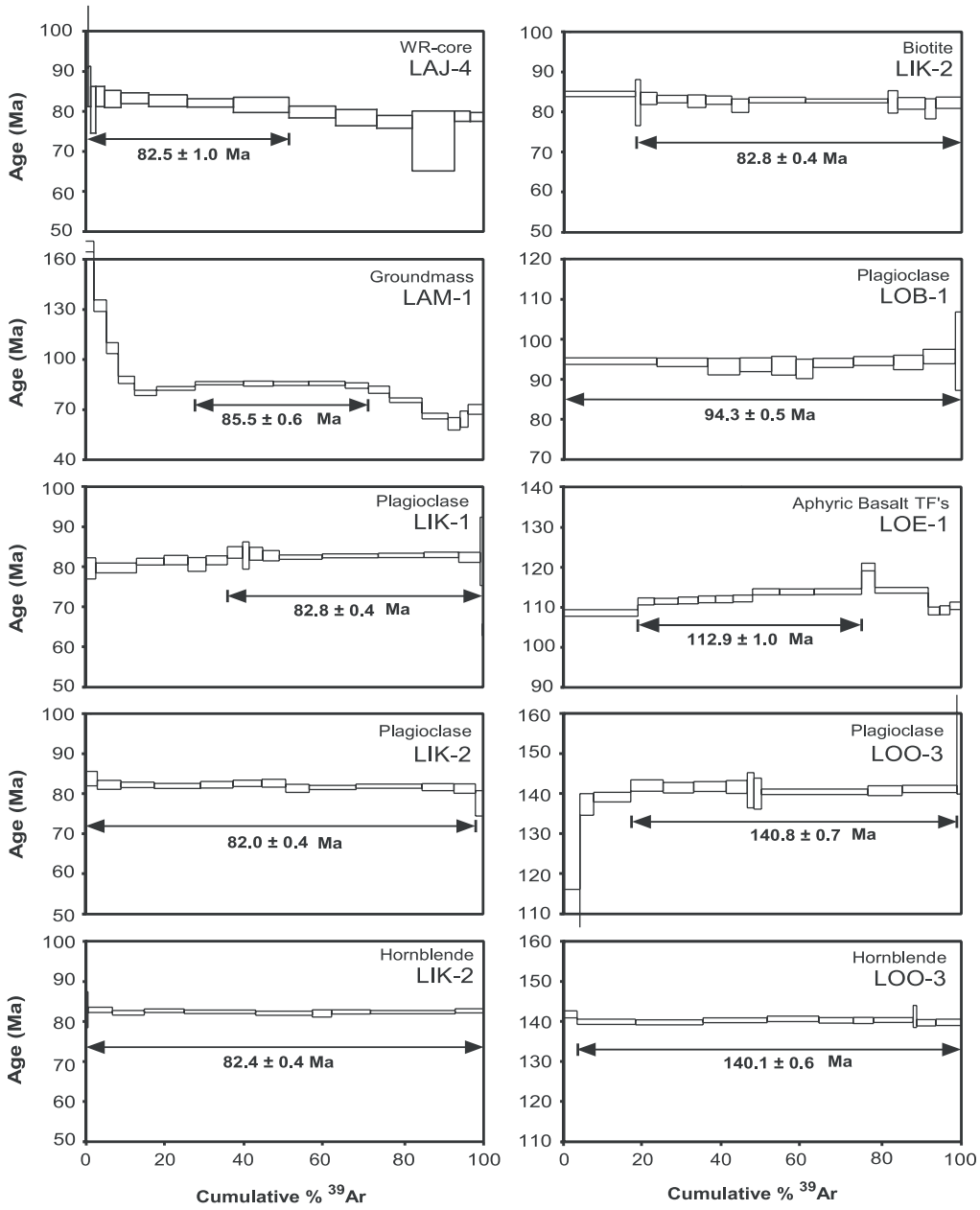

Figure 4. (continued)

least squares fits with correlated errors [*York*, 1969] using the ArArCALC v16 software [*Koppers*, 1998, 2002] (see also the http://earthref.org/tools/ararcalc.htm website). In this paper the errors on the $^{40}Ar/^{39}Ar$ ages are reported at the 95% confidence level; all other errors represent standard deviations.

[17] To determine whether an incremental heating experiment yields meaningful crystallization ages, we adopted quality criteria proposed by *Fleck et al.* [1977] and *Pringle* [1993] (1) high temperature plateaus in the age spectra should include more than three incremental heating steps and at least 50% of the total amount of $^{39}Ar_K$ released, (2) the plateau and isochron ages should be concordant at the 95% confidence level, (3) the $^{40}Ar/^{36}Ar$ intercepts on the isochron diagrams should be concordant with the atmospheric value of 295.5 at the 95% confidence level, and (4) the mean squared of weighted deviations [*York*, 1969; *Roddick*, 1978] for both the plateau ages (MSWD =

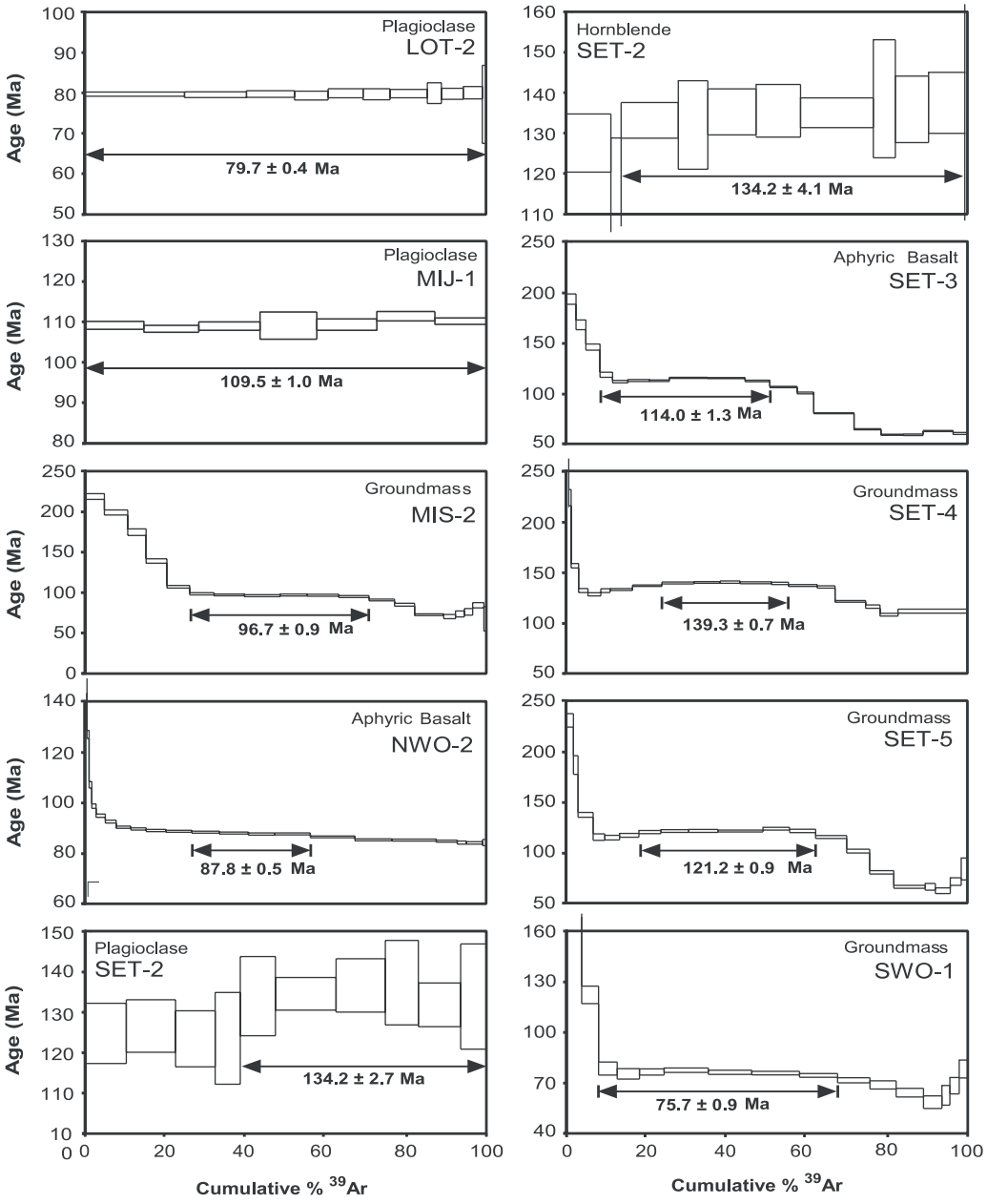

Figure 4. (continued)

SUMS/N-1) and isochron ages (MSWD = SUMS/N-2) should be sufficiently small compared to F-statistic critical values for significance. Although these criteria are well suited for evaluation of $^{40}Ar/^{39}Ar$ results from unaltered whole rock samples and mineral separates, they are not necessarily suitable for the evaluation of altered basaltic groundmass separates [*Koppers et al.*, 2000]. For a more detailed discussion on $^{40}Ar/^{39}Ar$ dating of altered groundmass samples we refer to Appendix A. Remaining excess argon due to incomplete degassing of the submarine basalts under hydrostatic pressure [*Dalrymple and Moore*, 1968] is likely not a problem in this study [*Koppers et al.*, 1998, 2000]. First, the studied rocks crystallized in water less than 1400 m deep or subaerially [*Schlanger et al.*, 1987; *Winterer et al.*, 1993; *Larson et al.*, 1995]. Second, most samples are abundantly vesiculated, which indicates that outgassing occurred upon eruption. And, finally, the samples do not contain significant amounts of (altered) glass and/or olivine, which are potential

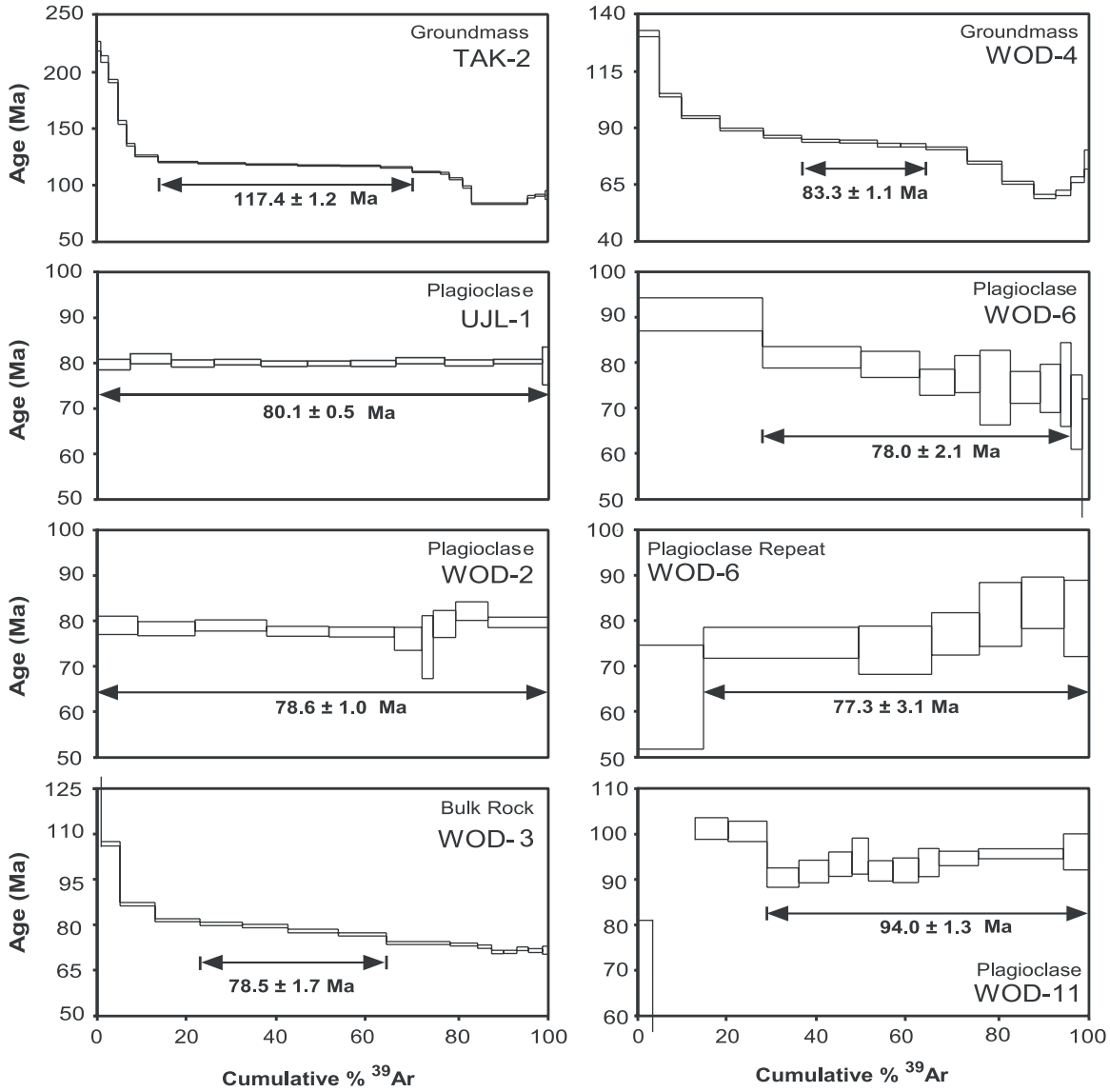

Figure 4. (continued)

sources of remaining excess argon in submarine basalts [*Dalrymple and Moore*, 1968; *Seidemann*, 1977, 1978]. As a result, we may use an atmospheric $^{40}Ar/^{36}Ar$ value of 295.5 for the calculation of the $^{40}Ar/^{39}Ar$ plateau ages, as is confirmed in the $^{40}Ar/^{36}Ar$ intercepts calculated from the isochrons.

3.2. Sr-Nd-Pb Isotope Geochemistry

[18] Sr-Nd-Pb isotope composition and dilution analyses were performed on whole rock powders and clinopyroxene, plagioclase, nepheline and hornblende separates. For two samples of Vlinder Guyot we analyzed the K-feldspar separated from the groundmass. Minerals separates were acid leached following the recipe for $^{40}Ar/^{39}Ar$ dating [*Koppers et al.*, 2000] but they were additionally treated by etching in 7% HF for 10 min. We removed the effects of seawater alteration on the whole rock samples using an acid leaching procedure that evolved from the procedure used by *Shimizu and Hart* [1973]. Leached whole rock powders were prepared by leaching of 6–25 gram of sample in an ultrasonic bath with (1) 250 mL ultra-pure 1 N HCl for 1 hour, (2) 250 mL 7 N HCl

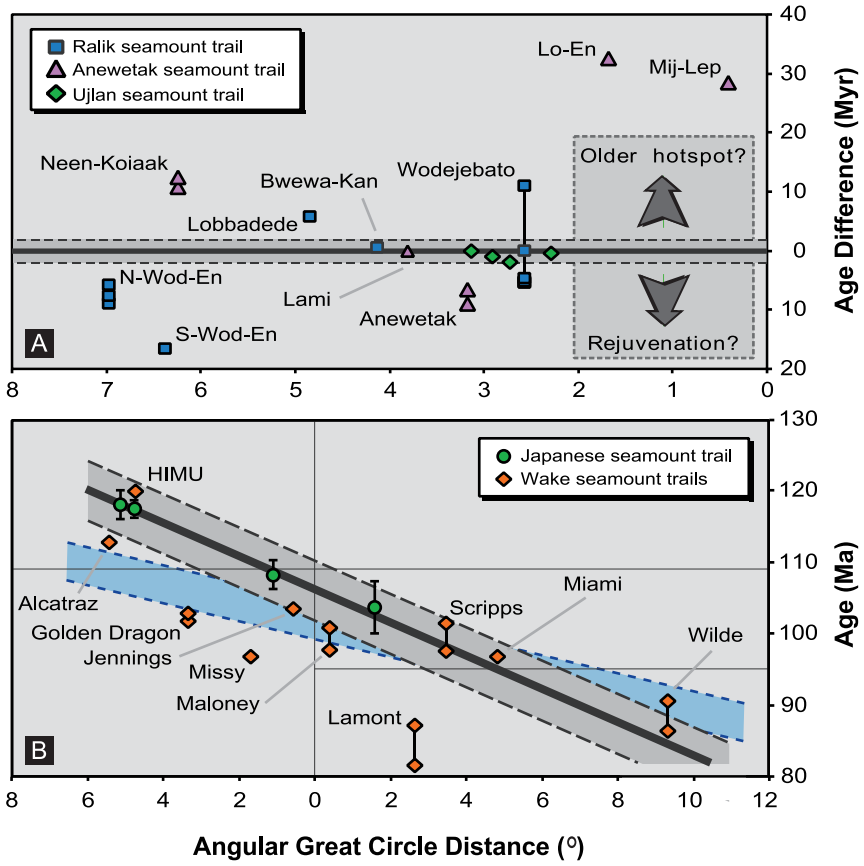

Figure 5. Age distributions and progressions in the West Pacific Seamount Province. (a) Age differences in the Ujlan, Anewetak, Ralik and Ratak seamount trails with respect to the 47.6 mm/yr age progression (horizontal zero line) for the Magellan seamount trail [*Koppers et al.*, 1998]. (b) Age progressions in the Northern and Southern Wake seamount trails with respect to the 48.1 mm/yr age progression (thick gray line) observed in the Japanese seamount trail. An alternative age progression line of 83.1 mm/yr (light blue area) is defined by Alcatraz and Scripps in the Northern Wake seamount trail. The angular great circle distances have been calculated relative to the minor bend in the Wake seamount trails at 22°58′N–155°44′E and 21°06′N–156°43′E, respectively.

for 2–8 hours, and optionally (3) 250 mL 7% HF for 10 min. Every 15 min the rock fraction was stirred; every 60 min the acids were refreshed. The temperature of the acid solutions was set between 35–60°C. Before dissolution, residues were washed 5 times in ultra-pure water, dried at a hot plate and checked microscopically for the presence of remaining secondary phases. Preparation of the samples, standard liquid chromatography and measurement of radiogenic Sr-Nd-Pb isotope compositions and Rb-Sr-Sm-Nd-U-Pb isotope dilution were all performed at the Vrije Universiteit Amsterdam using Finigan MAT-261 (fixed) and MAT-262 (moveable) multicollector systems. Rb-Sr, Sm-Nd and U-Th-Pb abundances were alternatively analyzed using XRF (Vrije Universiteit Amsterdam), INAA and ICP-MS (Activation Laboratories Ltd. in Canada).

3.3. Removal of Hydrothermal and Seawater Alteration

[19] Hydrothermal and seawater alteration may cause significant shifts in Sr- and Pb-isotopic signatures of submarine basaltic rocks. Another concern is the shift in parent-daughter ratios due to low temperature seawater alteration, introducing Rb and U [*Corliss*, 1970; *Hart*, 1969] which adds uncertainty to the radioactive ingrowth corrections for the studied Cretaceous seamount basalts. Acid leaching of whole rock powders (<125 μm) normally removes the anomalous isotopic signatures by the preferential dissolution of secondary alter-

ation phases [*Shimizu and Hart*, 1973; *Cheng et al.*, 1987; *Staudigel et al.*, 1991; *Pringle*, 1992; *Castillo et al.*, 1992; *Koppers et al.*, 1995]. Acid leaching also preferentially removes Rb-Sm-Nd-U-Th-Pb from basalts, whereas Sr is increased in basalts containing abundant plagioclase minerals [*Cheng et al.*, 1987]. Similar chemical depletions and enrichments are evident in our own leaching experiments, as reported in Appendix B. We find that measured parent-daughter ratios reflect the proportion of plagioclase and clinopyroxene in the residues, and not that of altered basaltic groundmass, which preferentially dissolves during leaching. This allows us to perform radiogenic ingrowth corrections in these acid-leached basalts with reasonable confidence, in particular, since the measured parent-daughter ratios are low ($^{87}Rb/^{86}Sr < 0.14$; $^{147}Sm/^{144}Nd < 0.14$; $^{238}U/^{204}Pb < 2.9$; $^{232}Th/^{204}Pb < 23$) reflecting typically low plagioclase and clinopyroxene values.

4. $^{40}Ar/^{39}Ar$ Geochronology and Age Progressions

[20] We have grouped the WPSP seamount trails according to region, age and azimuth (see colored lines in Figure 3a). The first group is located in the south of the WPSP and includes the Magellan, Ujlan, Anewetak, Ralik and Ratak seamount trails that have NW trends and range in age between 70–100 Ma (green; Figures 3d and 3e). The second and third groups are located in the north of the WPSP and include the EW trending Northern Wake, Southern Wake and Japanese seamount trails that range in age between 100–120 Ma (red; Figures 3b and 3c) and the NNE trending Typhoon group that is older than 120 Ma (blue; Figure 3c). All other seamounts, that are not uniquely associated with a particular seamount trail, are considered solitary seamounts. New incremental heating $^{40}Ar/^{39}Ar$ ages for these nine seamount trails were determined on groundmass separates, mineral separates (plagioclase, hornblende, biotite) and bulk-rock grain samples. These results are plotted as age plateau diagrams in Figure 4. In this section, we review these new age results together with all previously published $^{40}Ar/^{39}Ar$ ages for the WPSP as compiled in Table 1 and in the annotated bathymetric maps of Figure 3. Conventional K-Ar ages have been omitted from this compilation since these ages may be inaccurate due to pervasive seawater alteration [cf. *Koppers et al.*, 2000]. We will discuss the available $^{40}Ar/^{39}Ar$ geochronological evidence in terms of analytical (and geological) uncertainties and in terms of age progressions alongside these seamount trails.

4.1. The Magellan, Ujlan, Anewetak, Ralik, and Ratak Seamount Trails

[21] The Magellan seamounts and the Marshall Islands comprise five potential trails ranging in age between 70–100 Ma (Figures 3a, 3d, and 3e). All of them are short due to intermittent volcanic activity. Only one of them displays a linear age progression consistent with a singular hot spot origin, namely the Magellan seamount trail [*Koppers et al.*, 1998]. On the basis of new bathymetric data [*Smith and Sandwell*, 1996, 1997] we can now distinguish between these five different seamount trails that are only spaced 230–280 km apart and that have distinct isotopic signatures (see section 5.1).

4.1.1. Magellan Seamount Trail

[22] The Magellan seamount trail (MST; Figure 3d) includes three seamounts (Vlinder, Pako and Ioah) extending over Cretaceous seafloor that also includes some volcanic edifices that are notably older (Vlinder and Ita-Mai-Tai). The recombined $^{40}Ar/^{39}Ar$ age results of Vlinder (95.1 ± 0.5 Ma, $n = 5$), Pako (91.5 ± 0.3 Ma, $n = 2$) and Ioah (87.1 ± 0.3 Ma, $n = 2$) yield a well-constrained age progression at 47.6 ± 1.6 mm/yr for the MST [*Koppers et al.*, 1998]. Nonetheless, Vlinder guyot was build on top of an older volcano (102.4 ± 0.5 Ma; 101.6 ± 0.6 Ma; 100.2 ± 0.4 Ma) that still defines its western and northwestern deeper portion. Vlinder also features post-erosional volcanism occurring at least 20–30 Myr after drowning and erosion (based on subsidence models). In addition, Ita-Mai-Tai guyot (118.1 ± 0.5 Ma, $n = 3$) was formed 34–36 Myr before the MST hot spot arrived at the predicted location of this southern-most guyot in the MST. The latter volcanic stage is confirmed by Late-

Aptian hyaloclastite-rich turbidite flows as encountered on the apron of Ita-Mai-Tai guyot at DSDP Site 585 [*Wedgeworth and Kellogg*, 1987]. These deviations from a linear age progression indicate magma sources other than the Magellan hot spot to produce the older pedestal underneath Vlinder, the post-erosional volcano on top of Vlinder and the volcanic shield of Ita-Mai-Tai [*Koppers et al.*, 1998].

4.1.2. Ujlan Seamount Trail

[23] The Ujlan seamount trail is a short (~570 km) alignment that is located at the western site of the Ujlan-Anewetak cluster in the Marshall Islands (Figure 3d) (J. R. Hein et al., Geological, geochemical, geophysical and oceanographic data and interpretations of seamounts and Co-rich ferromanganese crusts from the Marshall Islands, KORDI-USGS R. V. *Farnella* cruise F10-89-CP, unpublished report, 1990). There are four dated features within a 100 km section of this trail, including Likelep (82.5 ± 0.2 Ma, n = 5), Lajutokwa (81.2 ± 0.5 Ma, n = 3), Lotab (79.7 ± 0.4 Ma) and Ujlan (80.1 ± 0.5 Ma). These average ages cluster in a narrow period with slightly older ages in its NW part. This distribution of ages is consistent with the local plate velocity derived from neighboring MST trail (Figure 5a). The average age of Likelep guyot includes ages on plagioclase, hornblende and biotite mineral separates of sample LIK-2 (82.0 ± 0.4 Ma; 82.4 ± 0.4 Ma; 82.8 ± 0.4 Ma), plagioclase sample LIK-1 (82.8 ± 0.4 Ma) and bulk-rock sample F1089CP 19–18 (82.4 ± 0.8 Ma); the combined age of Lajutokwa guyot includes plagioclase samples LAJ-1 (81.1 ± 0.7 Ma) and LAJ-2 (80.9 ± 0.7 Ma). All mineral separate analyses have concordant plateau, isochron and total fusion ages, their age plateaus represent between 60–100% of the total amount of $^{39}Ar_K$ released in 7–12 contiguous increments, and their trapped argon signatures are similar to atmospheric values. The concordant plagioclase, hornblende and biotite ages of LIK-2 also demonstrate the effective minimization of alteration in these mineral separates due to the applied acid leaching procedures. These $^{40}Ar/^{39}Ar$ ages agree with the Early Campanian foraminiferal ages of Likelep's carbonate cover [J. R. Hein et al., unpublished report, 1990; *Lincoln et al.*, 1993].

4.1.3. Anewetak Seamount Trail

[24] The Anewetak seamount trail (~860 km) includes the eastern site of the Ujlan-Anewetak cluster in the Marshall Islands (J. R. Hein et al., unpublished report, 1990) and is volumetrically more prominent than the Ujlan seamount trail (Figure 3d). This trail displays a very complex distribution of ages that is (largely) incompatible with the age progression at the MST (Figure 5a). For example, Neen-Koiaak (102.3 ± 0.3 Ma, n = 3), Lo-En (113.0 ± 0.9 Ma, n = 3) and Mij-Lep (106.0 ± 1.9 Ma, n = 1) display Early-Cretaceous ages inconsistent with the expected 100–80 Ma age range for the Anewetak seamount trail based on absolute Pacific plate motion models. The apparent anomalously old age for Lo-En guyot is confirmed by the presence of an Albian-age nanoflora in phosphatized clasts of pelagic limestone sampled at ODP Site 872 [*Watkins et al.*, 1995] and F1089CP dredge site D-33 [*Lincoln et al.*, 1993]. In this seamount trail only the ages of Anewetak atoll (77.5 ± 0.8 Ma, n = 4; 75.0 ± 0.8 Ma, n = 2) and Lami seamount (85.5 ± 0.6 Ma) fall within the 100–80 Ma stage pole for the Pacific plate. Despite the wide spread in the observed ages for the Anewetak seamount trail the quality of the $^{40}Ar/^{39}Ar$ age data is good. First, we note the age concordance of plagioclase samples NEK-1 (103.0 ± 0.7 Ma) and NEK-2 (102.5 ± 0.9 Ma), aphyric basalt sample LOE-1 (114.9 ± 2.2 Ma; 112.9 ± 1.0 Ma) and bulk-rock sample ODP-144 872C 18X1 88–93 (110.9 ± 2.8 Ma), and bulk-rock samples E-1-4-3A (77.1 ± 1.2 Ma; 77.8 ± 1.0 Ma) and E-1-5-6A (75.3 ± 1.2 Ma; 74.8 ± 1.0 Ma). Second, we note that plagioclase sample MIJ-1 and groundmass sample LAM-1 exhibit concordant plateau, isochron and total fusion ages, despite the fact that their age plateaus cover only 43–44% of the total amount of $^{39}Ar_K$ released.

4.1.4. Ralik Seamount Trail

[25] This seamount trail (~1,550 km) is located at the west side of the Marshall Islands (Figure 3e) [*Davis et al.*, 1989; *Lincoln et al.*, 1993] and

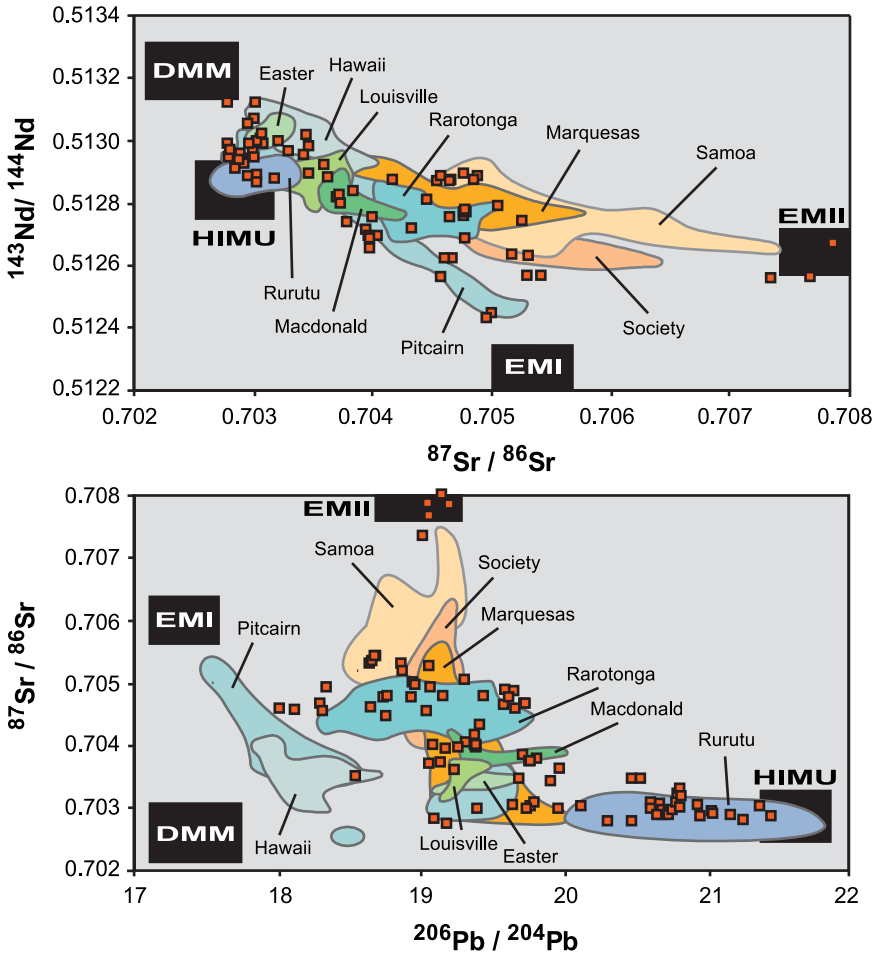

Figure 6. Radiogenic isotope correlation diagrams comparing ocean-island basalts for the Cenozoic and Mesozoic Pacific. To calculate equivalents to present-day mantle compositions, we applied a radiogenic ingrowth model for the Mesozoic mantle source (inferred from the WPSP basalts) using the best estimates of the initial ratios (Table 2), an average primordial mantle source with Rb/Sr = 0.030, Sm/Nd = 0.325 and U/Pb = 0.296 [*McDonough et al.*, 1992] and the $^{40}Ar/^{39}Ar$ ages of this study (Table 1). The composition of the mantle end-members DMM, HIMU, EMI and EMII are after *Zindler and Hart* [1986] and *Woodhead and Devey* [1993]. The SOPITA reference fields are denoted by light-colored areas [*McDonough and Chauvel*, 1991; *Staudigel et al.*, 1991; *Chauvel et al.*, 1992; *Farley et al.*, 1992; *Dupuy et al.*, 1993; *Hauri and Hart*, 1993; *Hauri et al.*, 1993; *Woodhead and Devey*, 1993; *Woodhead et al.*, 1993]; the WPSP basalts are denoted by red squares.

displays a very complex distribution of ages. Only the ages of Bwewa-Kan seamount (87.5 ± 0.8 Ma) and the oldest ages of the shield-building stage of Wodejebato guyot (ODP Site 877: 83.3 ± 1.1 Ma; Site 873: 81.9 ± 0.5 Ma, n = 3) may be compatible with the age progression at the MST (Figure 5a). North-Wod-En guyot (87.8 ± 0.5 Ma; 86.1 ± 0.7 Ma, n = 2; 85.4 ± 1.0 Ma) and South-Wod-En guyot (75.7 ± 0.9 Ma) most likely are too young, whereas Lobbadede guyot (94.3 ± 0.5 Ma) is too old to belong to the same hot spot trail. The older age of Lobbadede is confirmed by its pre-Cenomanian fossil ages as well as by the Albian fossil ages at Lewa guyot [*Lincoln et al.*, 1993] that is located just north of Lobbadede (Figure 3e). Ages from multiple sample sites at Wodejebato guyot demonstrate that shield-building volcanism continued for at least 4 Myr at the main summit (Site 877: 83.3 ± 1.1 Ma; Site 873: 81.9 ± 0.5 Ma, n = 3; Site 874: 78.6 ± 1.0 Ma; Site 876: 78.5 ± 1.4 Ma, n = 2) and at a satellite volcano on its NE rift (77.4 ± 1.8 Ma, n = 2). Moreover, volcaniclastic flows drilled at ODP apron Site 869 have been identified as an older volcanic phase (96.0 ± 0.6 Ma; 94.3 ± 0.4 Ma, n = 3; 91.8 ± 0.6 Ma) for Wodejebato guyot. This latter phase is also supported by the presence of

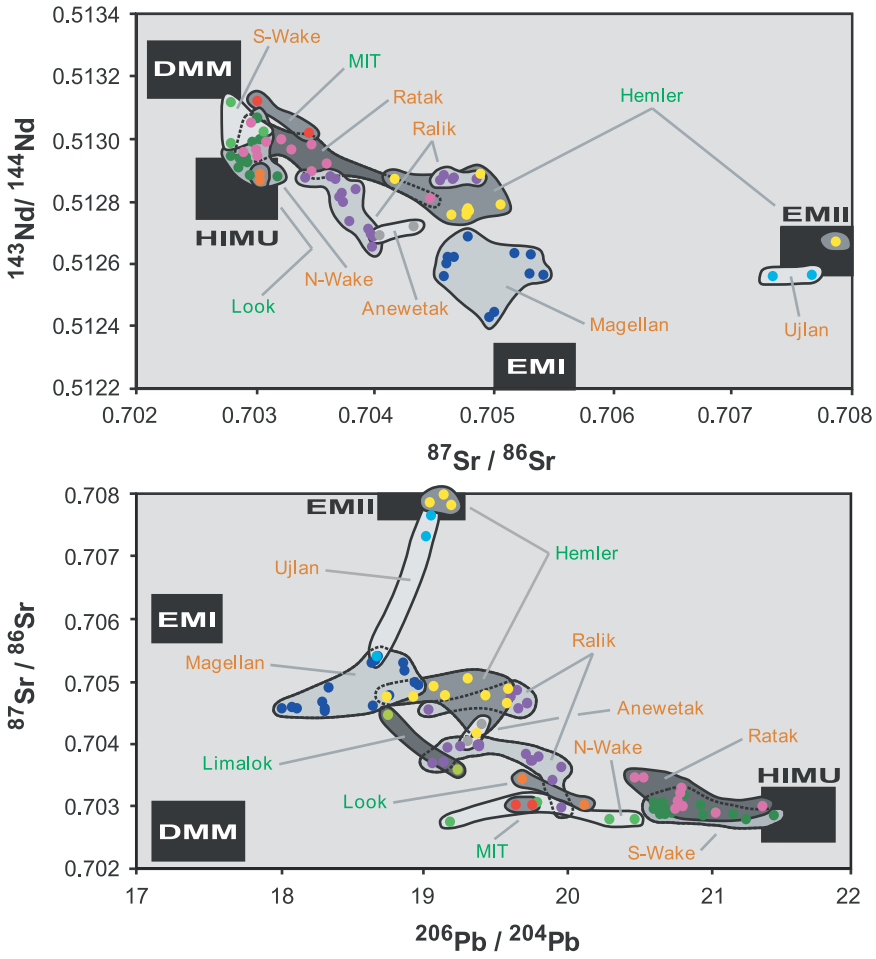

Figure 7. Radiogenic isotope correlation diagrams for ocean-island basalts of the WPSP organized according to the nine-studied seamount trails. See Figure 6 for references and applied ingrowth corrections.

Albian fossils at the south flank of Wodejebato [*Lincoln et al.*, 1993]. The quality of the plagioclase $^{40}Ar/^{39}Ar$ analyses meets the adopted quality criteria. However, the ages from the groundmass analyses BWE-1, WOD-3 and WOD-4 are less well defined; they yield narrow (28–41%) and slightly sloping age plateaus (Figure 4). Because all three groundmass plateau ages have similar total fusion ages, these analyses are considered fair estimates of their crystallization ages.

4.1.5. Ratak Seamount Trail

[26] The Ratak seamount trail is the most prominent and longest seamount trail (~1,650 km) in the Marshall Islands, although its continuation to the north of Ratak guyot is unclear (Figure 3e). Yet, only three guyots have been dated by $^{40}Ar/^{39}Ar$ geochronology: Ratak (85.3 ± 1.4 Ma, $n = 2$; 81.4 ± 0.7 Ma, $n = 2$), Erikub (87.1 ± 0.5 Ma, $n = 5$) and Limalok (68.2 ± 0.5 Ma, $n = 2$). The reproducibility of these bulk-rock and groundmass analyses implies that the plateau ages are reliable estimates of their crystallization ages. The possibility of an age progression in the Ratak seamount trail is inconsistent with the fact that the older Erikub guyot lies south of Ratak guyot (Figure 3e) [*Davis et al.*, 1989].

4.2. Japanese, Northern Wake, and Southern Wake Seamount Trails

[27] The Japanese and Wake seamounts comprise potential hot spot trails ranging between 100–120 Ma in age (Figures 3a, 3b, and 3c). These seamount trails display a minor change in azimuth from WNW to ENE, which is particularly evident from the Northern and Southern Wake seamount trails. Of these seamount trails only the Japanese

seamount trail (JST) exhibits an age progression consistent with a singular hot spot origin [*Winterer et al.*, 1993].

4.2.1. Japanese Seamount Trail

[28] The $^{40}Ar/^{39}Ar$ ages for Takuyo-Daini (118.1 ± 2.0 Ma), Takuyo-Daisan (117.5 ± 1.1 Ma, n = 2), Winterer (108.3 ± 2.0 Ma) and Isakov (103.7 ± 3.6 Ma) yield an age progression at 48.1 ± 4.5 mm/yr (r^2 = 0.994; MSWD = 0.34) for the JST (Figures 3b and 5b). This age progression is particularly evident because the JST delineates small-sized guyots that most likely are produced from monogenetic volcanic events, comparable to the seamounts of the well-defined Musicians [*Pringle*, 1993; *Koppers et al.*, 1998] and Foundation [*O'Connor et al.*, 1998] seamount trails. Additional evidence that reflects a single hot spot origin comes from the fact that no other seamount trail crosses the JST (Figure 3b) and that the thermal rejuvenation of the JST lithosphere is minimal [*Larson et al.*, 1995]. Despite large errors on the (unleached) bulk-rock analyses, we may consider these crystallization ages for the following reasons: (1) most samples are alkali-rich basalts, (2) the $^{40}Ar/^{39}Ar$ ages for acid-leached groundmass sample TAK-2 (117.4 ± 1.2 Ma) and unleached bulk-rock sample A5-37-3 (118.4 ± 3.6 Ma) are within error at the 95% confidence level, and (3) the radiometric ages agree with the late Aptian to early Albian palaeontological ages [*Winterer et al.*, 1993; *Premoli Silva et al.*, 1993].

4.2.2. Wake Seamount Trails

[29] The Northern Wake (~920 km) and Southern Wake (~980 km) seamount trails have parallel azimuths and a minor bend at 22°58′N–155°44′E and 21°06′N–156°43′E, respectively (Figure 3c). Their Sr-Nd-Pb isotopic signatures (see next Section) can be used to further distinguish between these trails since the Southern Wake seamount trail features HIMU-type signatures as opposed to more EM-type signatures for the Northern trail. The Northern Wake seamount trail was sampled only at Alcatraz (112.7 ± 0.8 Ma, n = 2; 117.8 ± 4.0 Ma) and Scripps (101.4 ± 1.4 Ma, n = 2); whereas the Southern Wake seamount trail was sampled at HIMU (119.9 ± 0.8 Ma, n = 3), Golden Dragon (102.1 ± 0.4 Ma, n = 2), Missy (96.7 ± 0.9 Ma), Jennings (103.4 ± 0.4 Ma, n = 2), Maloney (100.7 ± 0.6 Ma, n = 2; 97.7 ± 0.6 Ma), Lamont (87.2 ± 0.6 Ma; 81.6 ± 1.2 Ma, n = 2) and Miami (96.8 ± 1.2 Ma). Wilde guyot (90.6 ± 0.6 Ma; 86.4 ± 3.8 Ma) is not readily assigned to either one of these seamount trails (Figure 3c). In Figure 5b we plotted the age progressions along the Wake seamount trails with reference to their minor bends (origin positions). When assuming local plate velocities similar to that of the JST (48.1 mm/yr) we can reconcile only the old age of HIMU seamount with the ages of Scripps and Miami guyots; all other seamounts would be up to 16–20 Myr younger than the passage of both Wake hot spots. When assuming an age progression defined by Alcatraz and Scripps in the Northern Wake seamount trail (88.3 mm/yr) we can also include Jennings, Maloney and Miami guyots. In this case, however, HIMU seamount would be ~13 Myr too old, whereas other guyots may be up to 7 Myr too young. Unfortunately, these scenarios are not testable because the dated nephelinitic samples of Miami, Lamont and Scripps guyot are plausibly post-erosional summit eruptives [*Winterer et al.*, 1993] as reflected in the young age dates for Lamont guyot (81–87 Ma). In the discussion we will propose an alternative model that is consistent with the random distribution of ages in the Southern Wake seamount trail.

4.3. Typhoon Seamount Trail

[30] The Typhoon seamount trail (~260 km) is distinguished from the other WPSP seamount trails on basis of its NNE azimuth and older $^{40}Ar/^{39}Ar$ mineral ages of 134.2 ± 2.3 Ma (n = 2) for Seth guyot (Figure 3c). This seamount trail represents the oldest trace of absolute Pacific plate motion yet found. Groundmass samples SET-3, SET-4 and SET-5 yield horizontal age plateaus including 32–44% of the total amount of $^{39}Ar_K$ released in 5–6 contiguous increments. However, their ages exhibit an extended age range of ~25 Myr (SET-3 = 114.0 ± 1.3 Ma; SET-4 = 139.3 ± 0.7 Ma; SET-5 = 121.2 ± 0.9 Ma) as opposed to concordant plagioclase and horn-

blende ages (134.2 ± 2.7 Ma; 134.2 ± 4.1 Ma) for SET-2. They further exhibit significantly discordant plateau and total fusion ages, and extremely low molar K/Ca ratios (0.06–0.14). Together these observations suggest that most of their primary argon signature has been lost from these groundmasses due to alteration [*Koppers et al.*, 2000]. The ~25 Myr age range also appears incompatible with the relatively small volume of this guyot, which rather implies a short-lived volcanic history. Nevertheless, the well-defined $^{40}Ar/^{39}Ar$ mineral ages of SET-2 clearly indicate that volcanism started at least 134 Myr ago at Seth guyot.

4.4. Solitary Seamounts

[31] Solitary seamounts are defined as those volcanic edifices that morphologically cannot be associated with any of the nine studied WPSP seamount trails. Makarov guyot (Figure 3b) has been dated at 93.9 ± 2.6 Ma using the normal isochron method on an unleached bulk-rock sample [*Ozima et al.*, 1977]. The quality of this analysis, however, cannot be tested because no other $^{40}Ar/^{39}Ar$ analyses were performed for this guyot and because no plateau or total fusion ages were reported. ODP Site 878 was drilled on MIT guyot (Figure 3c) revealing three volcanic units: (1) a lower series of alkali basalts, (2) a middle series of basanites, and (3) an upper series of hawaiites [*Christie et al.*, 1995]. Basalts of the lower series yield an age of 123.3 ± 0.5 Ma (n = 5), whereas basalts of the middle and upper series yield a combined age of 120.1 ± 0.9 Ma (n = 4). These ages correspond perfectly to the stratigraphic relations at this drill site [*Erba et al.*, 1995] and the upper boundary of the reversed polarity Chron M1R as sampled in the upper series [*Pringle and Duncan*, 1995b]. Hemler guyot (Figure 3c) is located at the eastern end of the Dutton ridge [cf. *Smoot*, 1983]. Two total fusion experiments on nepheline (99.5 ± 1.2 Ma) and hornblende (100.7 ± 1.2 Ma) yield concordant ages resulting in an recombined age of 100.1 ± 0.8 Ma (n = 2). Look seamount (Figure 3e) is located between the Ralik and Ratak seamount trails [cf. *Lincoln et al.*, 1993] and is characterized by an exceptionally old age (140.4 ± 0.5 Ma, n = 2; 140.0 ± 1.6 Ma; 138.4 ± 1.0 Ma, n = 2). This age is exceptional considering the fact that all volcanism in the seamount trails of the Marshall Islands ranges in age between 69–113 Ma (see above). The quality of the $^{40}Ar/^{39}Ar$ analyses, nonetheless, meets the adopted quality criteria. Each incremental heating experiment yielded concordant plateau, isochron and total fusion ages that included at least 82% of the total amount of $^{39}Ar_K$ as released in more than 9 contiguous increments. The $^{40}Ar/^{36}Ar$ intercept values are indistinguishable from the atmospheric value.

5. Sr-Nd-Pb Geochemistry

[32] The Sr-Nd-Pb isotopic ratios measured for the WPSP basalts are listed in Table 2 and illustrated in Nd-Sr and Sr-Pb isotope correlation diagrams (Figures 6 and 7). In these diagrams we compare the Cretaceous WPSP data to the inferred mantle components after *Zindler and Hart* [1986] and the reference fields of SOPITA hot spot volcanism. It is evident that on a regional scale the isotopic fields of the WPSP and SOPITA are similar in diversity and the types of mantle end-members involved (Figure 6). For example, the WPSP basalts may cluster at extreme values close to the HIMU and EMII mantle components [*Davis et al.*, 1989; *Smith et al.*, 1989; *Staudigel et al.*, 1991; *Koppers et al.*, 1995] or they show evidence for the admixture of the EMI mantle component [*Koppers et al.*, 1998]. More importantly, each seamount trail reflects a distinct mantle source composition, as opposed to the extreme mantle source heterogeneity at the scale of the entire WPSP region (Figure 7). Such a unique isotopic discrimination allows for the geochemical mapping of Cretaceous hot spot volcanism in the WPSP through geological time. In the following we will discuss each seamount trail for its distinct mantle source composition, while drawing comparisons to the currently active intraplate volcanoes in the SOPITA region. We will limit this discussion to only highlight the most common or most prominent mantle components in each seamount trail that are required to

perform a basic geochemical mapping of the WPSP through time.

5.1. Magellan, Ujlan, Anewetak, Ralik, and Ratak Seamount Trails

[33] The seamount trails in the Marshall Islands and Magellan Seamounts cover almost the entire range of isotopic compositions in the SOPITA data arrays (Figure 7). First, basalts of the Ratak seamount trail are confined to extreme HIMU signatures with $^{206}Pb/^{204}Pb$ ratios that are generally higher than 20.6. Second, the Ujlan seamount trail has $^{87}Sr/^{86}Sr$ higher than 0.705 indicative of EMII signatures. Third, the Anewetak and Ralik seamount trails display isotopic compositions intermediate to these HIMU-EMII signatures. And, finally, the Magellan seamount trail (MST) shows evidence for a contribution from the EMI mantle component [*Koppers et al.*, 1998]. These are interesting observations, because all five seamount trails were formed within the 100–80 Ma period of Pacific plate motion and because they run sub-parallel within an area less than 1,000 km wide (Figures 3d and 3e). This puts strong constraints on the chemical geodynamics of the South Pacific mantle, as we will discuss later in this paper.

5.1.1. Magellan Seamount Trail

[34] Isotopic signatures of Vlinder, Pako, Ioah and Ita-Mai-Tai guyot point to the EMI mantle component. This is most evident since they have the lowest $^{206}Pb/^{204}Pb$ and $^{143}Nd/^{144}Nd$ ratios measured in the WPSP and, therefore, the MST most closely resembles the currently active Rarotonga hot spot in the SOPITA based on its isotope geochemistry [*Koppers et al.*, 1998].

5.1.2. Ujlan Seamount Trail

[35] Three samples have been analyzed from the Ujlan seamount trail (LIK-2, LOT-1 and LOT-2) showing an EMII signature comparable to the currently active Samoa hot spot in the SOPITA. Most illustrative of this signature are the extremely high $^{87}Sr/^{86}Sr$ ratios above 0.707 at low $^{143}Nd/^{144}Nd$ ratios. The good internal consistency of two leached whole rock (LOT-1, LOT-2) and one clinopyroxene (LOT-1) analyses for Lotab guyot demonstrates that seawater alteration was insignificant for these samples.

5.1.3. Anewetak Seamount Trail

[36] In this seamount trail only the anomalously older (>100 Ma) Lo-En and Neen-Koiaak guyots (see above) have been investigated for their Sr-Nd-Pb isotopic signatures. Two acid-leached whole rock samples from ODP Site 872 at the summit of Lo-En yield comparable isotopic signatures falling intermediate to the EMII-HIMU mixing line. These results are similar to the $^{87}Sr/^{86}Sr$ ratio (0.703694) measured from a plagioclase separate of the NEK-2 sample. Both Lo-En and Neen-Koiaak have significantly lower $^{87}Sr/^{86}Sr$ ratios than their neighboring Ujlan seamount trail, while having higher $^{143}Nd/^{144}Nd$ ratios between 0.5127–0.5128. For this reason, they most likely resemble the currently active Macdonald (or Rarotonga) hot spot in the SOPITA.

5.1.4. Ralik Seamount Trail

[37] Wodejebato guyot displays a large variation in the Sr-Nd-Pb isotopic systematics (Figure 7) and is comparable to the high $^{87}Sr/^{86}Sr$ fields of the Macdonald, Rarotonga and Society hot spots. Lavas forming the volcanic shield at Wodejebato (ODP Sites 873–877) have $^{87}Sr/^{86}Sr > 0.704$ as opposed to lower $^{87}Sr/^{86}Sr$ ratios for the NE-satellite volcano and the ODP apron Site 869 [*Koppers et al.*, 1995; *Janney et al.*, 1995]. Volcaniclastic materials at Site 869 are comparable in isotopic composition [*Janney et al.*., 1995] and $^{40}Ar/^{39}Ar$ age (~94 Ma) with Lobbadede guyot (Figure 3e). The signatures for North- and South-Wod-En guyot have slightly higher Pb-isotopic signatures at even lower $^{87}Sr/^{86}Sr$ ratios, as confirmed by independent clinopyroxene and plagioclase analyses. This may indicate some affinity with the currently active Rurutu hot spot in the Cook-Austral Islands.

5.1.5. Ratak Seamount Trail

[38] The two basanites from ODP Site 871 at the summit platform of Limalok guyot plot toward EMI [*Koppers et al.*, 1995] exhibiting an

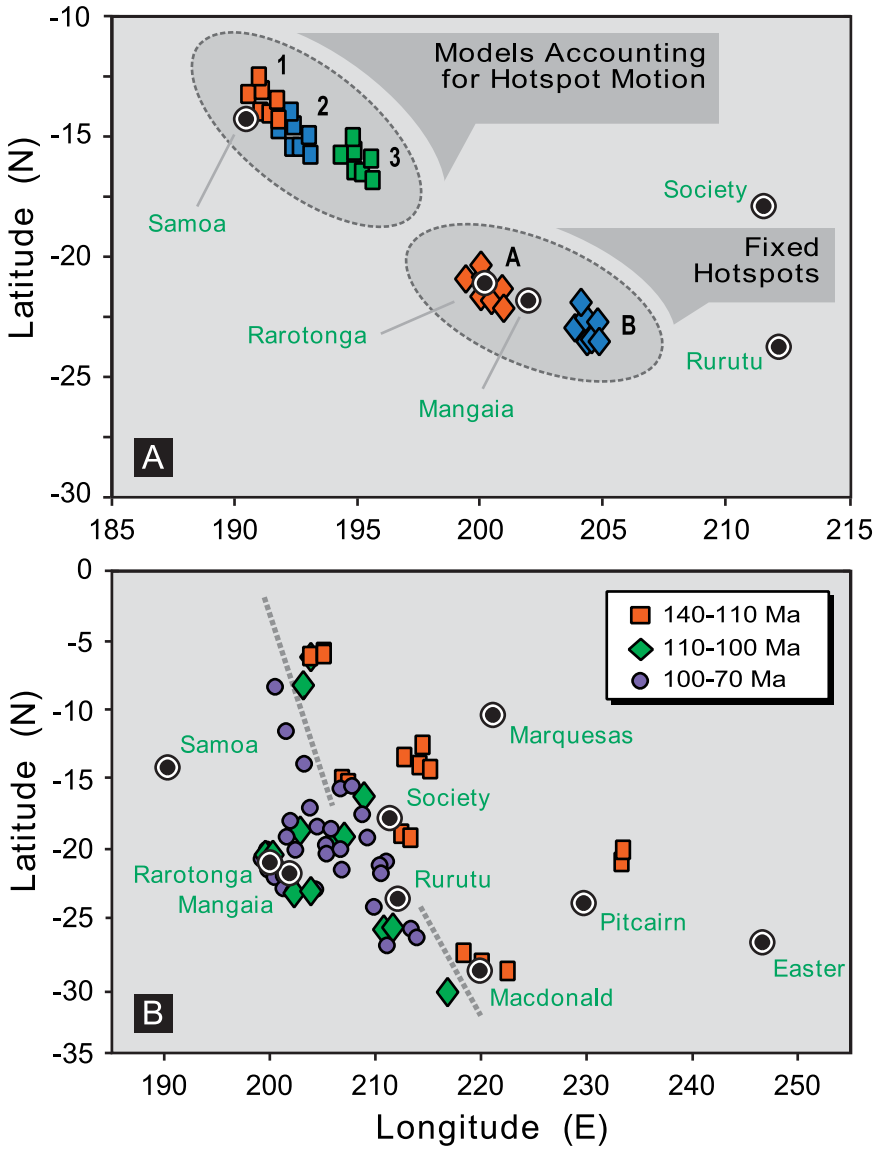

Figure 8. Plate tectonic reconstructions. (a) Backtrack reconstruction for the Magellan seamount trail. Models 1-2-3 represent "true" Pacific plate motion based on the angular plate velocities of *Steinberger* [2000] that account for hot spot motion and the "best-fit" Euler poles of *Koppers et al.* [2001]. Models A–B represent "conventional" Pacific plate motion based on the fixed hot spot hypothesis, using "best-fit" Euler poles of *Koppers et al.* [2001] in combination with estimates on the apparent angular plate velocities of *Wessel and Kroenke* [1997] and *Steinberger* [2000], respectively. For each model seven age dates for Vlinder, Pako and Ioah were used (Table 1) [*Koppers et al.*, 1998]. (b) Backtrack reconstruction of the WPSP according to seamount age, accepting model A. The $^{40}Ar/^{39}Ar$ ages used are listed in Table 1. The currently active hot spots of the SOPITA region (filled black circles) are shown for reference.

isotopic signature that partly coincides with the isotopic signature of the Rarotonga hot spot. Limalok, thus, exhibits an unexpected isotopic signature, considering the fact that all other samples from the Ratak, Erikub, Bikar and Majuro guyots typically have HIMU-type signatures with $^{206}Pb/^{204}Pb > 20.6$ [cf. *Davis et al.*, 1989; *Staudigel et al.*, 1991] similar to the Rurutu and Mangaia hot spots.

5.2. Northern Wake and Southern Wake Seamount Trails

[39] The majority of the seamounts and guyots studied in the Wake seamount trails display

$^{87}Sr/^{86}Sr$ ratios lower than 0.7035 while enveloping the entire range of $^{206}Pb/^{204}Pb$ ratios (18.7–21.5). Of these seamount trails the Southern Wake seamount trail is most remarkable since it exhibits HIMU signatures at $^{206}Pb/^{204}Pb$ ratios larger than 20.6 (Figure 7). These HIMU signatures are comparable to the isotope signatures of the current Rurutu hot spot and the Late Cretaceous Ratak seamount trail (see above).

5.3. Northern Wake Seamount Trail

[40] Alcatraz and Scripps guyot have been analyzed for the Northern Wake seamount trail and yield $^{206}Pb/^{204}Pb$ ratios between 19.1–20.6 at $^{87}Sr/^{86}Sr$ ratios lower than 0.7035 (Figure 7). Miami guyot can be included in this isotopic data array, but Wilde guyot exhibits too high $^{87}Sr/^{86}Sr$ ($\sim$0.705) and too low $^{143}Nd/^{144}Nd$ (<0.5128) probably due to its post-erosional character [*Winterer et al.*, 1993]. As a consequence, the basalts from Wilde guyot were most likely not produced by the Northern Wake mantle plume, but predominantly from lithospheric melts.

5.4. Southern Wake Seamount Trail

[41] HIMU seamount and Golden Dragon guyot were in previous studies characterized as typical HIMU type intraplate basalts [*Smith et al.*, 1989; *Staudigel et al.*, 1991]. For these basalts new Sr-Nd-Pb analyses were performed on hornblende, clinopyroxene and plagioclase mineral separates and on leached whole rock samples. Similar analyses were also performed on samples from Maloney guyot and Jennings guyot. Each analysis confirms the typical HIMU-type signature in the basalts of the Southern Wake seamount trail. The reproducibility for these mineral analyses is excellent, showing that the effects of seawater alteration are negligible. For example, mineral analyses for sample HIM-1 yield average $^{87}Sr/^{86}Sr_{(i)}$ at 0.702727 ± 10 (n = 5), $^{143}Nd/^{144}Nd_{(i)}$ at 0.512781 ± 6 (n = 4) and $^{206}Pb/^{204}Pb_{(i)}$ at 20.41 ± 16 (n = 3) as displayed in Figure B1. Only post-erosional volcanism at Lamont guyot (80–86 Ma) is deviating from this HIMU signature by exhibiting too low $^{206}Pb/^{204}Pb$ and, therefore, falling in the Northern Wake array.

5.5. Solitary Seamounts

[42] Despite the fact that the solitary seamounts cannot be associated with any of the studied WPSP seamount trails, they show Sr-Nd-Pb isotopic signatures quite similar to trails that are located closest. MIT guyot displays low $^{87}Sr/^{86}Sr$ in combination with intermediate $^{143}Nd/^{144}Nd$ and Pb-isotope signatures. This isotopic signature is similar only to the low $^{87}Sr/^{86}Sr$ lavas of the Marquesas hot spot of the SOPITA and falls close to the isotopic signatures of the Northern Wake seamount trail (Figure 7). Two volcanic edifices have been analyzed from Hemler guyot for Sr-Nd-Pb geochemistry [*Smith et al.*, 1989; *Staudigel et al.*, 1991]. Of these edifices the northern satellite volcano displays extreme EMII mantle source characteristics similar to the Samoan hot spot or the Late Cretaceous Ujlan seamount trail. Less extreme isotopic signatures are more typical for main Hemler volcano, which were reproduced by multiple clinopyroxene, plagioclase and nepheline mineral analyses (Table 2; Figure B1). Look seamount is located between the Ralik and Ratak seamount trails. Its isotopic signature measured from hornblende and clinopyroxene samples is likewise intermediate in composition between these two seamount trails. Because Look seamount is more than 50 Myr older than its surrounding seamounts, this may suggest that intraplate volcanism in the WPSP is principally controlled by lithospheric melting, as predicted in case of the weak Marquesian-type hot spot model. This coincidence has major geodynamic consequences, since it suggests that the ''enriched'' mantle compositions have been frozen-in as geochemical heterogeneities in the Pacific lithosphere, following earlier melting stages [cf. *Staudigel et al.*, 1991; *Phipps Morgan and Morgan*, 1999], and have been re-sampled during the formation of Look seamount.

6. Discussion

[43] The continuity in the geochemical characteristics of SOPITA hot spot volcanism back through

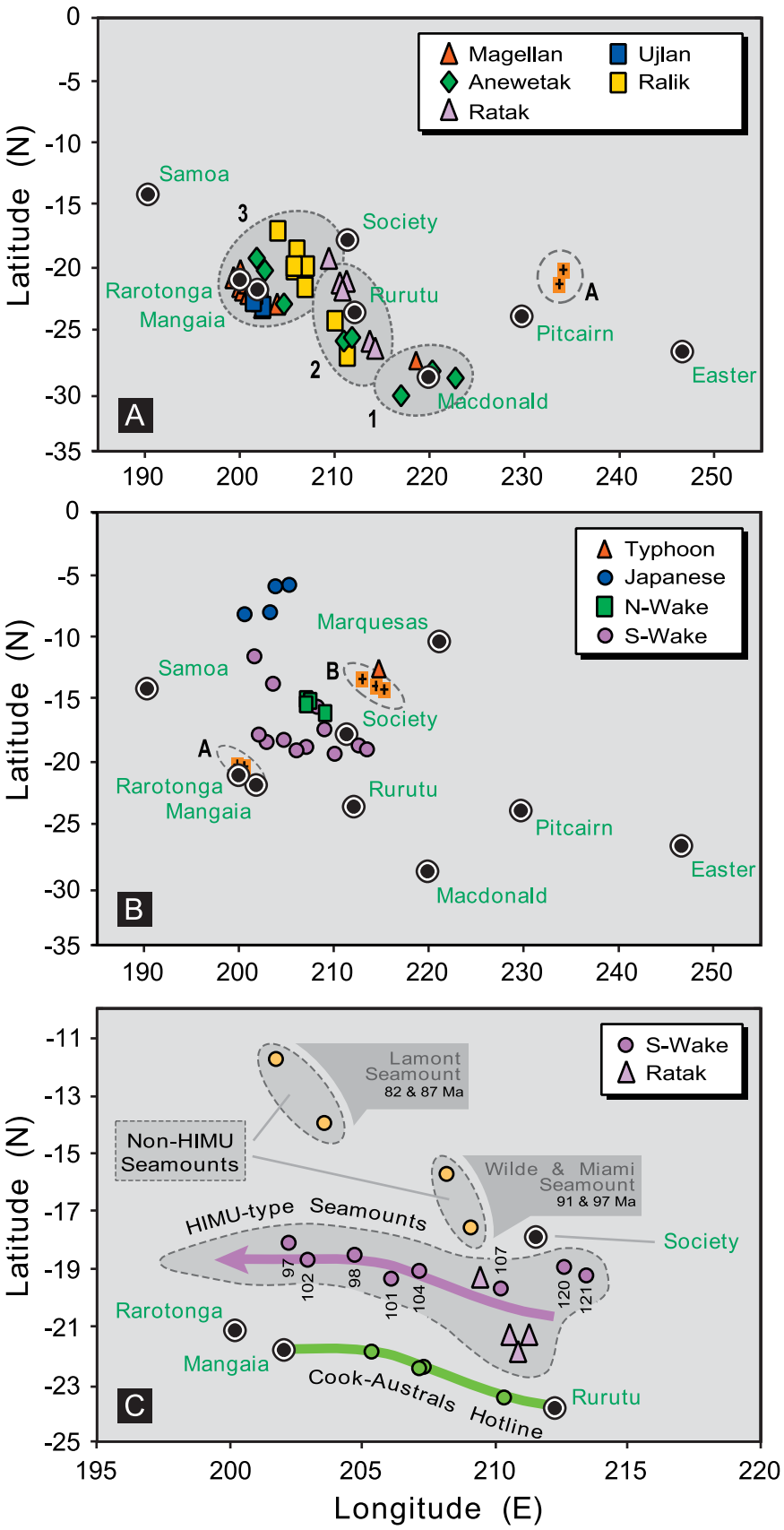
Magellan
Anewetak
Ratak
Ujlan
Ralik
Samoa
Society
Rarotonga
Mangaia
Rurutu
Pitcairn
Easter
Macdonald
A
1
2
3
Latitude (N)
Typhoon
Japanese
N-Wake
S-Wake
Marquesas
B
Lamont Seamount 82 & 87 Ma
Non-HIMU Seamounts
Wilde & Miami Seamount 91 & 97 Ma
HIMU-type Seamounts
97
102
98
101
104
107
120
121
Cook-Australs Hotline
C
Longitude (E)

time may be used to relate ancient seamounts to their present-day active source. In the following we will combine the reviewed $^{40}Ar/^{39}Ar$ ages and Sr-Nd-Pb isotope geochemistry to unravel some of the morphological and geochronological complexities of Western Pacific Seamount Province (WPSP). This allows us to resolve part of the evolution of intraplate volcanism in the South Pacific and their mantle sources, while addressing their longevity and (dis)continuity over the last 140 Myr. As will be shown in each section, most of our observations violate the basic assumptions that characterize the classical Wilson-Morgan hot spot model. This makes it clear that long-lived, deep and fixed plumes do not offer a satisfactory explanation for South Pacific intraplate volcanism. The consequences of this will be discussed in the last section, where we will review alternative models to explain intraplate volcanism of the South Pacific mantle. In these discussions, we will also investigate the structural control by the Pacific lithosphere itself, which is an often forgotten factor in the formation of intraplate volcanoes. We will argue that global intraplate volcanism is likely due to two main processes: (1) lithospheric extension, and (2) some modified plume concept. Such a modified plume concept may include both deep plumes and small shallow plumelets, whereby the latter may be rising from the top of superplumes. Plume-lithosphere interactions may also be required. However, we emphasize here that many of these concepts are based on the interpretation of geochemical data only that have very little (or no) spatial resolving power; in other cases, these concepts are based on geophysical models that have relatively little resolving power for the types of magma sources and their interaction with the lithosphere. Our understanding of global intraplate volcanism, therefore, will increase only if we collect and reconcile all available geophysical and geochemical data (or models) to find the best possible model.

6.1. SOPITA: WPSP Connection Revisited

[44] Plate tectonic reconstructions indicate that most WPSP seamounts originated in the NW part of the SOPITA region during the Cretaceous [*Ozima et al.*, 1977; *Duncan and Clague*, 1985; *Smith et al.*, 1989; *Staudigel et al.*, 1991; *Bergersen*, 1995; *Koppers et al.*, 1995, 1998]. This has been confirmed by measured southern paleolatitudes for the WPSP seamounts [*Sager and Pringle*, 1987; *Premoli Silva et al.*, 1993; *Sager et al.*, 1993b; *Winterer et al.*, 1993; *Tarduno and Sager*, 1995; *Tarduno and Gee*, 1995] and by similarities in their Sr-Nd-Pb isotopic signatures [*Davis et al.*, 1989; *Smith et al.*, 1989; *Staudigel et al.*, 1991; *Koppers et al.*, 1995, 1998]. Direct connections between individual Cretaceous hot spots and active hot spots in the SOPITA, however, are difficult to demonstrate, because (1) there is not one continuous volcanic trail that connects the WPSP to the SOPITA region, (2) hot spots are not necessarily fixed, and (3) individual hot spots may be too short-lived. Below we will reconstruct locations of the Cretaceous WPSP hot spots (using backtracking and hot spotting) and compare them to the SOPITA hot spots based on their Sr-Nd-Pb isotopic source characteristics. Such comparisons may allow us to distinguish between cogenetic pairs of hot spots, if these hot spots have maintained their distinct isotopic compositions and if they have longevities exceeding 40 Myr.

Figure 9. (opposite) Plate tectonic reconstructions. (a) Backtrack reconstruction of the Magellan, Ujlan, Anewetak, Ralik and Ratak seamount trails. Ellipses 1-2-3 outline a three-stage evolution of the Marshall and Magellan seamounts due to the passage of the Pacific plate over Macdonald, Rurutu and Rarotonga hot spot. A = Look seamount. (b) Backtrack reconstruction of the Typhoon, Japanese, Northern Wake and Southern Wake seamount trails. A, Hemler guyot; B, MIT guyot. (c) Detail of the Southern Wake and Ratak seamount trails. Note the pronounced ~1,000 km long age-trend for the exclusively HIMU-type seamounts that become younger from the east to the west. Numbers next to the S-Wake symbols are ages in Ma; ages for the Ratak seamounts range between 81–87 Ma. All backtrack reconstructions were based on Model A from Figure 8a using the "best-fit" Euler poles of *Koppers et al.* [2001] and apparent angular plate velocities of *Wessel and Kroenke* [1997]. The $^{40}Ar/^{39}Ar$ ages used are listed in Table 1. The currently active hot spots of the SOPITA region (filled black circles) are shown for reference.

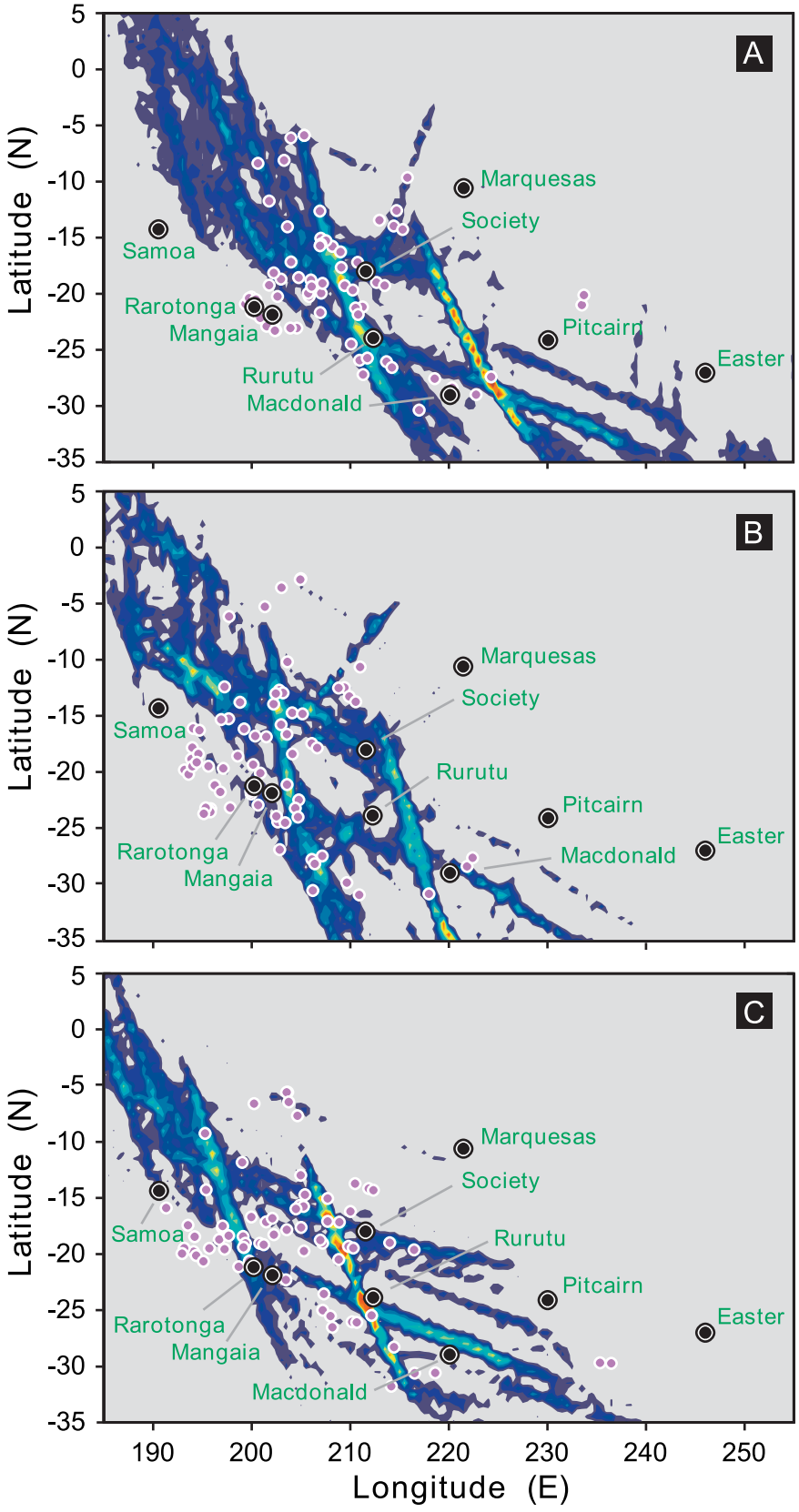
A
B
C
Latitude (N)
Longitude (E)
5
0
-5
-10
-15
-20
-25
-30
-35
190
200
210
220
230
240
250
Marquesas
Society
Samoa
Rarotonga
Mangaia
Rurutu
Macdonald
Pitcairn
Easter

6.1.1. Absolute Plate Motion in a Non-Fixed Hot Spot Frame of Reference

[45] Plate motions measured relative to hot spots are the net effect of lithospheric plate motion and hot spot motion. As a result, plate motion models should be corrected for hot spot motion, when applying backtrack reconstructions to find the "ancient" location of a hot spot during seamount formation. Uncorrected plate motion models, however, may still be very useful (as shown below), because they reflect the cumulative sum of subparallel plate and hot spot motions through geological time and, therefore, they may yield the "present-day" location of an (apparently) long-lived and drifted hot spot, in similar backtrack reconstructions. For fixed hot spots these "ancient" and "present-day" hot spot locations would coincide.

[46] We thus have to consider two types of angular plate velocities; one that includes hot spot motion and one that exclusively reflects the motion of the lithospheric plate. *Steinberger* [2000] estimated both types of angular plate velocities from his modeling of global mantle flow. We illustrate the differences in these plate motion models by reconstructing the location for the Magellan hot spot [*Koppers et al.*, 1998] using various fixed and mobile hot spot models (Figure 8a). Models including hot spot motion (models 1-2-3: squares) predict an "ancient" location for the Cretaceous Magellan hot spot close to Samoa. However, this "ancient" hot spot location is notably different from the reconstructed "present-day" location of the Magellan hot spot near Rarotonga (models A–B: diamonds) assuming fixed hot spots. Because the Magellan and Rarotonga hot spots bear close (but not exact) resemblance in Sr-Nd-Pb isotopic signatures (Figure 7) these reconstructions may indicate that the extension of the Rarotonga hot spot is indeed long-lived (at least 100 Myr) and that this hot spot could have moved from a location near Samoa to the southeast for more than 1,000 km (~10 mm/yr) since the Cretaceous.

6.1.2. Reconstruction of the WPSP Hot Spots

[47] Using the argument from above, we will evaluate the long-term geochemical history of the SOPITA hot spots by reconstructing the "present-day" hot spot locations for the WPSP seamount trails. In Figures 8b and 9 the WPSP hot spot locations are reconstructed based on model A in Figure 8a using the $^{40}Ar/^{39}Ar$ ages of Table 1 (this study) in combination with a new set of Euler poles of *Koppers et al.* [2001] and angular plate velocity estimates of *Wessel and Kroenke* [1997]. The resulting distribution of reconstructed hot spot locations is bimodal according to seamount age (Figure 8b). Long-lived WPSP hot spots older than 110 Ma would today be located east of the Macdonald-Rurutu-Society line; hot spots active between 70–110 Ma would be located to the west. As a direct result the older Typhoon, Japanese and Wake seamount trails do not match hot spot locations of the younger Magellan and Marshall seamount trails (compare Figures 9a and 9b) and yield "present-day" locations of their hot spots to the north of any currently active hot spot in the SOPITA. This disparity can be reconciled with the classical Wilson-Morgan hot spot hypothesis, only if the hot spots that produced the older seamount trails disappeared before the younger seamount trails were produced. This requires a discontinuation in the Early Cretaceous hot spot volcanism around 120–100 Ma. As we will show below, only the Southern Wake seamount trail appears to be as long-lived as 120 Myr, putting a maximum limit on the recorded duration of hot spot volcanism in the Pacific. Nonetheless, in all our reconstructions we still need to allow for 350–500 km of "individual" southward motion of this HIMU-type mantle

Figure 10. (opposite) Plate tectonic reconstructions comparing the conventional backtracking technique with the hot spotting technique of *Wessel and Kroenke* [1997]. (a) Comparison based on the stage pole model of Model A from Figure 8a using the "best-fit" Euler poles of *Koppers et al.* [2001] and apparent angular plate velocities of *Wessel and Kroenke* [1997]. (b) Comparison based on the stage pole model of *Wessel and Kroenke* [1997]. (c) Comparison based on the stage pole model of *Engebretson et al.* [1985]. In all diagrams the reconstructed backtrack locations (filled pink circles) have been calculated using the $^{40}Ar/^{39}Ar$ ages listed in Table 1. The currently active hot spots of the SOPITA region (filled black circles) are shown for reference.

source to make a perfect fit to the currently active Rurutu and Mangaia hot spots.

6.1.3. Hot Spotting Versus Backtracking

[48] Hot spot locations for ancient seamount trails may alternatively be reconstructed using the "hot spotting" technique of *Wessel and Kroenke* [1997, 1998]. In their technique, each seamount can be used to reconstruct its mantle flow line without knowledge of its age of formation. Combining the flow lines of multiple seamounts belonging to one and the same hot spot then should create multiple crossings at their "ancient" hot spot location. However, we have to assume that the WPSP seamounts were exclusively formed during single stages of hot spot volcanism, and that their hot spots are fixed in the mantle over long periods of geological time (100–200 Myr). Only in that case do these crossings coincide with the traditional "backtracked" hot spot locations.

[49] In Figure 10 we show results of three comparisons we made using the "hot spotting" and "backtracking" techniques for the WPSP seamounts based on three different stage pole models for the Pacific plate [*Engebretson et al.*, 1985; *Wessel and Kroenke*, 1997; *Koppers et al.*, 2001]. For reference, we also show the locations of the currently active hot spots of the SOPITA region. No direct overlap is apparent in any of these comparisons that may indicate long-lived and fixed locations for the WPSP hot spots. For example, one distinct cluster of backtrack locations falls in each comparison to the west of the entire "hot spotting" cluster. More importantly, most "hot spotting" crossings neither coincide with the WPSP backtrack clusters (based on accurate $^{40}Ar/^{39}Ar$ ages) nor with the current locations of the SOPITA hot spots. This does not necessarily indicate an error in the "hot spotting" technique [cf. *Aslanian et al.*, 1998; *Geli et al.*, 1998]. These observations rather may be explained by the intermittent style of hot spot volcanism in the WPSP and SOPITA regions, by the superposition of multiple hot spots on the evolution of single seamount trails (see below) or by extended periods of volcanism at individual seamounts. The fact that the western cluster of backtrack locations (80–100 Ma) shows no corresponding "hot spotting" cross indicates that no younger seamount trails are present on the Pacific plate to generate such a crossing. This follows since the "hot spotting" technique requires for every single hot spot trail to minimally include two segments that were formed during two (very) distinct stage poles, in order to be able to create clearly defined crossings. The periodic character of intraplate volcanism in the Pacific over the last 140 Myr (cf. Figure 2b) certainly minimizes such a coincidence. One might also invoke a linear source of intraplate volcanism rather than hot spot volcanism, such as *Bonatti and Harrison*'s [1976] mantle "hotline" (see below for a further discussion). More recently, it has been suggested that extension may cause plate thinning and mantle upwelling, which in turn may result in partial melting and the formation of intraplate volcanoes [e.g., *Winterer and Sandwell*, 1987; *Sandwell et al.*, 1995; *Favela and Anderson*, 2000]. In these alternative scenarios, intraplate volcanism is not related to plate motion (at least not directly) but to the architecture and physical make-up of the lithospheric plate, allowing for most of the observed discrepancies.

6.2. Non-Singular Hot Spot Models and the WPSP

[50] Simple continuous hot spot models do not adequately explain the WPSP. For example, two periods of Cretaceous volcanism can be distinguished in the seamount trails of the Marshall Islands and Magellan seamounts [*Davis et al.*, 1989; *Lincoln et al.*, 1993; *Winterer et al.*, 1993; *Haggerty and Premoli Silva*, 1995; *Koppers et al.*, 1998]. Their Late Cretaceous period of volcanism agrees well with the formation of the Musicians seamounts [*Pringle*, 1993], the Wentworth seamounts [*Pringle and Dalrymple*, 1993] and the Line Islands [*Schlanger et al.*, 1984] during the 100–80 Ma stage pole of Pacific plate motion [*Koppers et al.*, 1998]. They also have consistent northwestern azimuths (Figure 3) implying that the majority of these seamounts should have formed within this 100–80 Ma stage pole. However, the occurrence of volcanism prior

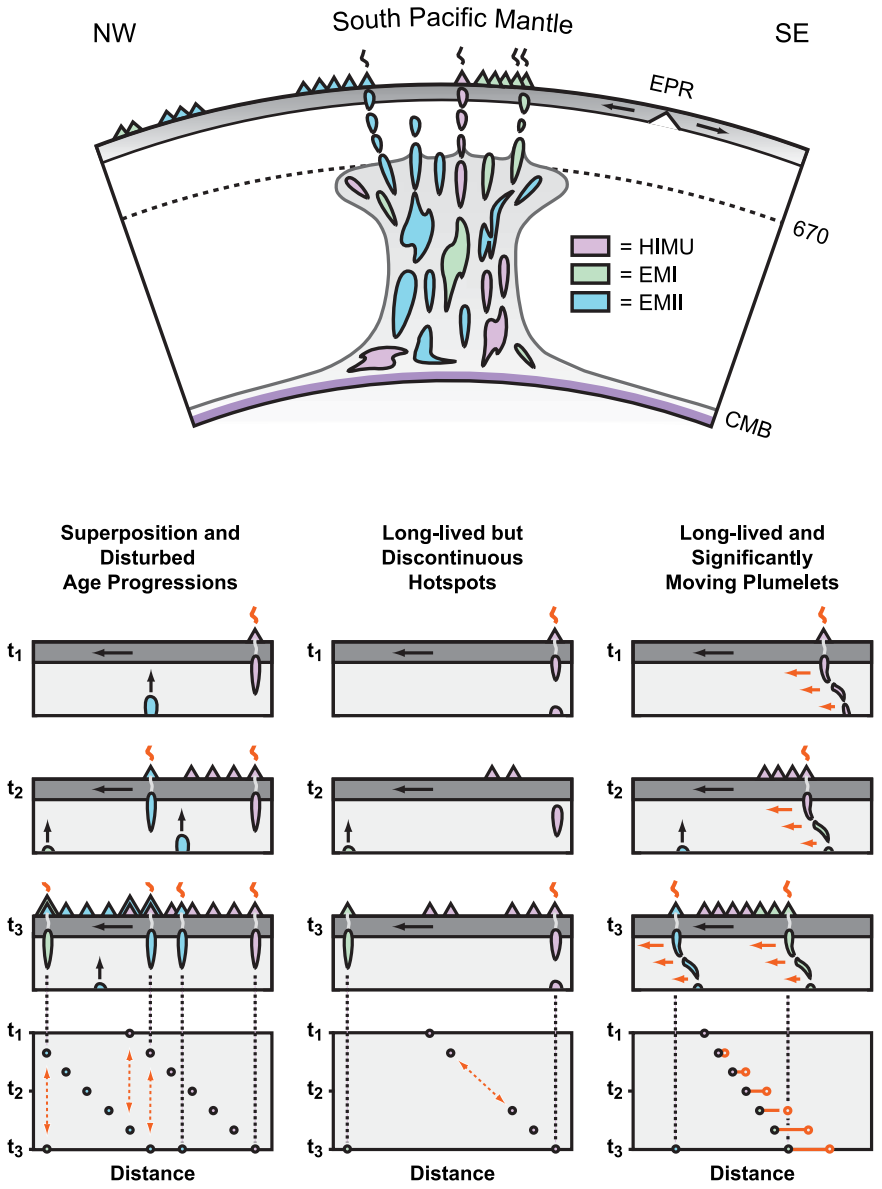

Figure 11. Adjusted model for weak Marquesian-type or secondary hot spots. Plumelets consisting of heterogeneous subducted materials are formed as small parasitic plumes from the top of a superplume [cf. *Courtillot et al.*, 2002]. During upwelling the entrained materials segregate into discrete plumelets with strong affinities toward one (or more) end-member mantle components such as HIMU, EMI and EMII. Depending on the size and continuity of these plumelets, hot spot volcanism may be produced following partial melting of the plumes and the oceanic lithosphere they penetrate. Melt residues (and terminated plumelets) will be mixed back into the asthenosphere. The localized formation of multiple plumelets results in complex age distributions along closely-spaced en echelon seamount trails with typical superposition of volcanism. Discontinuity and temporary terminations of the plumelets (at the base of the lithosphere) may lead to intermittent volcanism, and their motion within a more viscous upper mantle may cause significant changes in the observed age progressions. These diagrams are based on this review and partially by studies of *Duncan et al.* [1986], *Janney et al.* [1999], *Sleep* [1984], *McNutt et al.* [1997], *Steinberger and O'Connell* [1998] and *Courtillot et al.* [2002].

to 100 Ma is unanticipated and cannot be reconciled with a singular hot spot model, in particular, since individual guyots (Wodejebato, Vlinder) show evidence for both volcanic events.

[51] The backtrack reconstructions show that the age distributions within the Magellan, Ujlan, Anewetak, Ralik and Ratak seamount trails may be explained by the successive passage over the

currently active Macdonald, Rurutu and Rarotonga/Society hot spots between 120 and 80 Ma (compare Area 1, 2 and 3 in Figure 9a). This concurs with other studies on the Marshall Islands [e.g., *Lincoln et al.*, 1993] but this scenario is only partially supported by the observed Sr-Nd-Pb isotopic signatures in the WPSP seamounts. In most cases the "present-day" locations for the WPSP hot spots cannot be matched in isotopic space with the currently active SOPITA hot spots. For example, the Ralik seamounts that formed in "Area 2" do not resemble the typical HIMU isotope signatures for Rurutu since their $^{206}Pb/^{204}Pb$ ratios are all below 20, whereas the Ralik seamounts that formed in "Area 3" have $^{87}Sr/^{86}Sr$ ratios below 0.704 which is atypical for the Rarotonga and Society hot spots. The Ujlan seamounts have "present-day" locations near Rarotonga and Mangaia in "Area 3" but their $^{87}Sr/^{86}Sr$ ratios are unusually high. On the other hand, Lo-En guyot in the Anewetak seamount trail matches its predicted "present-day" location in "Area 1" with an isotopic signature that is comparable to the currently active Macdonald hot spot. A similar positive match has already been discussed for the Magellan and Rarotonga hot spots indicating that the Rarotonga hot spot may have been active over the last 100 Myr. These observations put important constraints on the chemical geodynamics of the South Pacific mantle, in particular, since the Magellan, Ujlan, Anewetak, Ralik and Ratak seamount trails cover the entire range of isotopic compositions (Figure 7) while being located only a few 100 km's apart (Figure 3). Most Cretaceous hot spots apparently ceased activity around 80 Ma in the Pacific. This is true also for the Magellan and Anewetak hot spots, which both terminate toward the SSE on the bathymetric maps in Figures 3d and 3e. As a consequence, the ancient South Pacific hot spots typically display intermittent activity and, in most cases, ceased to exist after ~20 Myr of intraplate volcanism. These hot spots, therefore, have to be comprised of short and small-volume plumelets with very distinct isotopic signatures that remain stable only on a relatively short ~20 Myr timescales in a configuration of closely-spaced conduits every 230–280 km.

[52] Further backtrack reconstructions demonstrate an age trend in the Southern Wake source region between 121 and 97 Ma toward the west (Figure 9c). This age-trend is entirely defined by HIMU-type seamounts with $^{206}Pb/^{204}Pb > 20.6$ and is almost 1000 km long. Neither uncertainties in absolute plate motion nor a western motion of the Southern Wake hot spot during the 125–110 and 110–100 Ma stage poles would account for this trend. The reason for this is that two neighboring seamounts (HIMU and Golden Dragon; Figure 3c) define both ends of this trend but have very different ages of 120 and 102 Ma. This leaves the possibility of intraplate volcanism along a "hotline" of closely-spaced conduits in the mantle [*Bonatti and Harrison*, 1976; *Epp*, 1984; *Maia and Diament*, 1991; *Janney et al.*, 1999] that were simultaneously active during the Cretaceous while generating an irregular age progression in the Southern Wake seamount trail (Figure 5b). More strikingly, the Southern Wake hot spot region closely resembles the present-day configuration of seamounts in the Cook-Austral Islands (Mangaia, Maria, Rimatara, Rurutu, Tubuai; Figure 9c) by its azimuth and length, but also by comparable HIMU-type mantle source characteristics (Figure 7) [*Palacz and Saunders*, 1986; *Nakamura and Tatsumoto*, 1988; *Hauri and Hart*, 1993] and its irregular age progression [*McDougall and Duncan*, 1980; *Turner and Jarrard*, 1982]. These observations strengthen the existence of the Rurutu-Ratak-Wake seamount trail [*Koppers et al.*, 1995] representing at least 120 Myr of hot spot volcanism. However, our current reconstruction rather indicates that this seamount trail is associated with a "hotline" in the Cook-Austral Islands [*Turner and Jarrard*, 1982] and not just the Rurutu hot spot [*Koppers et al.*, 1995]. Plate motion parallel to this hotline during both the 43–0 and 125–100 Ma stage poles most probably would have induced the irregular age progressions in the Cook-Austral and the Southern Wake seamount trails. Nonetheless, a southward hot spot motion during the 100–80 and 80–45 Ma stage poles would be required to explain the observed 350–500 km latitudinal offset between the Southern Wake and Cook-Austral hot spot regions (Figure 9c).

6.3. Short-Lived and Discontinuous Intraplate Volcanism

[53] Plate tectonic and geochemical correlations suggest that the basalts sampled in the WPSP and SOPITA regions have been produced from the same heterogeneous mantle source in the South Pacific over the last 120 Myr [cf. *Smith et al.*, 1989; *Staudigel et al.*, 1991; *Koppers et al.*, 1995]. This indicates that HIMU, EMI and EMII are enduring mantle sources on the scale of the WPSP and SOPITA. However, on the scale of single hot spots, we could establish cogenetic relations between only a few hot spots in the South Pacific over the last 140 Myr. In fact, the majority of the seamount trails in the Pacific basin were formed by pulses of short-lived volcanism not exceeding 40 Myr (Figure 2a) and occurring during the Cretaceous and over the last 30 Myr only (Figure 2b). These observations are in marked contrast to the continuous and long-lived character of Hawaiian-type hot spots (Figure 2a) [*Vogt*, 1972; *Pringle et al.*, 1994; *McNutt et al.*, 1997; *Koppers et al.*, 1998; *Clouard and Bonneville*, 2001] and any model explaining this type of intraplate volcanism has to identify a regional force that can turn on/off "hot spots" in a very large region. Other observations seem to violate the basic assumptions of the classical Wilson-Morgan hot spot hypothesis as well. First of all, it has been shown that Pacific hot spots display hot spot motions [*Gordon and Cape*, 1981; *Sager and Bleil*, 1987; *Tarduno and Cottrell*, 1997; *Cande et al.*, 1995; *Norton*, 2000; *Koppers et al.*, 2001] undermining the "fixed" character of standard hot spots. Second, most South Pacific hot spots have produced non-age-progressive seamount trails that show clear indications for repeated volcanic episodes and overprinting [e.g., *Bonatti and Harrison*, 1976].

[54] It thus becomes more attractive to view intraplate volcanism in the South Pacific region as the result of short-lived hot spots (in connection with deep "superplume" activity as envisioned by *McNutt* [1998]) and lithospheric extension. We will show that a combination of these "end-member models" is the most likely explanation for the above observations. Such a combined model has to be able to answer the following questions: How to explain the negative anomaly in the geoid that coincides with the uplifted SOPITA region? Is there a relation with the South Pacific "superplume" as shown in tomographic studies? Why are linear volcanic ridges associated with low gravity lineations in the oceanic crust? Why does intraplate volcanism (almost) never occur on older oceanic crust? Why is the maximum horizontal stress sub-parallel to the direction of absolute plate motion for Pacific oceanic crust younger than 80 Ma as shown in global stress compilations? Which process triggers the episodical activation of intraplate volcanism in the Cretaceous and again 30 Myr ago? Which process explains the high number of "short-lived" hot spots in the South Pacific mantle? Is there a relation with global plate re-organizations and the build-up of tensional stress in the Pacific plate? And, finally, how to explain the non-age-progressive nature of the WPSP and SOPITA seamount trails?

[55] Most of these questions will remain unanswered, but in the following we will discuss both models to illustrate the complexities that arise when adopting one of these models over the other. It will become clear that these simplified end-member models cannot explain all characteristics of intraplate volcanism in the South Pacific. For example, the existence of the "superplume" in the deep South Pacific mantle can be causally related to the "superswell" in the same area and, therefore, to regional lithospheric extension. The lithosphere may become weak due to this extension process and prone to intrusion of small plumelets that originated from the base of the lithosphere or the surface of the deep superplume. In such a "mixed" scenario it becomes unclear whether intraplate volcanism is caused by plumes or extension, both these processes seem to play an important role. Thermochemical convection experiments show further evidence for these kind of "mixed" scenarios, where superplume regimes oscillate vertically throughout the whole mantle (causing the superswells) on timescales exceeding 100 Myr, while thin plumelets rise from the top of these superplumes on much shorter timescales of ~20 Myr only [*Davaille et al.*, 2002, 2003]. The same experiments also show that deep mantle plumes (like Hawaii) may coexist with these superplume

regimes [*Davaille et al.*, 2002, 2003]; they may even be generated from the same boundary layer deep in the mantle [*Gu et al.*, 2001; *Romanowicz and Gung*, 2002; *DePaolo and Manga*, 2003]. It is important to realize that deep plumes, superplumes and lithospheric processes may all be the result of the same convecting Earth.

[56] In Figure 11 we start out by illustrating an adjusted hot spot model explaining "short-lived" intraplate volcanism in a "superplume" setting (like *McNutt* [1998]). Even though this may not be a comprehensive model, it clearly shows our new observations that contradict the standard hot spot hypothesis. This first "end-member model" assumes that small plumelets shoot off from the top of a superplume that is being deflected at the 670 km boundary layer [*Janney et al.*, 1999; *Courtillot et al.*, 2002] or at the bottom of the lithosphere [*McNutt*, 1998; *Romanowicz and Gung*, 2002] in a similar fashion as observed in thermochemical convection experiments [*Davaille*, 1999; *Davaille et al.*, 2002, 2003]. These plumelets can contain any mixture of the HIMU-EMI-EMII mantle components, but for simplicity we assume that the plumelets sample one of these components preferentially, thereby determining their distinct geochemical source characteristics. Depending on their size and buoyancy, these plumelets may rise through the upper mantle, and based on the structural make-up of the overlying lithosphere, they may successfully create magma conduits through the Pacific plate in order to produce intraplate volcanism. Long seamount trails of unique geochemical heritage can be produced only when several plumelets with the same mantle signature are (fortuitously) lined up underneath each other in the South Pacific mantle. Discontinuity in the arrival of separate plumelets may lead to intermittent hot spot volcanism, while simultaneous formation of multiple plumelets may result in "irregular" age progressions and "overprinting" along the seamount trails. Convectional mantle flow in the asthenosphere may deflect the thin mantle plumes and generate "apparently" faster or slower age progressions. In this alternative plume model, each plumelet is only shortly stable for 10–40 Myr before they dissipate or become less buoyant than the overlying lithosphere. These plumelets also need to be physically small (when compared to the Hawaiian plume) so they can coexist in the South Pacific mantle, spaced no more than 200–300 km apart, and still retain their distinct geochemical source characteristics. Large plumes of typical Hawaiian dimensions (~100 km) would be instable in this configuration, causing mantle plumes to merge, in particular, if they rise from deeper in the mantle [*Albers and Christensen*, 1996; *Davaille*, 1999; *Davaille et al.*, 2002, 2003]. This locates the origin of intraplate volcanism in the South Pacific mantle at rather shallow depths, possibly even shallower than the 400 km depth as based on the modeling of the negative geoid anomalies [*McNutt and Judge*, 1990].

[57] In the following we will review some extension-related processes that may explain some of the phenomena we have been describing for the South Pacific and WPSP seamount trails. These explanations do not exclude the presence of plumelets and/or superplumes in the South Pacific mantle, but we believe that these extension-related processes are complementary in our understanding of intraplate volcanism, in particular, as mechanisms that facilitate channeling of magmas through the oceanic lithosphere. As discussed by *Favela and Anderson* [2000] stress-induced magmatism and the reactivation of already existing fracture zones in the interior of oceanic lithospheres may explain short-lived volcanic chains, its intermittent character and the sometimes simultaneous eruption along mantle "hotlines" such as we have shown for the Wake seamount trail and Cook-Austral hot spot region. Local stress variations can reactivate seafloor structures, such as inactive transform faults [*Vogt*, 1974; *Jackson and Shaw*, 1975; *Bonneville and McNutt*, 1992; *Favela and Anderson*, 2000], while the progressive opening of these fractures continuously channels magma through the lithosphere to produce seamount trails [*Solomon and Sleep*, 1974; *Anguita and Hernan*, 1975; *Turcotte and Oxburgh*, 1978]. Age progressions may still be produced in these type of seamount trails, but continued volcanism over the length of the entire fracture zone will cause significant disturbances in the age progressions. Loading of the lithosphere by volcanic edifices [*Hieronymus*

and Bercovici, 1999, 2000] may cause lithospheric flexure and cracking followed by the formation of new volcanoes. Depending on lithosphere thickness, this process is expected to produce continuous volcanic ridges (thin lithosphere) or discretely spaced seamounts in a trail (thick lithosphere) with more or less linear age progressions. However, the formation of the first volcano in these seamount trails still requires an independent intraplate process, making these self-propagating volcanic trails a secondary lithospheric phenomenon. Intermittent seamount volcanism (as often observed in the WPSP and SOPITA) may be caused by regional stress changes that freeze and unfreeze lithospheric transform faults. This effect may be enhanced by sudden changes in the lithospheric thickness across the transforms causing thermal stress changes [*Sleep*, 2002]. This fate is more likely in the context of lithospheric stress changes than a fortuitous alignment of plumelets in the deep mantle (see Figure 11). The main source of these stress variations may be regional extensional stress that exists as a consequence of the pull of subducting slabs surrounding the Pacific plate and the push at the spreading ridges [*Solomon and Sleep*, 1974; *Wortel and Cloetingh*, 1981; *Zoback et al.*, 1989; *Sandwell et al.*, 1995]. Because of the high absolute plate velocity of the Pacific plate, the maximum tensional stress is expected to be orthogonal to the direction of absolute plate motion for the youngest part of this plate, but this effect should diminish toward older and more rigid lithosphere [*Sandwell et al.*, 1995]. This stress distribution is confirmed by the small number of stress measurements in the Pacific plate, as determined by the focal mechanisms of intraplate earthquakes [*Zoback et al.*, 1989]. Interestingly, the orientation of the maximum tensional stress seems to become sub-parallel to the absolute plate motion vector in Pacific crust older than 80 Ma [*Zoback et al.*, 1989]. The fact that only a very small number of earthquakes are recorded in the interiors of oceanic plates indicates that the strain build up can only be very minimal. In such a low strain setting we only can expect that far-field tensional stresses cause boudinage in the young part of the Pacific plate [*Winterer and Sandwell*, 1987; *Sandwell et al.*, 1995; *Wessel et al.*, 1996] resulting in cracking and intraplate magmatism in the thinnest lithosphere that is under higher tensional stress. Alternatively, thermal contraction in young lithosphere close to the spreading ridges [*Gans et al.*, 2003] may explain a similar buckling of the Pacific plate with seamount formation in the gravity lows.

[58] Assuming whole mantle convection and a "marble cake" nature of the mantle [*Allègre and Turcotte*, 1986; *Phipps Morgan and Morgan*, 1999], the delivery of the mantle components HIMU-EMI-EMII to the South Pacific volcanoes can be explained without the need for different "mantle plumes" ascending from the deep mantle in a closely-spaced configuration. Partial melting will preferentially sample the more fertile components [*Bonatti*, 1990; *Phipps Morgan and Morgan*, 1999; *Phipps Morgan*, 2001] in the asthenosphere, depending on their volatile content and on the depth of mantle upwelling under the extended South Pacific lithosphere. Variations in the depth of melting causes different mantle components to be sampled for different intraplate volcanoes, resulting in the unusual isotope compositions for the SOPITA and WPSP [*Vidal et al.*, 1984; *Zindler and Hart*, 1986; *Staudigel et al.*, 1991; *Woodhead and Devey*, 1993; this study]. As a consequence "hot spots" may become "wet" spots without plumes.

[59] We have shown that we can explain a large number of observations with the extensional models, but not all of them. The South Pacific region is clearly associated with a geoid low that cannot be explained by extension alone, but requires the dynamic support from a superplume originating deep in the mantle [cf. *McNutt*, 1998]. Also this model falls short of explaining recent tomographic images depicting a large-scale thermal upwelling starting at the core-mantle boundary and reaching all-the-way to the bottom of the Pacific lithosphere [cf. *Romanowicz and Gung*, 2002]. Nevertheless, the physical state of the lithosphere plays an important role during intraplate volcanism; we often seem to forget that intraplate magmas need to find their way through a rigid oceanic lithosphere; plumes cannot burn themselves holes to reach the surface, but they need to take advantage of any existing weak spot or fracture zone to have a change to penetrate the overlying lithosphere. However, there is still an important question to answer

with respect to the waxing and waning of intraplate volcanism in the regional Pacific. Massive volcanism in the South Pacific has been recorded once during the Cretaceous and again starting 30 Myr ago, separated by a 30–40 Myr quiescence period (Figure 2b). If both volcanic episodes are caused by superplume activity, why do we see an enormous burst of flood basalt volcanism during the Cretaceous maybe causing the normal magnetic quite zone [cf. *Larson*, 1991] and other global phenomena, which seem to be completely absent for the modern equivalent of the superplume? Does this mean that the current superplume is another variety of superplumes, or is this a second and weaker phase in the succession of an oscillating superplume [cf. *Davaille et al.*, 2002]. Explaining this periodicity in the light of lithospheric extension is equally difficult, because the last major plate reorganization in the Pacific is synchronous with a reorganization of the Pacific-Farallon fracture zones around Chron 23 or 48–50 Ma [*Hey et al.*, 1988]. This would require a long period of strain build-up (~20 Myr) without significant volcanism before intraplate volcanism starts to increase in the SOPITA region around 30 Ma (Figure 2b).

7. Summary

[60] The $^{40}Ar/^{39}Ar$ ages of seamount formation in the West Pacific Seamount Province (WPSP) range from 134 to 69 Ma and describe five different stage poles of absolute plate motion. Sr-Nd-Pb isotopic signatures indicate that the WPSP seamount trails exhibit distinct mantle source characteristics, which is in sharp contrast to the extreme isotopic variation in the entire WPSP mantle region. Most prominent are the HIMU signatures at $^{206}Pb/^{204}Pb$ larger than 20.6 for the Southern Wake and Ratak seamount trails and the EMII signatures at $^{87}Sr/^{86}Sr$ larger than 0.705 for the Ujlan seamount trail. Other seamount trails have signatures intermediate to these extreme cases or they show a potential contribution from the EMI mantle component, such as is the case for the Magellan seamount trail. On the basis of these profound differences in Sr-Nd-Pb isotope geochemistry we were able to map out the WPSP hot spots and start to relate them to currently active hot spots in the South Pacific Isotopic and Thermal mantle Anomaly (SOPITA).

[61] Of the eleven hot spots that are currently active in the SOPITA we could identify only two hot spots that appear to be long-lived and that have Cretaceous counterparts in the WPSP. Plate reconstructions show that the Southern Wake seamount trail most likely originated from the Mangaia-Rurutu "hotline" in the Cook-Austral Islands, whereas the Magellan seamount trail may have originated from the Rarotonga hot spot. Combined with similarities in their Sr-Nd-Pb isotope characteristics, our hot spot mappings suggest that these WPSP seamount trails are closely related to the Mangaia, Rurutu and Rarotonga hot spots in the SOPITA region and have been active, therefore, up to 120 Myr. These mappings also indicate that their mantle source regions maintained their distinct geochemical HIMU, EMI and EMII signatures over long periods of geological time.

[62] All other hot spots in our reconstructions show discontinuous volcanism. For example, the Typhoon and Japanese hot spots were terminated during the Early Cretaceous, whereas the currently active Samoan, Society, Pitcairn and Marquesas hot spots apparently have no long-lived counterparts in the WPSP. Most of these hot spots may have become active over the last 20–30 Myr only. Even though we could demonstrate the longevity of some weak Marquesas-type or secondary hot spots in the South Pacific, their style of volcanism typically has been intermittent over the last 140 Myr, resulting in numerous seamount trail segments that represent no more than 10–40 Myr of hot spot volcanism. In addition, we confirm that some mantle sources, such as the Mangaia-Rurutu "hotline" in the Cook-Austral Islands have moved 300–500 km over the last 100 Myr (3–5 mm/yr).

[63] From our observations it is clear that most premises of the classical Wilson-Morgan hot spot hypothesis appear to be violated for the hot spots in the South Pacific mantle. All studied hot spots violate one or more assumptions of a classical hot spot: (1) none of them are active continuously, (2) most are short-lived or intermittently active,

(3) some show evidence of hot spot motion, and (4) most have poor age progressions, if any at all. On top of this we have strong evidence for volcanism along mantle "hotlines" and the "superposition" of hot spot volcanism. We thus conclude that long-lived, deep and fixed mantle plumes cannot explain intraplate volcanism in the South Pacific mantle over the last 140 Myr.

[64] Short-lived and discontinuous hot spot volcanism of the South Pacific mantle, therefore, seems best explained by a prolonged "broad-scale" mantle upwelling enclosing many "plumelets" of distinct Sr-Nd-Pb isotopic signature that remain stable on short ~20 Myr timescales in a configuration of closely-spaced but dynamic diapirs. This would require a different style of hot spot volcanism with a rather shallow origin in the upper mantle, and in other studies, these alternate hot spots have been earmarked as weak "Marquesian-type" or "secondary" hot spots [*Duncan et al.*, 1986; *Haase*, 1996; *Courtillot et al.*, 2002]. The question remains which process(es) drive(s) the upwelling of these plumelets? The formation of these plumelets may be related to the inferred "superplume" in the South Pacific that may have been slowly oscillating vertically over the last 140 Myr with a periodicity of 80–90 Myr. This phenomenon is also observed in thermochemical convection experiments [*Davaille*, 1999; *Davaille et al.*, 2002, 2003] and has been used to explain periodic volcanism in the Line Islands during the Cretaceous [*Davis et al.*, 2002]. The plumelets may also be attracted by a thinning of the lithosphere due to intraplate extension or they may represent the loci of a "wet" heterogeneous mantle spot that does not require physical plumes at all. In these cases, the periodicity of the intraplate volcanism can also be explained by changes in the local stress field following major plate re-organizations in the global plate circuit. These tensional stresses may also be the result of lithospheric uplift due to the upwelling of the South Pacific superplume itself.

[65] This work and previous studies have rendered the simple and elegant "hot spot" model insufficient to explain the age distribution and source region characteristics of intraplate volcanoes in the South Pacific. Abandoning the hot spot model has been resisted, because many aspects of plate tectonics appear to depend on it, and for this reason, most authors have explained apparent inconsistencies by modifying the hot spot model. This effectively leads to new models that retain the concept of mantle plumes, but that lack both simplicity and predictive power. New models that call on "extension" are indeed simple and they can explain most characteristics of the Earth's intraplate volcanism, but they don't allow us to predict the nature of age progressions along the volcanic chains they produce and, therefore, it is difficult to independently test their validity. For this reason, Occam's Razor asks us to choose the most simple model, but all that we can observe is either quite complicated and/or it lacks predictive powers that would allow us to test these hypotheses. We have argued in this paper that we require a process that forces regional magmatism from a large-scale source of buoyancy below (like the rise of plumelets shooting off the top of a superplume) and we require a process that acts from above, as lithospheric extension opens up pathways that allow the lithosphere to be penetrated by magma. This is not a simple solution any more, so we either keep searching for better simple models or we accept that nature is more complicated than Occam's Razor suggests.

Appendix A: On Groundmass $^{40}Ar/^{39}Ar$ Dating

[66] Dating groundmass samples using $^{40}Ar/^{39}Ar$ geochronology has become a powerful tool when determining the age progressions along seamount trails [cf. *Koppers et al.*, 1998]. This is particularly true since crystalline groundmasses provide crystallization ages concordant to $^{40}Ar/^{39}Ar$ ages of comagmatic minerals, despite the inability to perform isochron calculations for many of such experiments and typical age plateau widths ranging between 30 to 70% of the total amount of $^{39}Ar_K$ released [*Koppers et al.*, 2000]. In this Appendix, we like to draw attention to some important observations that can be made when interpreting the age spectra from typical groundmass $^{40}Ar/^{39}Ar$ analyses.

[67] The observed argon release patterns in Figure 4 for the groundmass samples LAM-1, NWO-2, SWO-1, WOD-3, WOD-4, MIS-2, and TAK-2 are characterized by: (1) too high apparent ages for the low temperature increments, (2) accurate age plateaus at the intermediate temperature increments, and (3) too low apparent ages for the high temperature increments. The low temperature sections are further characterized by higher K/Ca ratios and higher atmospheric components than observed for the age plateau. These observations can only be explained by the recoil of $^{39}Ar_K$ (increasing apparent ages) in combination with the preferential degassing of alteration phases as located in-between and on the surfaces of plagioclase, clinopyroxene and Ti-magnetite crystallites (increasing K/Ca ratios and the atmospheric component). The intermediate temperature sections exhibit age plateaus that are high in their radiogenic component (98–100%) and have rather constant K/Ca ratios that are equal to or higher than the bulk-groundmass K/Ca ratios. We conclude that the contributions of alteration and $^{39}Ar_K$ recoil to the groundmass age plateaus are negligible, and that these age plateaus most likely represent degassing of the interstitial spaces (high K/Ca) instead of groundmass plagioclase (low K/Ca). In most cases, the plateau ages are concordant to their total fusion ages. The high temperature sections are further characterized by a spike in the release of $^{37}Ar_{Ca}$ paralleled by strong decreases in the K/Ca ratios, reflecting the preferential outgassing of the calcium-rich phases, such as clinopyroxene and plagioclase. Their low apparent ages are explained by either the recoil loss of $^{37}Ar_{Ca}$ or the redistribution of $^{39}Ar_K$ into the high temperature, low-potassium phases.

[68] In contrast, the release patterns for groundmass samples BWE-1, BAT-1 and GRA-1 yield no horizontal age spectra (Figure 4). The persisting effects of $^{39}Ar_K$ recoil in the alteration phases of the groundmass best explain these discordant experiments. If alteration increasingly contributes to the groundmasses, then $^{39}Ar_K$ recoil will result in decreasing age spectra from high apparent ages in the low temperature sections to low apparent ages in the high temperature sections, not exhibiting age plateaus. This effect will be even more significant considering the low-potassium nature of these groundmasses (K/Ca < 0.2 [*Koppers*, 1998]).

Appendix B

B1. Effects of Acid Leaching on Whole Rock Samples

[69] The main difficulty in the geochemical study of ancient seamount basalts is the common occurrence of alteration products in their groundmass. The amount of low temperature alteration in these submarine samples is completely determined by the proximity of seawater—an important source of K, Rb, Sr and U [*Corliss*, 1970; *Hart*, 1969; *Honnorez*, 1981; *Staudigel and Hart*, 1983]. A continued exposure to seawater leads to the progressive weathering of Tertiary and, in particular, Cretaceous submarine basalts [*Corliss*, 1970; *Hart*, 1969]. For example, low temperature alteration increases the $^{87}Sr/^{86}Sr$ ratios [*Spooner*, 1976; *Staudigel and Hart*, 1983; *Cheng et al.*, 1987] and, over longer periods of time, it may also decrease the $^{143}Nd/^{144}Nd$ ratios and LREE [*Staudigel and Hart*, 1983; *Cheng et al.*, 1987]. In here we will assess the success of acid leaching on basaltic samples in minimizing such alteration signatures in their Sr-Nd-Pb isotopes and major-trace element geochemistry. The acid leaching procedures were already outlined in section 3.2; the discussed data are listed in Table 2 (isotopes) and Appendix D (major and trace elements).

B2. Acid Leaching for Sr-Nd-Pb Isotope Geochemistry

[70] Figure B1 presents the $^{87}Sr/^{86}Sr_{(i)}$ ratios from multiple phases in 9 different samples of Golden Dragon, Hemler, HIMU, Lobbadede and N-Wod-En guyot. Seawater alteration is evident for the "unleached" whole rock powders (UWR) since they always display higher $^{87}Sr/^{86}Sr_{(i)}$ ratios than their acid-leached whole rock powders (LWR) and minerals. Seawater alteration also caused a lowering in the $^{143}Nd/^{144}Nd_{(i)}$ ratios [*Cheng et al.*, 1987] as observed for the "unleached" samples HIM-1 (UWR = 0.512780; CPX = 0.512888) and HIM-4 (UWR = 0.512900; HBL = 0.512994). These systematics illustrate the effective removal of alter-

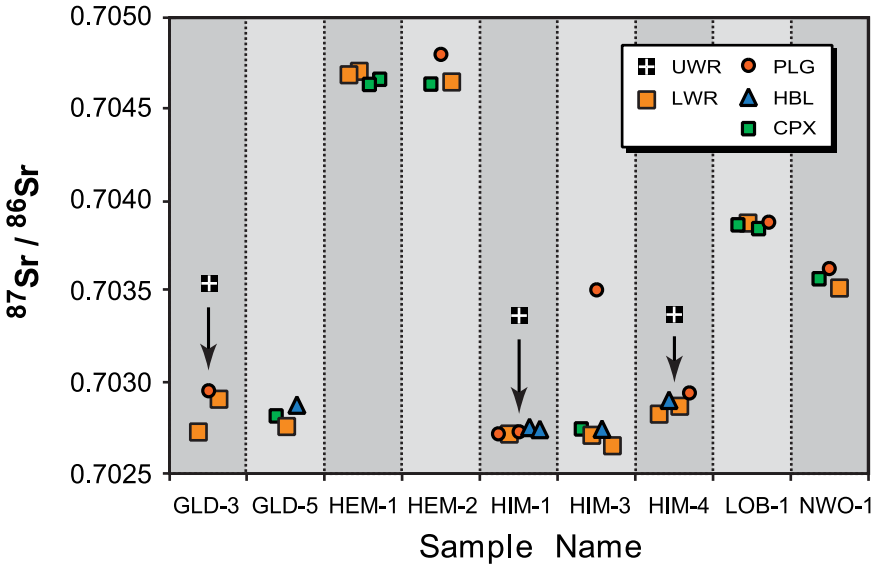

Figure B1. Acid leaching effects on $^{87}Sr/^{86}Sr$ for different types of basaltic phases. Note the pronounced down-shift from unleached whole rock signatures to acid-leached mineral and whole rock signatures. Data are listed in Table 2.

ation (Cretaceous seawater $^{87}Sr/^{86}Sr$ ~0.7072) due to acid leaching of the basaltic rock and its mineral phases. This removal is also implied by the consistency in $^{87}Sr/^{86}Sr$, $^{143}Nd/^{144}Nd$ and $^{206}Pb/^{204}Pb$ ratios measured for comagmatic mineral phases (see Table B1).

[71] The $^{87}Sr/^{86}Sr_{(i)}$ ratios for some LWR are lower compared to their mineral phases. From this observation we conclude that Rb introduced by seawater alteration may not always be entirely removed by acid leaching. The measured Rb/Sr ratios, therefore, are slightly higher than the primary Rb/Sr ratios of the basalt residues and cause an overcorrection for radiogenic ingrowth and decrease the $^{87}Sr/^{86}Sr_{(i)}$ ratios. This presumes that the mineral phases measured (e.g., clinopyroxene, hornblende) are not significantly changed by alteration. However, in a few cases (HIM-3 plagioclase, HEM-2 nepheline) the mineral phases still show anomalously high $^{87}Sr/^{86}Sr$ ratios, indicating that alteration (authegenic feldspars

Table B1. Reproducibility of Sr-Nd-Pb Isotope Measurements for Comagmatic Minerals[a]

		Phase Count				Initial Ratios					
Lab Code	Seamount Name	CPX	HBL	PLAG	LWR	$^{87}Sr/^{86}Sr$	n	$^{143}Nd/^{144}Nd$	n	$^{206}Pb/^{204}Pb$	n
GLD-5	Golden Dragon	1	1		1			0.512781 ± 25	3		
HEM-1	Hemler	2				0.704653 ± 18	2	0.512641 ± 1	2	18.75 ± 15	2
HEM-2	Hemler	1			1	0.704647 ± 4	2	0.512639 ± 14	2		
HIM-1	HIMU		2	2	1	0.702727 ± 10	5	0.512781 ± 6	4	20.31 ± 2	2
HIM-2	HIMU	1	2			0.512786 ± 3	3				
HIM-3	HIMU	1	1	1	2	0.702709 ± 43	4	0.512783 ± 10	3	20.24 ± 19	2
ITA-1	Ita Mai Tai			1	1	0.512503 ± 46	2				
JLW-1	Jalwoj	2				0.703626 ± 13	2	0.512732 ± 8	2	18.90 ± 6	2
LOB-1	Lobadede	2		1	1	0.703864 ± 17	3	0.512570 ± 6	2	19.12 ± 1	2
LOO-2	Look	1			1	0.702861 ± 4	2	0.512711 ± 1	2		
NWO-2	N-Wod-En	2		1	1	0.703571 ± 51	3	0.512768 ± 6	3	19.61 ± 14	2
PAK-1	Pako	1		1	1	0.705147 ± 74	3	0.512450 ± 1	2	18.40 ± 2	3
OMA-1	Vlinder			1	1	0.704453 ± 44	2			17.93 ± 16	2
VLI-4	Vlinder			1	1	0.704470 ± 27	2			18.21 ± 24	2
VLI-5	Vlinder	1	1		1			0.512648 ± 32	2	18.77 ± 3	2

[a] For mass fractionation corrections, standard values and within-run errors see Table 2.

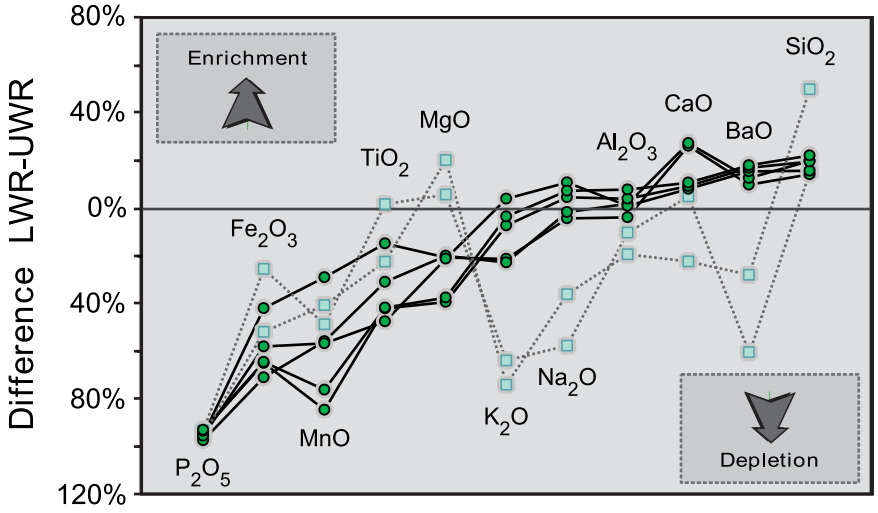

Figure B2. Depletion diagram for major elements. The elements are plotted in ascending order from the largest depletion to the largest enrichment in the hawaiites (green circles). Hornblende basanites are denoted by light blue squares. Data are listed in Appendix C.

and clays) was not completely removed by acid leaching. The measured range in $^{87}Sr/^{86}Sr_{(i)}$ ratios is nevertheless small (<0.0002, without UWR), in particular, when considering the complete range of $^{87}Sr/^{86}Sr_{(i)}$ compositions measured for the WPSP basalts (0.7025–0.7075; Figure 6, 7). Similar relations hold for the $^{143}Nd/^{144}Nd$ and Pb-isotope ratios indicating that acid leaching minimizes the isotopic alteration signatures in the altered WPSP basalts and minerals.

B3. Acid Leaching for Major and Trace Geochemistry

[72] In Figures B2 and B3 the depletion-enrichment of the LWR analyses with respect to UWR

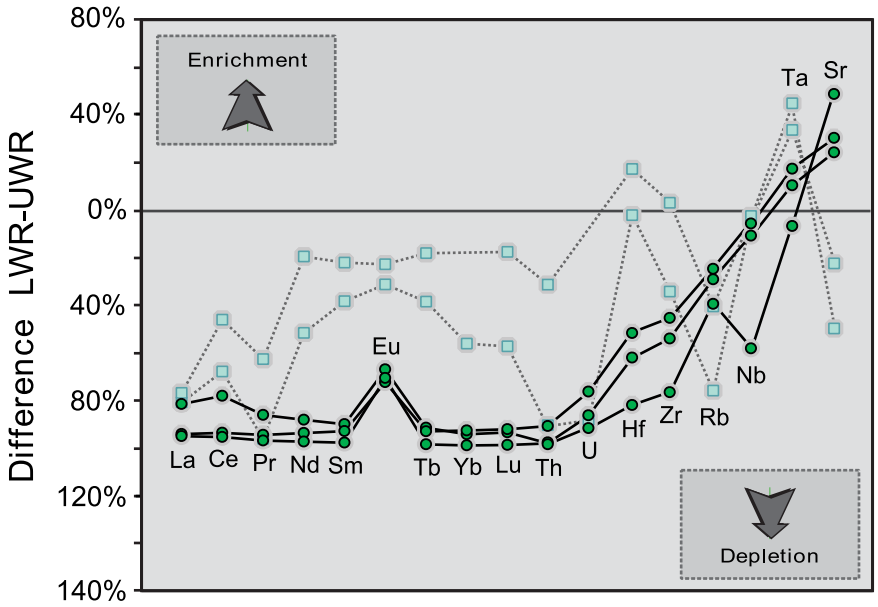

Figure B3. Depletion diagram for REE (La-Ce-Pr-Nd-Sm-Eu-Yb-Lu) and a selection of trace elements (Sr-Rb-Th-U-Ta-Nb-Zr-Hf). The elements are plotted in ascending order (except Eu) from the largest depletion to the largest enrichment in the hawaiites (green circles). Hornblende basanites are denoted by light blue squares. Data are listed in Appendix C.

analyses are plotted for major and trace elements. In these diagrams an overall depletion of P_2O_5, Fe_2O_3, MnO, TiO_2, MgO and most of the trace elements is evident. These depletions increase in stronger leaching experiments and for some elements are almost complete (P_2O_5 and all REE). The profound negative spike for P_2O_5, U and Th may be explained by the preferential dissolution of groundmass (apatite) and secondary phosphates in the residues. In addition, the loss of ignition (LOI in Appendix C) was decreased by 29 ± 16% indicating that leaching (partially) removed the hydrated alteration minerals (clays, zeolites, phosphates). This is also indicated by depletions of Cs (59 ± 27%) and Rb (34 ± 26%), which are elements typically introduced by seawater alteration [*Honnorez*, 1981]. All these observations point to the preferential dissolution of altered groundmass in the acid-leached basalts [cf. *Cheng et al.*, 1987].

[73] Rock type, on the other hand, seems to control the extent to which elements remain in the residues. For the hawaiites an enrichment of Sr and BaO is apparent. Also note here that the overall depletion of the REEs results in a positive Eu-anomaly due to an increased modal plagioclase in the leaching residue. However, for the hornblende basanites an enrichment of MgO, TiO_2 (compared to the hawaiites), Ta, Nb, Zr and Hf is apparent. In both cases, the enrichments may be explained by the predominance of phenocrystic phases (plagioclase; hornblende) in the major and trace element inventory of the acid leaching residues.

[74] In conclusion, the geochemical systematics of the unleached and acid-leached powders suggest that the parent-daughter ratios in the leaching residues reflect the proportion of plagioclase over clinopyroxene in the basalts, and not that of alteration products in the groundmass. Moreover, the depletion of Sm-Nd and U-Th-Pb to low concentrations during leaching suggests that Sm/Nd, U/Pb and Th/Pb ratios of the residues resemble primary (mineral) ratios. The significant decrease in the Rb/Sr ratios during acid leaching also seems due to phase removal, rather than chemical fractionation during acid leaching [*Cheng et al.*, 1987]. We can, therefore, perform approximate corrections for radiogenic ingrowth in acid-leached basaltic samples.

Appendix C: $^{40}Ar/^{39}Ar$ Analytical Data

[75] The reduced data for each performed $^{40}Ar/^{39}Ar$ analyses are listed in separate data tables, organized according to seamount name.[1] The $^{40}Ar/^{39}Ar$ data tables in this appendix are divided into three sections: (1) sample information, (2) data from the incremental heating analyses, and (3) the age results. A few data tables include data from duplicate analyses or total fusion experiments (as notified in the tables). The data listed for the $^{40}Ar/^{39}Ar$ experiments are as follows:

argon laser wattage (or temperature in degrees Celsius)	in W
atmospheric component in ^{36}Ar	$^{36}Ar(a)$
calcium-derived ^{37}Ar	^{37}Ar
chlorine-derived component in ^{38}Ar	$^{38}Ar(cl)$
potassium-derived component in ^{39}Ar	$^{39}Ar(k)$
sum of radiogenic and atmospheric components in ^{40}Ar	$^{40}Ar^*(a)$
increment size	^{39}Ar in%
percentage radiogenic component in ^{40}Ar	$^{40}Ar^*$ in%
molar K/Ca ratio	K/Ca
weighted $^{40}Ar/^{39}Ar$ age and 2σ uncertainty plus error in J - value	in Ma
$^{40}Ar/^{36}Ar$ isochron intercept and 2σ uncertainty mean squared weighted deviation	MSWD
number of increments included in age calculation	n

The crosses "**X**" in the data section identify those increments used to calculate the plateau age, whereas the letters "**Z**" denote increments (within error to the plateau age) added for the isochron calculation. MSWD's for the plateau and inverse isochron ages were calculated based on [N-1] and [N-2] degrees of freedom, respectively. For a data compilation see Table 1. This data set can also be downloaded from the EarthRef Digital Archive by

[1] Supporting appendices are available at ftp://agu.org/apend/gc/2003GC000533.

following the http://earthref.org/cgi-bin/erda.cgi?n=148 link.

Appendix D: Major and Trace Element Data

[76] In this Appendix we present the geochemical data for unleached (UWR) and acid-leached (LWR) whole rock basalts as determined by XRF, INA, ICP-MS and ICP-AES. For details concerning analytical procedures and the accuracy of the presented data, the reader is referred to *Koppers* [1998]. The major elements were determined using XRF with the exception of BaO (ICP-MS) or BaO, Fe2O3, CaO and Na2O (INA). The trace elements were determined using ICP-MS, XRF or INA (Eu, Lu and Sm; light-gray background). This data set can also be downloaded from the EarthRef Digital Archive by following the http://earthref.org/cgi-bin/erda.cgi?n=149 link.

Acknowledgments

[77] We thank Jason Phipps Morgan and Jason Morgan for many discussions on absolute Pacific plate motions. Dave Sandwell's help with GMT was greatly appreciated. Jim Hein and Alicé Davis of the USGS, Warren Smith of the Scripps Institution of Scripps rock depository and Y. Pushcharovsky of the USSR Academy of Sciences are thanked for providing key samples to this study. Most of the material in this paper is based on the Ph.D. thesis of AAPK at the Vrije Universiteit Amsterdam, which provided the analytical facilities and a dynamic research group, including Gareth Davies and Ed Verdurmen. This work was supported by NWO, the Netherlands Foundation of Scientific Research (NWO Project 750.60.005) and NSF grants (OCE 91-02183; 97-30394). Samples were collected during the TUNES04 and TUNES06 expeditions of the Scripps Institution of Oceanography (HS), the R/V *Moana Wave* MW8805 expedition of the Hawaiian Institute of Geophysics (F. K. Duennebier and S. O. Schlanger, MW88-05 Marshall Islands guyots cruise report, April 24–May 30 1988, Guam to Guam, unpublished report, 80 pp., 1988), and the R/V *Farnella* F1089CP expedition of the United States Geological Survey and KORDI (Hein et al., unpublished report, 1990). Samples were also obtained from ODP Leg 143 [*Sager et al.*, 1993a] and Leg 144 [*Premoli Silva et al.*, 1993], from the ZETES IV expedition of the Scripps Institution of Oceanography, and from the R/V *Conrad* cruise 2610 and R/V *Vema* cruise 33–12 of the Lamont-Doherty Geological Observatory. We like to thank Bob Duncan, Anne Davaille and Chatherine Chauvel for thoughtful and detailed reviews that helped to improve this manuscript.

References

Abrams, L. J., R. L. Larson, T. H. Shipley, and Y. Lancelot, Cretaceous volcanic sequences and Jurassic oceanic crust in the east Mariana and Pigafetta basins of the Western Pacific, in *The Mesozoic Pacific: Geology, Tectonics, and Volcanism*, *Geophys. Monogr. Ser.*, vol. 77, edited by M. S. Pringle et al., pp. 77–101, AGU, Washington, D. C., 1993.

Albers, M., and U. R. Christensen, The excess temperature of plumes rising from the core-mantle boundary, *Geophys. Res. Lett.*, *23*, 3567–3570, 1996.

Allègre, C. J., and D. L. Turcotte, Implications of a two component marble cake mantle, *Nature*, *323*, 123–127, 1986.

Anderson, D. L., Top-down tectonics?, *Science*, *293*, 2016–2018, 2001.

Anderson, D. L., Plate tectonics as a far-from-equilibrium self-organized system, in *Plate Boundary Zones*, *Geodyn. Ser.*, vol. 30, edited by S. Stein and J. Freymueller, pp. 411–425, 2002.

Anguita, F., and F. Hernan, A propagating fracture model versus a hotspot origin for the Canary Islands, *Earth Planet. Sci. Lett.*, *27*, 11–19, 1975.

Aslanian, D., L. Geli, and J.-L. Olivet, Hotspotting called into question, *Nature*, *396*, 127, 1998.

Bemis, K. G., and D. K. Smith, Production of small volcanoes in the Superswell region of the south Pacific, *Earth and Planetary Science Lett.*, *118*: *251–262*, 1993.

Bergersen, D. D., Cretaceous hotspot tracks through the Marshall Islands, *Proc. Ocean Drill. Program Sci. Results*, *144*, 605–613, 1995.

Bonatti, E., Not so hot "hotspots" in the oceanic mantle, *Science*, *250*, 107–111, 1990.

Bonatti, E., and C. G. A. Harrison, Hotlines in the Earth's mantle, *Nature*, *263*, 402–404, 1976.

Bonneville, A., and M. McNutt, Shear strength of the great Pacific fracture zones, *J. Geophys. Res.*, *19*, 2023–2026, 1992.

Cande, S. C., and D. V. Kent, A new geomagnetic polarity time scale for the Late Cretaceous and Cenozoic, *J. Geophys. Res.*, *97*, 13,917–13,951, 1992.

Cande, S. C., C. A. Raymond, J. Stock, and W. F. Haxby, Geophysics of the Pitman fracture zone and Pacific-Antarctic plate motions during the Cenzoic, *Science*, *207*, 947–953, 1995.

Castillo, P. R., The Dupal anomaly as a trace of the upwelling lower mantle, *Nature*, *336*, 667–670, 1988.

Castillo, P. R., P. A. Floyd, and C. France-Lanord, Isotope geochemistry of Leg 129 basalts: Implications for the origin of the widespread Cretaceous volcanic event in the Pacific, *Proc. Ocean Drill. Program Sci. Results*, *129*, 405–513, 1992.

Cazenave, A., and C. Thoraval, Mantle dynamics constrained by degree 6 surface topography, seismic tomography and geoid: Inference on the origin of the south Pacific superswell, *Earth Planet. Sci. Lett.*, *122*, 207–219, 1994.

Chauvel, C., A. W. Hofmann, and P. Vidal, HIMU-EM: The French Polynesian connection, *Earth Planet. Sci. Lett.*, *110*, 99–119, 1992.

Chen, C.-Y., and F. A. Frey, Origin of Hawaiian tholeiite and alkalic basalt, *Nature*, *302*, 785–789, 1983.

Cheng, Q., K.-H. Park, J. D. MacDougall, A. Zindler, G. W. Lugmair, J. Hawkins, P. Lonsdale, and H. Staudigel, Isotopic evidence for a hotspot origin of the Louisville seamount chain, in *Seamounts, Islands and Atolls*, *Geophys. Monogr. Ser.*, vol. 43: edited by B. H. Keating et al., pp. 283–296, AGU, Washington, D. C., 1987.

Christie, D. M., J. J. Dieu, and J. S. Gee, Petrologic studies of basement lavas from northwest Pacific guyots, *Proc. Ocean Drill. Program Sci. Results*, *144*, 495–512, 1995.

Clague, D. A., G. B. Dalrymple, T. L. Wright, F. W. Klein, R. Y. Koyanagi, R. Decker, and D. W. Thomas, The Hawaiian-Emperor chain, in *The Eastern Pacific Ocean and Hawaii: The Geology of North America*, edited by E. L. Winterer, D. M. Hussong, and R. W. Decker, pp. 187–287, Geol. Soc. Am., Boulder, Colo., 1989.

Clouard, V., and A. Bonneville, How many Pacific hotspots are fed by deep-mantle plumes?, *Geology*, *29*, 695–698, 2001.

Corliss, J. B., The origin of metal-bearing submarine hydrothermal solutions, *J. Geophys. Res.*, *76*, 8128–8138, 1970.

Crough, S. T., Thermal origin of mid-plate hotspot swells, *Geophys. J. R. Astron. Soc.*, *55*, 451–469, 1978.

Courtillot, V., A. Davaille, J. Besse, and J. Stock, Three distinct types of hotspots in the Earth's mantle, *Earth Planet. Sci. Lett.*, *205*, 295–308, 2002.

Dalrymple, G. B., and J. G. Moore, Argon-40: Excess in submarine pillow basalts from Kilauea volcano, Hawaii, *Science*, *161*, 1132–1135, 1968.

Dana, J. D., Geology, in *United States Exploring Expedition 10: Philadelphia (C. Sherman) With Atlas*, edited by C. Wilkes, 756 pp., Putnam, New York, 1849.

Darwin, C., On certain areas of elevation and subsidence in the Pacific and Indian Oceans, as deduced from the study of coral formations, *J. Geol. Soc. London*, *2*, 552–554, 1837.

Darwin, C., The structure and distribution of coral reefs, 344 pp., Appleton, New York, 1842.

Davaille, A., Simultaneous generation of hotspots and superswells by convection in a heterogeneous planetary mantle, *Nature*, *402*, 756–760, 1999.

Davaille, A., F. Girard, and M. Le Bars, How to anchor hotspots in a convecting mantle, *Earth Planet. Sci. Lett.*, *203*, 621–634, 2002.

Davaille, A., M. Le Bars, and C. Carbonne, Thermal convection in a heterogeneous mantle, *Comptes Rendus Geosci.*, *335*, 141–156, 2003.

Davis, A. S., M. S. Pringle, L.-B. G. Pickthorn, D. A. Clague, and W. C. Schwab, Petrology and age of alkalic lava from the Ratak chain of the Marshall Islands, *J. Geophys. Res.*, *94*, 5757–5774, 1989.

Davis, A. S., L. B. Gray, D. A. Clague, and J. R. Hein, The Line Islands revisited: New $^{40}Ar/^{39}Ar$ geochronologic evidence for episodes of volcanism due to lithospheric extension, *Geochem. Geophys. Geosyst.*, *3*(3), 1018, doi:10.1029/2001GC000190, 2002.

DePaolo, D. J., and M. Manga, Deep origin of hotspots: The mantle plume model, *Science*, *300*, 920–921, 2003.

Detrick, R. S., and S. T. Crough, Island, subsidence, hotspots, and lithospheric thinning, *J. Geophys. Res.*, *83*, 1236–1244, 1978.

Dickinson, W. R., Geomorphology and geodynamics of the Cook-Austral island-seamount chain in the South Pacific Ocean: Implications for hotspots and plumes, *Int. Geol. Rev.*, *40*, 1039–1075, 1998.

Duncan, R. A., and D. A. Clague, Pacific plate motion recorded by linear volcanic chains, in *The Ocean Basins and Margins*, edited by A. E. A. Nairn, F. L. Stehli, and S. Uyeda, pp. 89–121, Plenum, New York, 1985.

Duncan, R. A., and M. A. Richards, Hotspots, mantle plumes, flood basalts, and true polar wander, *Rev. Geophys.*, *29*, 31–50, 1991.

Duncan, R. A., M. T. McCulloch, H. Barszus, and D. R. Nelson, Plume versus lithosphere sources for melts at Ua Pou, Marquesas Islands, *Nature*, *322*, 534–538, 1986.

Dupuy, C., P. Vidal, R. C. Maury, and G. Guille, Basalts from Mururoa, Fangataufa and Gambier islands (French Polynesia): Geochemical dependence on the age of the lithosphere, *Earth Planet. Sci. Lett.*, *117*, 89–100, 1993.

Engebretson, D. C., A. Cox, and R. G. Gordon, Relative motions between oceanic and continental plates in the Pacific basin, *Spec. Pap. Geol. Soc. Am.*, *206*, 59, 1985.

Epp, D., Possible perturbations to hotspot traces and implications for the origin and structure of the Line Islands, *J. Geophys. Res.*, *89*, 11,273–11,286, 1984.

Erba, E., I. Premoli Silva, and D. K. Watkins, Cretaceous calcareous plankton biostratigraphy of Sites 872 through 879, *Proc. Ocean Drill. Program Sci. Results*, *144*, 157–169, 1995.

Farley, K. A., J. H. Natland, and H. Craig, Binary mixing of enriched and undegassed (primitive?) mantle components (He, Sr, Nd, Pb) in Samoan lavas, *Earth Planet. Sci. Lett.*, *111*, 183–199, 1992.

Favela, J., and D. L. Anderson, Extensional tectonics and global volcanism, in *Problems in Geophysics for the New Millennium*, edited by E. Boschi, G. Ekstrom, and A. Morelli, pp. 463–498, Ed. Compositori, Bologna, Italy, 2000.

Fleck, R. J., J. F. Sutter, and D. H. Elliot, Interpretation of discordant $^{40}Ar/^{39}Ar$ age-spectra of Mesozoic tholeiites from Antarctica, *Geochim. Cosmochim. Acta*, *41*, 15–32, 1977.

Foulger, G. R., and J. H. Natland, Is "hotspot" volcanism a consequence of plate tectonics?, *Science*, *300*, 921–922, 2003.

Gans, K. D., D. S. Wilson, and K. C. Macdonald, Pacific Plate gravity lineaments: Diffuse extension or thermal contraction?, *Geochem. Geophys. Geosyst.*, *4*(9), 1074, doi:10.1029/2002GC000465, 2003.

Geli, L., D. Aslanian, J.-L. Olivet, I. Vlastelic, L. Dosso, H. Guillou, and H. Bougault, Location of Louisville hotspot and origin of Hollister ridge: Geophysical constraints, *Earth Planet. Sci. Lett.*, *164*, 31–40, 1998.

Gordon, R. G., and C. D. Cape, Cenozoic latitudinal shift of the Hawaiian hotspot and its implications for true polar wander, *Earth Planet. Sci. Lett.*, *153*, 171–180, 1981.

Gu, Y. J., A. M. Dziewonski, W. J. Su, and G. Ekstrom, Models of the mantle shear velocity and discontinuities in the pattern of lateral heterogeneities, *J. Geophys. Res.*, *106*, 11,169–11,189, 2001.

Haase, K. M., The relationship between the age of the lithosphere and the composition of oceanic magmas: Constraints on partial melting, mantle sources and the thermal structure of the plates, *Earth Planet. Sci. Lett.*, *144*, 75–92, 1996.

Haggerty, J. A., and I. Premoli Silva, Comparison of the origin and evolution of northwest Pacific guyots drilled during Leg 144, *Proc. Ocean Drill. Program Sci. Results*, *144*, 935–949, 1995.

Harada, Y., and Y. Hamano, Recent progress on the plate motion relative to the hotspots, in *The History and Dynamics of Global Plate Motions*, *Geophys. Monogr. Ser.*, vol. 121, edited by M. A. Richards, R. G. Gordon, and R. D. van der Hilst, pp. 327–338, AGU, Washington, D. C., 2000.

Hart, S. R., K, Rb, Cs contents and K/Rb, K/Cs ratios of fresh and altered submarine basalts, *Earth Planet. Sci. Lett.*, *6*, 295–303, 1969.

Hart, S. R., A large scale isotope anomaly in the Southern Hemisphere mantle, *Nature*, *309*, 753–757, 1984.

Hart, S. R., et al., Vailulu'u undersea volcano: The new Samoa, *Geochem. Geophys. Geosyst.*, *2*, Paper number 2000GC000108, 2000.

Hauri, E. H., and S. R. Hart, Re-Os isotope systematics of HIMU and EMII oceanic island basalts from the south Pacific Ocean, *Earth Planet. Sci. Lett.*, *114*, 353–371, 1993.

Hauri, E. H., W. Shimizu, J. J. Diru, and S. R. Hart, Evidence for hot spot-related carbonatic metasomatism in the oceanic upper mantle, *Nature*, *365*, 221–227, 1993.

Hauri, E. H., J. A. Whitehead, and S. R. Hart, Fluid dynamic and geochemical aspects of entrainment in mantle plumes, *J. Geophys. Res.*, *99*, 24,275–24,300, 1994.

Hawkins, J. W., P. F. Lonsdale, and R. Batiza, Petrologic evolution of the Louisville seamount chain, in *Seamounts, Islands and Atolls*, *Geophys. Monogr. Ser.*, vol. 43, edited by B. H. Keating, P. Fryer, and R. Batiza, pp. 235–254, AGU, Washington, D. C., 1987.

Henderson, L. J., Motion of the Pacific plate relative to the hotspots since the Jurassic and model of oceanic plateaus of the Farallon plate, Ph.D. thesis, 312 pp., Norwestern Univ., Evanston, Ill., 1985.

Henderson, L. J., and R. G. Gordon, Fixed hotspots and recurrent volcanism along the Line Islands chain, *Geol. Soc. Am. Abstr. Programs*, *14*, 513, 1982.

Hess, H. H., Drowned ancient islands of the Pacific basin, *Am. J. Sci.*, *244*, 772–791, 1946.

Hey, R. N., H. W. Menard, T. M. Atwater, and D. W. Caress, Changes in direction of seafloor spreading revisited, *J. Geophys. Res.*, *93*, 2803–2811, 1988.

Hieronymus, C. F., and D. Bercovici, Discrete, alternating hotspot islands formed by interaction of magma transport and lithospheric flexure, *Nature*, *397*, 604–607, 1999.

Hieronymus, C. F., and D. Bercovici, Non-hotspot formation of volcanic chains: Control of tectonic and flexural stresses on magma transport, *Earth Planet. Sci. Lett.*, *181*, 539–554, 2000.

Hofmann, A. W., and W. M. White, Mantle plumes from ancient oceanic crust, *Earth Planet. Sci. Lett.*, *57*, 421–436, 1982.

Honnorez, J., The aging of the oceanic crust at low temperature, in *The Sea*, edited by C. Emiliani, 525–587, John Wiley, Hoboken, N. J., 1981.

Jackson, E. D., Linear volcanic chains on the Pacific plate, in *The Geophysics of the Pacific Ocean Basin and its Margins*, *Geophys. Monogr. Ser.*, vol. 19, edited by G. H. Sutton, M. H. Manghnani, and R. Moberly, pp. 319–336, AGU, Washington, D. C., 1976.

Jackson, E. D., and H. R. Shaw, Stress fields in central portions of the Pacific plate: Delineated in time by linear volcanic chains, *J. Geophys. Res.*, *80*, 1861–1874, 1975.

Janney, P. E., P. R. Castillo, and P. E. Baker, Petrology and geochemistry of basaltic clasts and hyaloclastites from volcaniclastic sediments at Site 869, *Proc. Ocean Drill. Program Sci. Results*, *143*, pp. 263–267, 1995.

Janney, P. E., P. R. Castillo, and R. Paterno, Isotope geochemistry of the Darwin Rise seamounts and the nature of long-term mantle dynamics beneath the south central Pacific, *J. Geophys. Res.*, *104*, 10,571–10,589, 1999.

Koppers, A. A. P., $^{40}Ar/^{39}Ar$ geochronology and isotope geochemistry of the West Pacific seamount province: Implications for absolute Pacific plate motions and the motion of hotspots, Ph.D. thesis, Vrije Univ., Amsterdam, Netherlands, 1998.

Koppers, A. A. P., ArArCALC—software for $^{40}Ar/^{39}Ar$ age calculations, *Comp. Geosci.*, *28*, 605–619, 2002. (Available at http://earthref.org/tools/ararcalc.htm)

Koppers, A. A. P., H. Staudigel, D. M. Christie, J. J. Dieu, and M. S. Pringle, Sr-Nd-Pb isotope geochemistry of Leg 144 west Pacific guyots: Implications for the geochemical evolution of the "SOPITA" mantle anomaly, *Proc. Ocean Drill. Program Sci. Results*, *144*, 535–545, 1995.

Koppers, A. A. P., H. Staudigel, J. R. Wijbrans, and M. S. Pringle, The Magellan seamount trail: Implications for Cretaceous hotspot volcanism and absolute Pacific plate motion, *Earth Planet. Sci. Lett.*, *163*, 53–68, 1998.

Koppers, A. A. P., H. Staudigel, and J. R. Wijbrans, Dating crystalline groundmass separates of altered Cretaceous seamount basalts by the $^{40}Ar/^{39}Ar$ incremental heating technique, *Chem. Geol.*, *166*, 139–158, 2000.

Koppers, A. A. P., J. Phipps Morgan, W. J. Morgan, and H. Staudigel, Testing the fixed hotspot hypothesis using $^{40}Ar/^{39}Ar$ age progressions along seamount trails, *Earth Planet. Sci. Lett.*, *185*, 237–252, 2001.

Larson, R. L., Geological consequences of superplumes, *Geology*, *19*, 963–966, 1991.

Larson, R. L., E. Erba, M. Nakanishi, D. D. Bergersen, and J. M. Lincoln, Stratigraphic, vertical subsidence, and paleolatitude histories of Leg 144 guyots, *Proc. Ocean Drill. Program Sci. Results*, *144*, 915–933, 1995.

Lincoln, J. M., M. S. Pringle, and I. Premoli Silva, Early and Late Cretaceous Volcanism and reef-building in the Marshall Islands, in *The Mesozoic Pacific: Geology, Tectonics, and Volcanism*, *Geophys. Monogr. Ser.*, vol. 77, edited by M. S. Pringle et al., pp. 279–305, AGU, Washington, D. C., 1993.

Lonsdale, P., Geography and history of the Louisville hotspot chain in the southwest Pacific, *J. Geophys. Res.*, *93*, 3078–3104, 1988.

Maia, M., and M. Diament, An analysis of the altimetric geoid in various wavebands in the Central Pacific ocean: Constraints on the origin of intraplate features, *Tectonophysics*, *190*, 133–153, 1991.

McDonough, W. F., and C. Chauvel, Sample contamination explains the PB isotopic composition of some Rurutu island and Sasha seamount basalts, *Earth Planet. Sci. Lett.*, *105*, 397–404, 1991.

McDonough, W. F., S. Sun, A. E. Ringwood, E. Jagoutz, and A. W. Hofmann, K, Rb and Cs in the Earth and moon and the evolution of the Earth's mantle, *Geochim. Cosmochim. Acta*, *56*, 1001–1012, 1992.

McDougall, I., Postassium-argon ages from lavas of the Hawaiian Islands, *Geol. Soc. Am. Bull.*, *75*, 107–128, 1964.

McDougall, I., Volcanic island chains and sea floor spreading, *Nature*, *231*, 141–144, 1971.

McDougall, I., and R. A. Duncan, Linear volcanic chains: Recording plate motions?, *Tectonophysics*, *63*, 275–295, 1980.

McNutt, M. K., Superswells, *Rev. Geophys*, *36*, 211–244, 1998.

McNutt, M., and K. M. Fischer, The South Pacific superswell, in *Seamounts, Islands and Atolls*, *Geophys. Monogr. Ser.*, vol. 43, edited by B. H. Keating, P. Fryer, R. Batiza, and G. W. Boehlert, pp. 25–34, AGU, Washington, D. C., 1987.

McNutt, M. K., and A. V. Judge, The superswell and mantle dynamics beneath the South Pacific, *Science*, *248*, 969–975, 1990.

McNutt, M. K., L. Sichoix, and A. Bonneville, Modal depths from shipboard bathymetry: There IS a south Pacific Superswell, *Geophys. Res. Lett.*, *23*, 3397–3400, 1996.

McNutt, M. K., D. W. Caress, J. Reynolds, K. A. Jordahl, and R. A. Duncan, Failure of plume theory to explain midplate volcanism in the southern Austral islands, *Nature*, *389*, 479–482, 1997.

Menard, H. W., Marine geology of the Pacific, 271 pp., McGraw-Hill, New York, 1964.

Menard, H. W., Darwin reprise, *J. Geophys. Res.*, *89*, 9960–9968, 1984a.

Menard, H. W., Origin of guyots: The Beagle to Seabeam, *J. Geophys. Res.*, *89*, 11,117–11,123, 1984b.

Morgan, W. J., Convection plumes in the lower mantle, *Nature*, *230*, 42–43, 1971.

Morgan, W. J., Deep mantle convection plumes and plate motions, *Am. Assoc. Petrol. Geol. Bull.*, *56*, 42–43, 1972a.

Morgan, W. J., Plate motions and deep mantle convection, *Geol. Soc. Am. Mem.*, *132*, 7–122, 1972b.

Nagihara, S., C. R. B. Lister, and J. G. Sclater, Reheating of old lithosphere: Deductions from observations, *Earth Planet. Sci. Lett.*, *139*, 91–104, 1996.

Nakamura, Y., and M. Tatsumoto, Pb, Nd, and Sr isotopic evidence for a multicomponent source for rocks of Cook-Austral Islands and heterogeneities of mantle plumes, *Geochim. Cosmochim. Acta*, *52*, 2909–2924, 1988.

Nakanishi, M., Topographic expression of five fracture zones in the northWestern Pacific Ocean, in *The Mesozoic Pacific: Geology, Tectonics, and Volcanism*, *Geophys. Monogr. Ser.*, vol. 77, edited by M. S. Pringle et al., 121–136, 1993.

Nakanishi, M., K. Tamaki, and K. Kobayashi, Magnetic anomaly lineations from late Jurassic to Early Cretaceous in the west-central Pacific Ocean, *Geophys. J. Int.*, *144*, 535–545, 1992.

Nikishin, A. M., P. A. Ziegler, D. Abbott, M.-F. Brunet, and S. Cloetingh, Permo-Triassic intra-plate magmatism and rifting in Eurasia: Implications for mantle plumes and mantle dynamics, *Tectonophysics*, *351*, 3–39, 2002.

Norton, I. O., Global hotspot reference frames and plate motion, in *The History and Dynamics of the Global Plate Motions*, *Geophys. Monogr. Ser.*, vol. 121, edited by M. A. Richards, R. G. Gordon, and R. D. van der Hilst, pp. 339–357, AGU, Washington, D. C., 2000.

O'Connor, J. M., P. Stoffers, and J. R. Wijbrans, Migration rate of volcanism along the Foundation chain, SE Pacific, *Earth Planet. Sci. Lett.*, *164*, 41–59, 1998.

Ozima, M., M. Honda, and K. Saito, $^{40}Ar/^{39}Ar$ ages of guyots in the Western Pacific and discussion of their evolution, *Earth Planet. Sci. Lett.*, *51*, 475–485, 1977.

Palacz, Z., and A. D. Saunders, Coupled trace element and isotope enrichment in the Cook-Austral-Samoa Islands, southwest Pacific, *Earth Planet. Sci. Lett.*, *79*, 270–280, 1986.

Parsons, B., and J. G. Sclater, An analysis of the variation of ocean floor bathymetry and heat flow with age, *J. Geophys. Res.*, *82*, 803–827, 1977.

Phipps Morgan, J., Thermodynamics of pressure release melting of a veined plum pudding mantle, *Geochem. Geophys. Geosyst.*, *2*, Paper number 2000GC000049, 2001.

Phipps Morgan, J., and W. J. Morgan, Two-stage melting and the geochemical evolution of the mantle: A recipe for mantle plum-pudding, *Earth Planet. Sci. Lett.*, *170*, 215–239, 1999.

Premoli Silva, I., J. Haggerty, and F. Rack, *Proceedings of the Ocean Drilling Program, Initial Reports*, vol. 144, Ocean Drilli. Program, College Station, Tex., 1993.

Pringle, M. S., Geochronology and petrology of the Musicians seamounts, and the search of hotspot volcanism in the Cretaceous Pacific, Ph.D. Thesis, Univ. of Hawaii, Honolulu, 1992.

Pringle, M. S., Age progressive volcanism in the Musicians seamounts: A test of the hotspot hypothesis for the late Cretaceous Pacific, in *The Mesozoic Pacific: Geology, Tectonics, and Volcanism*, *Geophys. Monogr. Ser.*, vol. 77, edited M. S. Pringle et al., pp. 187–216, Washington, D. C., 1993.

Pringle, M. S., and G. B. Dalrymple, Geochronological constraints on a possible hotspot origin for Hess Rise and the Wentworth seamount chain, in *The Mesozoic Pacific: Geology, Tectonics, and Volcanism*, *Geophys. Monogr. Ser.*, vol. 77, edited M. S. Pringle et al., pp. 263–277, AGU, Washington, D. C., 1993.

Pringle, M. S., and R. A. Duncan, Radiometric ages of basement lavas recovered at Sites 865, 866, and 869, in *Proc. Ocean Drill. Program Sci. Results*, *143*, 277–283, 1995a.

Pringle, M. S., and R. A. Duncan, Radiometric ages of basement lavas recovered at Lo-En, Wodejebato, MIT, and Taikuyo-Daisan guyots, ODP Leg 144, northWestern Pacific ocean, *Proc. Ocean Drill. Program Sci. Results*, *144*, 547–557, 1995b.

Pringle, M. S., A. A. P. Koppers, H. Staudigel, and J. R. Wijbrans, Cretaceous Pacific volcanism: Distribution in space, time, and source composition, *U.S. Geol. Surv. Circ.*, *1107*, 256, 1994.

Roddick, J. C., The application of isochron diagrams in $^{40}Ar/^{39}Ar$ dating: A discussion, *Earth Planet. Sci. Lett.*, *41*, 233–244, 1978.

Romanowicz, B., and Y. Gung, Superplumes from the core-mantle boundary to the base of the lithosphere, *Science*, *296*, 513–516, 2002.

Sager, W. W., and U. Bleil, Latitudinal shift of Pacific hotspots during the late Cretaceous and early Tertiary, *Nature*, *326*, 488–490, 1987.

Sager, W. W., and M. S. Pringle, Paleomagnetic constraints on the origin and evolution of the Musicians and south Hawaiian seamounts, central Pacific Ocean, in *Seamounts, Islands and Atolls*, *Geophys. Monogr. Ser.*, vol. 43, edited by B. H. Keating et al., pp. 133–162, AGU, Washington, D.C., 1987.

Sager, W. W., et al., *Proceedings of the Ocean Drilling Program*, *Initial Reports*, vol. 143, Ocean Drill. Program, College Station, Tex., 1993a.

Sager, W. W., R. A. Duncan, and D. W. Handschumacher, Paleomagnetism of the Japanese and Marcus-Wake seamounts, Western Pacific Ocean, in *The Mesozoic Pacific: Geology, Tectonics, and Volcanism*, *Geophys. Monogr. Ser.*, vol. 77, edited M. S. Pringle et al., pp. 401–435, AGU, Washington, D. C., 1993b.

Sandwell, D. T., E. L. Winterer, J. Mammerickx, R. A. Duncan, M. A. Lynch, D. Levitt, and C. L. Johnson, Evidence for diffuse extension of the Pacific plate from Pukapuka ridges and cross-grain gravity lineations, *J. Geophys. Res.*, *100*, 15,087–15,099, 1995.

Schlanger, S. O., et al., Geology and Geochronology of the Line Islands, *J. Geophys. Res.*, *89*, 11,261–11,272, 1984.

Schlanger, S. O., H. C. Jenkyns, and I. Premoli Silva, Volcanism and vertical tectonics in the Pacific basin related to global Cretaceous transgressions, *Earth Planet. Sci. Lett.*, *52*, 435–449, 1981.

Schlanger, S. O., J. F. Campbell, and J. W. Jackson, Post-Eocene subsidence of the Marshall Islands recorded by drowned atolls on Harrie and Sylvania guyots, in *Seamounts, Islands and Atolls*, *Geophys. Monogr. Ser.*, vol. 43, edited by B. H. Keating et al., pp. 165–174, AGU, Washington, D. C., 1987.

Seidemann, D. E., Effects of submarine alteration on K-Ar dating of deep-sea igneous rocks, *Geol. Soc. Am. Bull.*, *88*, 1660–1666, 1977.

Seidemann, D. E., $^{40}Ar/^{39}Ar$ studies of deep-sea igneous rocks, *Geochim. Cosmochim. Acta*, *42*, 1721–1734, 1978.

Shimizu, N., and S. R. Hart, Differential dissolution technique (DDT): Chemical separation of crystals from glass, *Year Book Carnegie Inst. Washington*, *72*, 268–270, 1973.

Sleep, N. H., Tapping of magmas from ubiquitous mantle hetereogeneities: An alternative to mantle plumes?, *J. Geophys. Res.*, *89*, 10,029–10,041, 1984.

Sleep, N. H., Local lithospheric relief associated with fracture zones and ponded plume material?, *Geochem. Geophys. Geosyst.*, *3*(12), 8506, doi:10.1029/2002GC000376, 2002.

Smith, A. D., and C. Lewis, The planet beyond the plume hypothesis, *Earth Sci. Rev.*, *48*, 135–182, 1999.

Smith, W. H. F., and D. Sandwell, Predicted bathymetry: New global seafloor topography from satellite altimetry, *Eos Trans. AGU*, *77*(46), 315, 1996.

Smith, W. H. F., and D. T. Sandwell, Global sea floor topography from satellite altimetry and ship depth soundings, *Science*, *277*, 956–962, 1997.

Smith, W. H. F., H. Staudigel, A. B. Watts, and M. S. Pringle, The Magellan seamounts: Early Cretaceous record of the south Pacific isotopic and thermal anomaly, *J. Geophys. Res.*, *94*, 10,501–10,523, 1989.

Smoot, N. C., Guyots of the Dutton ridge at the Bonon/Mariana trench juncture as shown by multi-beam surveys, *J. Geol.*, *91*, 211–220, 1983.

Solomon, S. C., and N. H. Sleep, Some simple physical models for absolute plate motions, *J. Geophys. Res.*, *79*, 2557–2567, 1974.

Spooner, E. T. C., The strontium isotopic composition of seawater, and seawater-oceanic crust interaction, *Earth Planet. Sci. Lett.*, *31*, 167–174, 1976.

Staudigel, H., and S. R. Hart, Alteration of basaltic glass: Mechanisms and significance for the oceanic crust-seawater budget, *Geochim. Cosmochim. Acta*, *47*, 337–350, 1983.

Staudigel, H., K.-H. Park, M. S. Pringle, J. L. Rubenstone, W. H. F. Smith, and A. Zindler, The longevity of the south Pacific isotope and thermal anomaly, *Earth Planet. Sci. Lett.*, *102*, 24–44, 1991.

Stefanick, M., and D. M. Jurdy, The distribution of hotspots, *J. Geophys. Res.*, *89*, 9919–9925, 1984.

Steinberger, B., Plumes in a convecting mantle: Models and observations for individual hotspots, *J. Geophys. Res.*, *105*, 11,127–11,152, 2000.

Steinberger, B., and R. J. O'Connell, Advection of plumes in mantle flow: Implications for hotspot motion, mantle viscosity and plume distribution, *Geophys. J. Int.*, *132*, 412–434, 1998.

Tarduno, J. A., and R. D. Cottrell, Paleomagnetic evidence for motion of the Hawaiian hotspot during formation of the Emperor seamounts, *Earth Planet. Sci. Lett.*, *153*, 171–180, 1997.

Tarduno, J. A., and J. Gee, Large-scale motion between Pacific and Atlantic hotspots, *Nature*, *378*, 477–480, 1995.

Tarduno, J. A., and W. W. Sager, Polar standstill of the mid-Cretaceous Pacific plate and its geodynamic implications, *Science*, *269*, 956–959, 1995.

Taylor, J. R., An introduction to error analysis, 270 pp., Univ. Science Books, Mill Valley, Calif., 1982.

Turcotte, D. L., and E. R. Oxburgh, Intra-plate volcanism, *Philos. Trans. R. Soc. London*, *288*, 561–579, 1978.

Turner, D. L., and R. D. Jarrard, K-Ar dating of the Cook-Austral Island chain: A test of the hotspot hypothesis, *J. Volcanol. Geothermal Res.*, *12*, 187–220, 1982.

Vidal, P., C. Chauvel, and R. Brousse, Large mantle heterogeneity beneath French Polynesia, *Nature*, *307*, 536–538, 1984.

Vogt, P. R., Evidence for global synchronism in mantle plume convection, and possible significance for geology, *Nature*, *240*, 338–342, 1972.

Vogt, P. R., Volcano spacing, fractures, and thickness of the lithosphere, *Earth Planet. Sci. Lett.*, *21*, 235–252, 1974.

Wang, S., and R. Wang, Current plate velocities relative to hotspots: Implications for hotspot motion, mantle viscosity and global reference frame, *Earth Planet. Sci. Lett.*, *189*, 133–140, 2001.

Watkins, D. K., P. N. Pearson, E. Erba, F. R. Rack, I. Premoli Silva, H. W. Bohermann, J. Fenner, and P. R. N. Hobbs, Stratigraphy and sediment accumulation patterns of the upper Cenozoic pelagic carbonate caps of guyots in the northWestern Pacific ocean, *Proc. Ocean Drill. Program Sci. Results*, *144*, 675–689, 1995.

Watts, A. B., J. K. Weissel, R. A. Duncan, and R. L. Larson, Origin of the Louisville ridge and its relationship to the Eltanin fracture zone system, *J. Geophys. Res.*, *93*, 3051–3077, 1988.

Wedgeworth, B., and J. Kellogg, A 3-D gravity-tectonic study of Ita Mai Tai guyot: An uncompensated seamount in the east Mariana Basin, in *Seamounts, Islands and Atolls*, *Geophys. Monogr. Ser.*, vol. 43, edited by B. H. Keating et al., pp. 73–84, AGU, Washington, D. C., 1987.

Wessel, P., and L. W. Kroenke, A geometric technique for relocating hotspots and refining absolute plate motions, *Nature*, *387*, 365–369, 1997.

Wessel, P., and L. W. Kroenke, The geometric relationship between hotspots and seamounts: Implications for Pacific hotspots, *Earth Planet. Sci. Lett.*, *158*, 1–18, 1998.

Wessel, P., and W. H. F. Smith, New version of the generic mapping tools released, *Eos Trans. AGU*, *76*(29), 329, 1995.

Wessel, P., L. W. Kroenke, and D. Bercovici, Pacific plate motion and undulations in geoid and bathymetry, *Earth Planet. Sci. Lett.*, *140*, 53–66, 1996.

White, W. M., and A. W. Hofmann, Sr and Nd isotope geochemistry of oceanic basalts and mantle evolution, *Nature*, *296*, 821–825, 1982.

Wijbrans, J. R., M. S. Pringle, A. A. P. Koppers, and R. Scheveers, Argon geochronology of small samples using the Vulkaan argon laserprobe, *Proc. K. Ned. Akad. Wet. Biol. Chem. Geol. Phys. Med. Sci.*, *98*, 185–218, 1995.

Wilson, J. T., A possible origin of the Hawaiian Islands, *Can. J. Phys.*, *41*, 863–870, 1963.

Winterer, E. L., En enchelon volcanic ridges along seamount chains result from episodic changes in stress orientations that open cracks to the asthenosphere and permit magma ascent: They do not require plumes, *Eos Trans. AGU*, *83*(47), Fall Meet. Suppl., Abstract S72C-01, 2002.

Winterer, E. L., and D. T. Sandwell, Evidence from en-echelon cross-grain ridges from tensions cracks in the Pacific plate, *Nature*, *329*, 534–537, 1987.

Winterer, E. L., J. H. Natland, R. J. Van Waasbergen, R. A. Duncan, M. K. McNutt, C. J. Wolfe, I. Premoli Silva, W. W. Sager, and W. V. Sliter, Cretaceous guyots in the northwest Pacific: An overview of their geology and geophysics, in *The Mesozoic Pacific: Geology, Tectonics, and Volcanism*, *Geophys. Monogr. Ser.*, vol. 77, edited by M. S. Pringle et al., pp. 307–334, AGU, Washington, D. C., 1993.

Wolfe, C., and M. K. McNutt, Compensation of Cretaceous seamounts of the Darwin rise, *J. Geophys. Res.*, *96*, 2363–2374, 1991.

Woodhead, J. D., Temporal geochemical evolution in oceanic intra-plate volcanics: A case study from the Marquesas (French Polynesia) and comparison with other hotspots, *Contrib. Mineral. Petrol.*, *111*, 458–467, 1992.

Woodhead, J. D., and C. W. Devey, Geochemistry of the Pitcairn seamounts: I. Source character and temporal trends, *Earth Planet. Sci. Lett.*, *116*, 81–99, 1993.

Woodhead, J. D., P. Greenwood, R. S. Harmon, and P. Stoffers, Oxygen isotope evidence for recycles crust in the source of EM-type ocean island basalts, *Nature*, *362*, 809–813, 1993.

Wortel, R., and S. Cloetingh, On the origin of the Cocos-Nazca spreading center, *Geology*, *9*, 425–430, 1981.

York, D., Least squares fitting of a straight line with correlated errors, *Earth Planet. Sci. Lett.*, *5*, 320–324, 1969.

Zindler, A., and S. Hart, Chemical geodynamics, *Annu. Rev. Earth Planet. Sci.*, *14*, 493–571, 1986.

Zoback, M. L., et al., Global patterns of tectonic stress, *Nature*, *341*, 291–298, 1989.